CELL BIOLOGY OF SETTLEMENT AND ADHESION PROCESSES OF BIOFOULING ALGAE

by Stephanie Eleanor Mary Thompson

A thesis submitted to The University of Birmingham for the degree of
DOCTOR OF PHILOSOPHY

School of Biosciences
The University of Birmingham
July 2007

Abstract

The aim of the research presented in this thesis was to investigate the cell biology behind the settlement and adhesion processes of biofouling algae.

Using the fluorescent dye FM 1-43 in *Ulva* zoospores to follow membrane recycling, rapid mass membrane retrieval of FM 1-43-labelled plasma membrane was found to occur to an endosomal compartment during settlement.

Biolistic delivery of dextran Oregon Green BAPTA-1 and Texas Red enabled ratiometric imaging with a 5-fold greater response to Ca^{2+}-ionophores than AM-ester Ca^{2+} indicators. During settlement, zoospores exhibited both localised and diffuse increases in cytosolic calcium implying a role in secretion of the adhesive.

Secretion of redox-active substrates was detected using amperometry when settled spores were mechano-stimulated. Secretory events were similar to those seen in bovine chromaffin cells with the presence of foot signals in the recordings implying a role for a 'fusion pore' in exocytosis.

Using DAF-FM DA nitric oxide (NO) production in *Seminavis robusta* was found to be 4-fold greater on a surface to which the cells adhered weakly than on a surface to which they attached more strongly. Increased NO reduced attachment strength and it is thought that NO may play a signalling and/or regulatory role in diatom adhesion.

Acknowledgements

I would like to especially thank my supervisors Jim and Maureen Callow at the University of Birmingham and Colin Brownlee and Alison Taylor (who became an additional supervisor) at the Marine Biological Association, Plymouth for all their help and advice throughout my PhD. Funding for the project was provided by the Biotechnological and Biological Sciences Research Council (BBSRC) and the Marine Biological Association. Funding though the BBSRC Doctoral Training Program allowed invaluable experience in travelling to and presenting at an international conference.

At Birmingham, special thanks must go to John Finlay for his helpful discussions that stimulated new ideas. Also thanks to everyone in the lab past and present for their assistance, especially Michele and Kat. Thanks also to the department of Computer Science for use of their printers.

In Plymouth, much gratitude is owed to Alison Taylor for devoting so much of her time to assist me with patch clamping and amperometry. In addition, Glen Wheeler was invaluable in development of methods for calcium imaging. John Bothwell developed the macros for Scion Image. Special thanks to Paul Pickerill for finding space for me in his house each year despite the building work!

I would particularly like to thank my parents for their financial and emotional support, which made it possible for me to do my two previous degrees and my sisters for their guidance throughout. And last but most importantly I thank Simon for putting up with my sustained weekly commute throughout the seaweed season and for making the effort to proof read a biologists thesis!

LIST OF CONTENTS

Appendix I – Stacks macros for ratio images in Scion Image

Appendix II – Guillards F/2 medium for diatoms

Appendix III – Patch clamping

Papers not included in the web version of this thesis:

Appendix IV – Thompson, S.E.M., Callow, J.A., Callow, M.E., Wheeler, G.L., Taylor, A.R., Brownlee, C. (2007). Membrane recycling and calcium dynamic during settlement and adhesion of zoospores of the green alga *Ulva linza*. *Plant, Cell and Environment*, **30**, 733-744.

Appendix V – Thompson, S.E.M., Taylor, A.R., Callow, M.E., Callow, J.A. To be submitted. The role of nitric oxide in diatom adhesion in relation to substratum properties.

LIST OF FIGURES

LIST OF TABLES

Abbreviations

AHL – *N*-acylhomoserine lactone

AM – Acetoxymethyl

BAPTA – 1,2-bis(o-aminophenoxy)ethane-N,N,N’, N’-tetraacetic acid

$[Ca^{2+}]_{cyt}$ – Cytosolic calcium

CDPK – Calcium-dependent protein kinase

CFME – Carbon-fibre microelectrodes

CFW – Calcofluor White

CLSM – Confocal laser scanning microscope

DAF-FM – 4-amino-5-methylamino-2',7'-difluorofluorescein diacetate

DAG – Diacylglycerol

DAPI – 4',6-diamidino-2-phenylindole

DMSO – Dimethyl sulfoxide

dsRNA – double stranded RNA

EPS – Extracellular polymeric substances

ESTs – Expressed sequence tags

IP_3 – Inositol 1,4,5-triphosphate

LUT – Look up table

MAPK – Mitogen-activated protein kinase

mRNA – messenger RNA

MS – Mechanosensitive

MVB – Multi-vesicular body

NA – Numerical aperture

NO – Nitric oxide

NOS – Nitric oxide synthase

NMMA - N_{ω}-Methyl-L-arginine acetate

OG – Oregon Green

PCR – Partially coated reticulum

PDMSE – Polydimethyl siloxyl elastomer

PIP_2 – Phosphatylinositol 4,5-bisphosphate

PLC – Phospholipase C

PMT – Photon multiplier tube

RNAi – RNA interference

SEM – Scanning Electron Micrograph

SNAP – *S*-nitroso-*N*-acetylpenicillamine

SNARE – Soluble NSF (*N*-ethylmaleimide-sensitive fusion protein) attachment protein receptor

TBT – Tri-butyl tin

TEM – Transmission Electron Microscope

TIRF – Total Internal Reflection Fluorescence

TR – Texas Red

Glossary

Amperometry – Electrochemical measurement of secretion. Secretion of oxidisable products at the surface of an electrode is measured as an oxidation current, which provides information on the quantity of molecule released and the spatio-temporal characteristics of its secretion.

AM-ester – Cell permeable form of a dye. It is cleaved intracellularly by esterases to yield the active form.

Apical papilla – The dome at the anterior of the *Ulva* zoospore where the base of the flagella are. Thought to be the main sensing area in *Ulva* zoospores.

Compartmentalisation – When dye is sequestered into membrane-bound compartments and organelles where it is unavailable to respond to changes in the ion concentration of interest in the cytosol.

Dextran – Cell-impermeable form of a dye.

Endocytosis – The process of vesicle recovery from the plasma membrane and uptake of extracellular molecules.

Endosome – A cellular compartment where endocytosed material is transported to.

Exocytosis – The process by which secretory products are released from a cell via transport in vesicles to the plasma membrane where the vesicle fuses and the contents of the vesicle are extruded from the cell.

Fusion pore – A channel that forms in the early stages of exocytosis before full fusion of the vesicle and plasma membrane through which leakage of the vesicle contents occurs.

Oxidation – Loss of electrons from a chemical species.

Patch clamping – Measurement of electrical currents from ion channels through creation of an electrical seal between the plasma membrane and a filled glass micropipette.

Raphe – Slit in the cell wall (frustule) of a diatom through which adhesive is secreted.

Redox-active – A substance that is easily oxidised or reduced.

Redox potential - The tendency of a chemical species to acquire electrons and thereby be reduced. Each species has its own intrinsic reduction potential; the more positive the potential, the greater the species' affinity for electrons and tendency to be reduced.

Reduction – Addition of electrons to a chemical species.

1: GENERAL INTRODUCTION

1.1 Rationale behind the project

This project is concerned with aspects of the cell biology of adhesion by the marine fouling alga *Ulva linza* Linnaeus syn *Enteromorpha linza*[1] and two fouling diatom species. Diatoms form microfouling slimes and *Ulva* is the most common macrofouling algae on ships. Marine biofouling has been a major problem over centuries of boat use as the accumulation of undesirable organisms increases hydrodynamic drag (Schultz & Swain, 2000) thereby increasing fuel costs. Fouled ship hulls burn up to 40% more fuel due to the increased drag (Champ, 2000). Increased fuel consumption is also an environmental issue (Evans, 1999). In addition, biofouling is a major problem on smaller boats with owners spending considerable amounts of time and money on the removal of biofouling organisms. Biofouling also causes structural problems for offshore oil rigs due to an increased load on the structure and regular cleaning by divers is required.

Antifouling paints such as those that use copper or TBT have had far reaching effects on the environment (see Alzieu *et al.* (1986); Claisse & Alzieu (1993); Davies *et al.* (1997) and Law *et al.*, (1998)). A global ban on the use of TBT antifouling paints will be effective from 2008 but environmental impacts from using the replacement organic

[1] *Enteromorpha* has only recently been incorporated into the genus *Ulva* due to molecular data providing strong evidence that the two genera are not sufficiently distinct in their morphologies to be classed separately. Both *Ulva* and *Enteromorpha* can show the same morphologies depending on environmental conditions (TAN, I. H., BLOMSTER, J., HANSEN, G., LESKINEN, E., MAGGS, C. A., MANN, D. G., SLUIMAN, H. J., STANHOPE, M. J. (1999). Molecular phylogenetic evidence for a reversible morphogenetic switch controlling the gross morphology of two common genera of green seaweeds, *Ulva* and *Enteromorpha*. *Mol. Biol. Evol.* **16**(8): 1011-1018.) *Enteromorpha* has therefore been reduced to synonymy with *Ulva* and papers cited that refer to *Enteromorpha* encompass *Ulva* synonymously.

booster biocides are unknown and they may be equally or even more toxic to the environment than TBT (Evans *et al.*, 2000). Siloxane elastomers form the basis of non-toxic foul-release coatings. These are hydrophobic coatings and release macrofouling algae under the correct hydrodynamic conditions (termed 'self-cleaning') due to their surface physico-chemical and mechanical properties. Although these low surface energy coatings minimise the adhesive strength of macrofouling algae such as *Ulva* (Finlay *et al.*, 2002a), diatom slimes accumulate due to their increased strength of adhesion on the hydrophobic surfaces (Holland *et al.*, 2004).

It is thought that interfering with bioadhesion of fouling algae is the best approach to developing environmentally safe antifouling strategies and one of the main areas where greater knowledge is needed is in understanding the cellular processes involved in adhesive secretion of these biofouling algae (Callow *et al.* (1997); Callow & Callow (2002) and Stanley *et al.* (1999)).

1.2 General ecology and physiology of *Ulva* zoospores

Ulva is found in the intertidal zone of the shore. It colonises substrates by releasing many microscopic swimming zoospores at a rate of 10^5-10^6 per plant per day (Maggs & Callow, 2003) (Figure 1-1a). An isomorphic alternation of generations occurs with haploid gametophytic plants producing biflagellate gametes and diploid sporophytic plants producing haploid zoospores (Maggs & Callow, 2003). The zoospores are released a few days before spring tide and settle, often gregariously, on detection of preferable substrata by secreting a preformed adhesive. The spores then germinate and grow to form the familiar adult plant (Figure 1-1b). This project focuses on the mechanisms underlying settlement of the zoospores.

The swimming zoospore is generally pyriform in shape and ~5 μm long with four anterior flagella (Figure 1-1c-d) that are lost upon permanent adhesion. The anterior end is the narrowest with large numbers of Golgi-derived electron-dense vesicles containing the adhesive needed for settlement (Callow & Evans, 1974) (Figure 1-2a). The apical papilla (Figure 1-1d) is also present at the anterior. It forms a dome where the base of the flagella are (Evans & Christie, 1970) and it is speculated that this may be the main 'sensing' area of the zoospore (Callow *et al.*, 1997). The chloroplast and nucleus occupy the posterior end of the zoospore (Figure 1-2b).

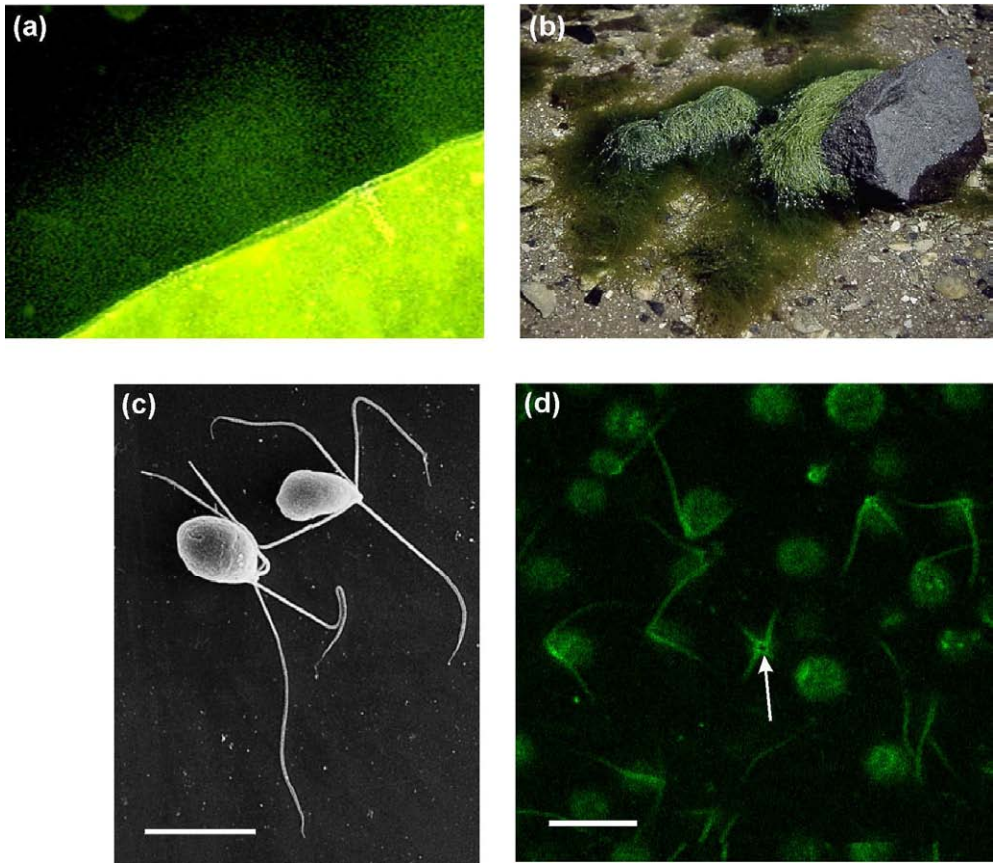

Figure 1-1 (a) Release of spores from the edge of a dried out thallus after flooding with seawater. **(b)** The familiar adult form of *Ulva* in its typical habitat. **(c)** Scanning Electron Micrograph (SEM) of zoospores showing the four flagella. **(d)** Confocal laser scanning image of zoospores loaded with FM 1-43 (see Chapter 3) which has labelled the flagella and anterior region of the zoospore. The dark region in the centre of the flagella (arrow) is the apical papilla. Scale bar in (c) and (d) = 10 µm. (a), (b) and (c) were kindly provided by Prof. J.A. Callow.

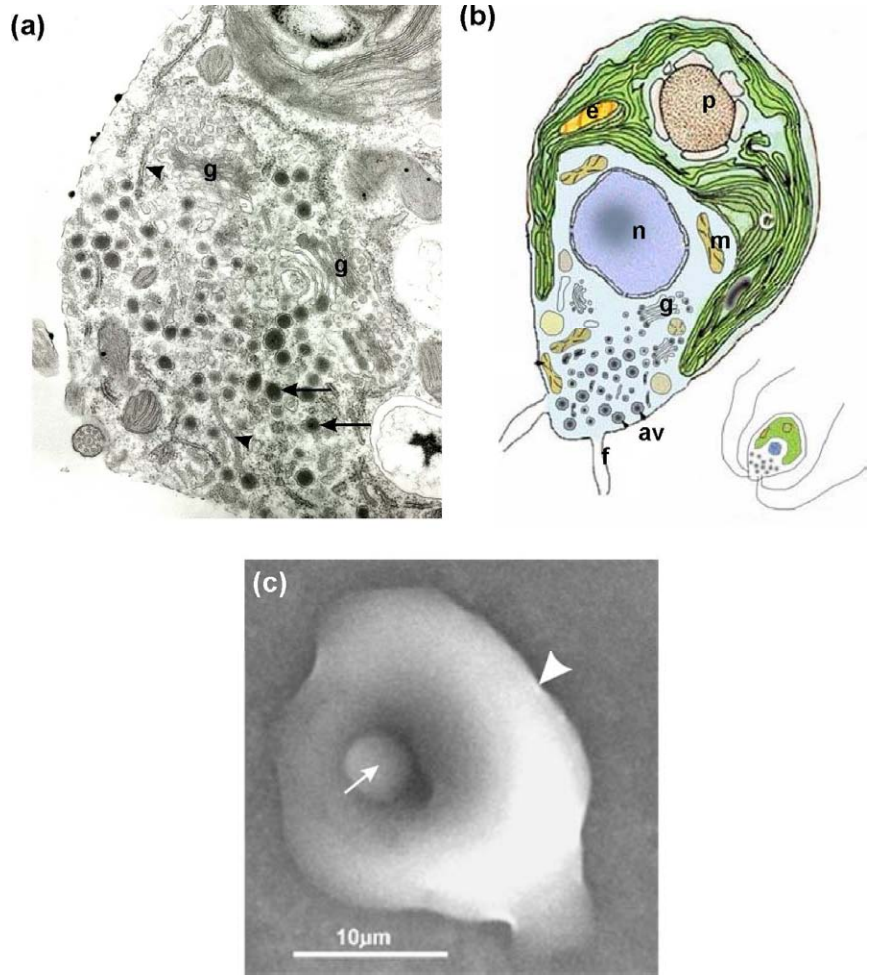

Figure 1-2 Cellular structure of the *Ulva* zoospore and visualisation of the adhesive. **(a)** Transmission electron micrograph of the anterior region of a motile spore (kindly provided by Prof. LV Evans – see Evans & Christie (1970) for preparation methods), illustrating the extensive network of Golgi bodies (g), endoplasmic reticulum (arrowheads) and electron-dense 'adhesive' vesicles (examples arrowed). **(b)** Diagrammatic view of a motile spore illustrating key features. av = adhesive vesicles; c = chloroplast; e = eyespot; f = flagellum; g = Golgi body; m = mitochondrion; n = nucleus; p = pyrenoid. **(c)** An environmental scanning electron micrograph of a settled *Ulva* zoospore (arrow) surrounded by the gel-like adhesive (arrowhead marks the extent of the adhesive). Using environmental-SEM the spore adhesive is visualised in its hydrated state without fixation or dehydration under a very low vacuum using water as the imaging gas (Callow *et al.*, 2003). (b) and (c) were kindly provided by Prof. J.A. Callow.

1.3 Settlement and adhesion of *Ulva*

1.3.1 Settlement cues

Settlement cues for motile spores range from features associated with the substratum to biological and chemical conditions (Maggs & Callow, 2003). Much research has been conducted recently on settlement cues for *Ulva* zoospores (see Callow *et al.* (2000b); Callow *et al.* (2002); Finlay *et al.* (2002a); Joint *et al.* (2000), Patel *et al.* (2003) and Youngblood *et al.* (2003)) showing that zoospores prefer to settle on organically conditioned hydrophobic rough surfaces and actively seek the angle between a ridge and valley to settle in as the increased contact area reduces the amount of energy required for adhesion (Callow *et al.*, 2002). Rough surfaces provide a greater surface area so that the spore is protected from desiccation and wave action (Maggs & Callow, 2003). Hydrophobic surfaces repel water, aiding adhesion by allowing closer contact between the adhesive and surface. Spores are however more easily removed from hydrophobic than hydrophilic surfaces due to a weak strength of attachment (Callow *et al.*, 2000b). Environmental scanning electron microscopy studies have shown that as the wettability of a surface increases, the adhesive spreads further and there is therefore a higher surface area of contact between the spore and a hydrophilic surface (Callow *et al.*, 2005), which may explain why a spore shows stronger attachment strength.

Zoospores are negatively phototactic (Callow & Callow, 2000) and tend to settle gregariously which is thought to be of adaptive value due to the reduced turbulence that zoospores experience when they are settled in a group (Finlay *et al.*, 2002b). Attachment of zoospores is enhanced by the presence of a bacterial biofilm with greater numbers settling on surfaces with a higher bacterial cover (Joint *et al.*, 2000).

It is thought that the presence of bacteria gives either a topographic and/or physico-chemical cue for settlement. Settlement of the zoospores may depend on a signal produced by bacteria (Joint *et al.*, 2000). 'Quorum sensing' involves the use of diffusible chemical signal molecules by bacteria that upon reaching a threshold level activate target genes that are used by the bacteria to regulate population growth. *Ulva* zoospores have been shown to exploit this bacterial system with enhanced settlement in the presence of quorum sensing *N*-acylhomoserine lactone (AHL) signals from bacteria (Joint *et al.*, 2002; Wheeler *et al.*, 2005).

1.3.2 The process of settlement and adhesion

Zoospores adhere at their greatest rate during the first 30 minutes after release. They vary in their speed of settlement and a proportion in the sample (up to 50%) will not settle (Callow *et al.*, 1997) the behavioural reason perhaps being that prolonging swimming will enable the spore to encounter a wider range of potential settlement sites thereby increasing the likelihood of finding a more favourable surface for settlement (Callow *et al.*, 2001). There are several stages in the settlement of a zoospore listed below:

1. Settlement begins when the swimming behaviour of the zoospore changes from random motion to a more localised searching pattern. Contact is made between the apical papilla and the surface and a small amount of elastic material has been seen to be released, termed temporary adhesive (Callow *et al.*, 1997).

2. The zoospore then spins on its apical papilla ‘sensing’ the surface (Callow & Callow, 2000) for seconds to minutes until it either permanently adheres or swims off.

3. Permanent adhesion occurs when the zoospore stops spinning and releases its adhesive vesicles to form an adhesive pad (Figure 1-2c) and changes from a pear-shape to become more rounded. The process of permanent adhesion lasts approximately 2 minutes.

4. The flagella are then withdrawn into the cell and the flagella sheaths discarded.

Approximately 20 min after adhesion the spore starts to produce a cell wall (Callow & Callow, 2000); the attached spore germinates within approximately 24 h and within days grows into a sporeling, which then develops into the mature, sessile plant (Callow *et al.*, 2000a). The adhesive undergoes rapid progressive curing by cross-linking becoming harder over time (Stanley *et al.*, 1999; Callow *et al.*, 2000a; Humphrey *et al.*, 2005). Callow *et al.*, (1997) used video microscopy to observe intense cytoplasmic activity in the anterior region of the zoospore as it undergoes permanent attachment and it is thought that this is due to the movement of the adhesive vesicles to the cell membrane. When secretion and membrane traffic was inhibited using the fungal antibiotic Brefeldin A, the proportion of zoospores settling was reduced by ~50 % (Callow *et al.*, 2001) providing evidence that exocytosis of adhesive materials is required for adhesion to occur.

1.4 Exocytosis and endocytosis

1.4.1 Current knowledge of endocytosis in plants

Endocytosis is the process of vesicle recovery from the plasma membrane. It is thought that a major role of endocytosis in eukaryotes is to balance exocytosis and prevent cell expansion as well as regulating membrane recycling, repair and internalisation of receptors during signalling processes (Marcote *et al.*, 2000). In plants endocytic retrieval of plasma membrane and associated proteins occurs through clathrin-coated pits. This material then passes through partially coated reticulum (PCR) (early endosome) and multi-vesicular bodies (MVBs) (late endosomes) before appearing in the vacuole (Geldner, 2004) (Figure 1-3). Partially coated reticulum has been shown to exist in many higher-plant species and is a series of interconnected tubular membranes with coated regions which is thought to act as a sorting endosome with material to be recycled being sent to the Golgi and material to be degraded being sent to the MVBs (Marcote *et al.*, 2000). The sorting is essential in controlling levels of receptors and transporters at the cell surface (Geldner, 2004). Endosomes therefore play a crucial role in signal transduction and development.

The study of plant cell endocytosis is less advanced in comparison to animals and yeast at least in part due to the cell wall barrier limiting the use of cell markers (Emans *et al.*, 2002). In particular, examples of endocytosis in algae are difficult to find. Membrane recycling occurs in response to mechanical wounding in the giant unicellular alga *Ventricaria ventricosa* where endocytosis involving coated pits allows transformation of maternal tonoplast into protoplast plasma membrane (Shepherd *et al.*, 2004) and in *Fucus distichus* zygotes membrane recycling occurs during polar growth of the rhizoid (Belanger & Quatrano, 2000).

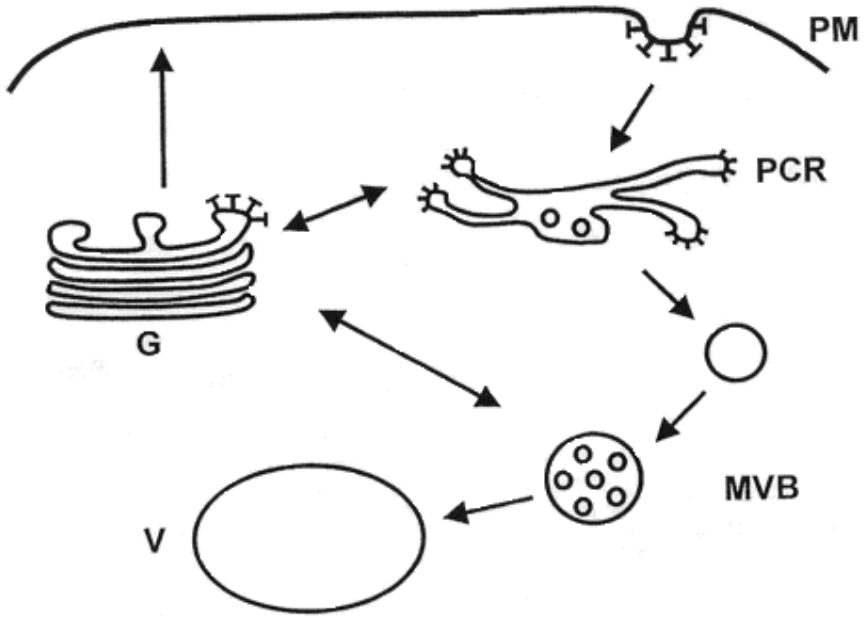

Figure 1-3 The endocytic pathway in plant cells (from Marcote *et al*. (2000)). Markers internalised in plant cells first appear in the partially coated reticulum (PCR). Markers that follow the degradative pathway then appear in multivesicular bodies (MVBs) and the central vacuole (V) with recycling occurring in the Golgi apparatus (G). PM = plasma membrane.

1.4.2 Optical detection of exocytosis and endocytosis

When zoospores adhere to a surface there is a large release of Golgi-derived vesicles containing glycoprotein adhesive at the anterior end of the zoospore (Evans & Christie, 1970). It is important to study this mass vesicle release and recycling in order that we may determine what signal response pathways underlie the detection of a favourable surface and trigger the cell to release its vesicles and adhere to the surface.

Imaging the release of the adhesive vesicles is difficult (Callow *et al.*, 1997) and advanced microscopy is required to provide the resolution required for imaging single secretory events. Total Internal Reflection Fluorescence (TIRF) microscopy can be used to visualise vesicles that are loaded with fluorescent dye. TIRF microscopy gives low background interference because light is only reflected internally at the glass-cell interface. The evanescence produced illuminates the sample to a depth of less than 100 nm (Zenisek *et al.*, 2000) therefore only events at the immediate cell membrane are observed. Unfortunately, it is not possible to use TIRF for imaging exocytosis in *Ulva* zoospores because the vesicles are too small to visualise using this technique (Pers. Comm. Dr R. H. Chow, University of Southern California).

Exocytosis and endocytosis of single vesicles or at a whole cell level can be viewed using styryl dyes such as FM 1-43 which have a high affinity for lipid membranes and bind to the cell membrane with their hydrophobic tail but cannot penetrate into the cytosol due to its two highly charged nitrogen atoms (Betz & Bewick, 1992). They are almost non-fluorescent in aqueous solution fluorescing strongly upon membrane binding (Cousin & Robinson, 1999). Styryl dyes differ from other dyes as they stain the vesicle membrane and not the lumen. Also, staining and cytoplasmic destaining of

the dye depends on the intensity of vesicle release (Betz *et al.*, 1992). As FM 1-43 only labels membranes it can only enter the cell from the cell exterior if the plasma membrane has been internalised hence the presence of FM 1-43 in the cell interior indicates internalisation of plasma membrane via endocytosis has occurred (Emans *et al.*, 2002).

1.4.3 Electrochemical detection of secretion

In addition to optical techniques for detection of secretion, electrochemical techniques are available such as amperometry. If the secreted product is redox-active then this sensitive technique has the potential to provide high spatiotemporal resolution of individual secretory exocytotic events (Travis & Wightman, 1998). Carbon-fibre microelectrodes that have been calibrated in the electron acceptor ferricyanide are used non-invasively to directly measure individual vesicle release events over time (Chow *et al.*, 1992). Secretion in a specific region of the cell (such as the anterior or posterior) can be studied as well as the kinetics of vesicle secretion such as whether a fusion pore forms in the early stages of exocytosis (Chow *et al.*, 1992; Monck & Fernandez, 1992). However, this technique depends on the contents of the released vesicles being readily oxidised. If this is not the case then vesicles can be artificially loaded with a redox-active substrate (Kim *et al.*, 2000).

Of interest in this project was whether zoospores release oxidisable substances during and/or after settlement as cross-linking has been shown to be important in curing the adhesive (Stanley *et al.*, 1999; Humphrey *et al.*, 2005). Eggs of the brown alga *Fucus* release oxidisable phenolics when forming a cell wall and vesicle release has been recorded recently using amperometry (Pers. Comm. Dr. A.R. Taylor, Marine

Biological Association of the UK). Therefore, another area of interest at settlement is whether cross-linking oxidisable agents are released from spores to cure the adhesive.

1.5 Calcium and its role in adhesion

1.5.1 Signalling in plants

Plants and algae continually respond to their environment via signal transduction processes that are initiated by various stimuli, in *Ulva* zoospores these are likely to include light, nutrients, gravity and surface-related features such as the presence of a bacterial biofilm or physicochemical properties.

The signals are perceived by different receptors, usually proteins, at the plasma membrane, in the cytosol or in other cellular compartments. There are at least three different classes of cell surface receptors – G protein-coupled, enzyme-linked and ion channel-linked. Activation of G protein-coupled receptors occurs through the binding of a ligand, resulting in the interaction of the G_{α} subunit of a trimeric G protein with the receptor. The G_{α} subunit is a GTPase that upon binding undergoes a conformational change that results in the dissociation of bound GDP (inactive state), which is replaced by GTP (active state). The G_{α} subunit then dissociates from the $G_{\beta\gamma}$ subunit. Dissociation of the ligand from the receptor causes G_{α} to bind to the effector (eg. adenylyl cyclase), activating it. Activation is short-lived as GTP is hydrolysed to GDP causing G_{α} to dissociate from the effector and reassociate with the $G_{\beta\gamma}$ subunit (Lodish *et al.*, 2004).

Enzyme-linked receptors are often protein kinases. When the signalling dimer binds to the receptor it causes it to dimerize which leads to phosphorylation and activation of the receptor. In turn the activated receptor can then phosphorylate and activate

other downstream proteins or it can interact with other membrane-bound or diffusible proteins such as Ras or G-proteins. Ion-channel-linked receptors are coupled to plasma membrane channels that open when a signal molecule binds to the receptor (Buchanan *et al.*, 2000).

Two of the essential/key elements of the signalling pathway that transduce the signal are cytosolic calcium and protein kinases. Calcium-dependent protein kinases link the two pathways. Protein kinases are enzymes that phosphorylate and thereby alter the activity of target proteins. Calcium-dependent protein kinases (CDPKs) have been discovered in the green alga *Chlamydomonas* (Pinontoan *et al.*, 2000), *Dunaliella tertiolecta* (Siderius *et al.*, 1997) and *Closterium ehrenbergii* (Yuasa & Hashimoto, 2006).

In *Arabidopsis*, signal transduction of the plant hormones ethylene and cytokinin occurs through two-component signalling pathways (Kieber, 1997; Hwang & Sheen, 2001). Two-component systems consist of a histidine protein kinase that senses the output and a response regulator that mediates the output (Hwang & Sheen, 2001). An ethylene receptor named ETR1 identified through ethylene-insensitive mutants has been discovered in *Arabidopsis*. The ETR1 gene encodes a protein that shows similarity to bacterial two-component histidine kinases and is localised to a membrane. The perception of ethylene is thought to begin with the binding of ethylene to ETR1 either as homo- or heterodimers which then leads to the inactivation of CTR1 kinase activity (a serine/threonine protein kinase similar to the Raf family). Inactivation of CTR1 then allows the activation of downstream components possibly through a mitogen-activated protein kinase (MAPK) cascade most likely resulting in

alterations in gene expression such as elevation of gene transcription of plant defence genes (Kieber, 1997).

Signalling pathways can include both static receptors located in the plasma membrane or other intracellular organelle membranes and diffusible components that can move freely in the cytosol. An example of a signalling pathway containing both static and diffusible elements is that involving activation of phospholipase C (PLC). Phosphatidylinositol 4,5-bisphosphate (PIP_2) is the substrate for PLC and it is cleaved to form two products: a soluble second messenger, inositol 1,4,5-triphosphate (IP_3) and diacylglycerol (DAG), which remains membrane-bound. IP_3 is then able to mobilise Ca^{2+} stores in the ER and vacuole by binding to specific receptors in their membranes that act as Ca^{2+} channels (Buchanan *et al.*, 2000). In the alga *Phaeocystis globosa*, photostimulation induces IP_3-triggered [Ca^{2+}] oscillations in the lumen of granules and in the cytosol which trigger exocytosis (Quesada *et al.*, 2006). In the flagellate green alga *Spermatozopsis* the IP_3-triggered Ca^{2+} signal in response to light has been found to occur through the activation of PLC which is coupled to a G-protein and the photoreceptor rhodopsin (Calenberg *et al.*, 1998). The function of the rhodopsin-coupled G-protein has been speculated to be in regulation of the voltage-gated Ca^{2+} channels in the eyespot (Calenberg *et al.*, 1998) (see section 1.6.2 for discussion of the Ca^{2+} channels present in the rhodopsin signalling pathway).

1.5.2 Calcium as a signalling messenger

There are a number of messengers in plant cells used in signalling pathways including Ca^{2+}, lipids and cyclic GMP. Calcium is a very common signalling messenger in animal and plant cells and cytosolic free calcium ($[Ca^{2+}]_{cyt}$) has been shown to respond to more stimuli than any other messenger (Sanders *et al.*, 1999). Calcium has

a high affinity for a range of binding proteins that transduce the signal, for example, calmodulin. This high affinity results in free Ca^{2+} being rapidly bound on entering the cell restricting the rate of diffusion in the cytosol and resulting in localised Ca^{2+} gradients that allow spatially distinct patterns in Ca^{2+} signalling (Sanders *et al.*, 1999). Specificity of Ca^{2+} signalling also results from differences in the kinetics of stimulus-induced increases in $[Ca^{2+}]_{cyt}$ which can result in oscillations and waves of $[Ca^{2+}]_{cyt}$ which have been shown to correlate with the degree of stimulus and the magnitude of the final response (McAinsh & Hetherington, 1998).

$[Ca^{2+}]_{cyt}$ is kept low, in the nM range in order to keep the cell responsive to further Ca^{2+} signals. This is brought about by efflux of Ca^{2+} out of the cytosol and into compartments such as the vacuole or through the plasma membrane. The efflux of Ca^{2+} is by energised transport using ATP-driven pumps (Sanders *et al.*, 1999) as Ca^{2+} is transported against the concentration gradient to restore $[Ca^{2+}]_{cyt}$ to resting levels. Influx into the cytosol from organelles or through the plasma membrane is down a concentration gradient from high to low $[Ca^{2+}]$. It can therefore occur passively through ion channels that are permeable to Ca^{2+} resulting in an increase from nanomolar to micromolar levels of $[Ca^{2+}]_{cyt}$.

1.5.3 Stimuli that are known to affect cytosolic calcium

In plants there are many known Ca^{2+}-mediated processes with many different physiological stimuli both abiotic and biotic being shown to evoke changes in $[Ca^{2+}]_{cyt}$ (see Table 1-1 for examples) and strong evidence that Ca^{2+} plays a central role in many key events in the plant cell (Sanders *et al.*, (1999); Trewavas & Knight (1994)). Touching, cold-shock and elicitors all cause elevations in $[Ca^{2+}]_{cyt}$ of varying length in *Nicotiana plumbaginifolia* (Knight *et al.*, 1991). It is postulated that of the

physiological stimuli listed in Table 1-1, touch is the stimulus most likely to initiate settlement in *Ulva* zoospores.

Table 1-1 Some physiological stimuli that elevate $[Ca^{2+}]_{cyt}$ in plant cells (taken from Sanders *et al.* (1999)).

Stimulus	***Example of response***
Red light	Photomorphogenesis
Abscisic acid	Stomatal closure
Gibberellin	α-Amylase secretion
Salinity/drought	Proline synthesis
Hypoosmotic stress	Osmoadaptation
Touch	Growth retardation
Fungal elicitors	Phytoalexin synthesis
Cold	*KIN1* gene expression
Heat shock	Thermotolerance
Oxidative stress	Free radical scavenger induction
NOD factors	Root hair curling

1.5.4 The role of calcium in exocytosis in plant cells

It is thought that the major regulatory role of Ca^{2+} in the cell is in the control of exocytosis (Battey & Blackbourn, 1993). In plant and animal cells secretion is triggered by a rise in $[Ca^{2+}]_{cyt}$ from ~10^{-7} to 10^{-6} M (Steer, 1988) allowing fusion and movement of vesicles using the actin/myosin pathway. Direct evidence for control of exocytosis by Ca^{2+} has come from electrophysiological studies of whole-cell membrane capacitance. The plasma membrane acts as a capacitor, the value of which is linearly proportional to the surface area of the membrane (Thiel & Battey, 1998) hence an increase in capacitance indicates exocytosis has occurred as the plasma membrane surface area has increased. This can be monitored by using the whole-cell patch clamp technique (Zorec & Tester, 1992; Carroll *et al.*, 1998). A rise in $[Ca^{2+}]_{cyt}$ to 1 µM in barley aleurone protoplasts (Zorec & Tester, 1992), maize root cap protoplasts (Carroll *et al.*, 1998) and maize coleoptile protoplasts (Sutter *et al.*, 2000) has been shown to cause an increase in plasma membrane capacitance implying an increase in surface area caused by exocytosis. However a Ca^{2+}-independent exocytotic pathway has also been found in barley aleurone protoplasts thought to be involved in cell expansion (Homann & Tester, 1997).

In algae, an increase in $[Ca^{2+}]_{cyt}$ is thought to be responsible, at least in part, for inducing cell wall exocytosis and signalling the development of the *Fucus serratus* egg (Roberts *et al.*, 1994). Calcium-regulated secretion has recently been discovered in the unicellular marine alga *Phaeocystis globosa*. Blue light stimulates an increase in $[Ca^{2+}]_{cyt}$ which in turn stimulates the exocytosis of organic material into the surrounding seawater (Chin *et al.*, 2004).

The endomembrane system, cytoskeleton and plasma membrane are all involved in secretion and both vesicle movement and fusion require Ca^{2+} in plants (Steer, 1988). Using electron microscopy, the presence of cytoplasmic microtubules has been documented in *Ulva* zoospores where the microtubules form an 'umbrella' running the length of the cell body with particular abundance close to the plasma membrane (Evans & Christie, 1970). The cytoplasmic microtubule network present in the swimming zoospore appears to be lost on settlement (Evans & Christie, 1970). Microtubules give structural support (Hoffman, 1967) which may become unnecessary once the cell has germinated and developed a cell wall. An additional function of the microtubules is suggested by their orientation. They lead towards the apical papilla which is the direction of transport for the adhesive vesicles. It is therefore possible that the microtubules direct the adhesive vesicles from the site of production in the Golgi apparatus to the plasma membrane in the *Ulva* zoospore. This has been found to occur in the fucoid *Hormosira banksii* (Schoenwaelder & Clayton, 1999) and has been suggested for the unicellular red alga *Glaucosphaera vacuolata* (Wilson *et al.*, 2006) in conjunction with microfilaments. Ca^{2+} levels affect microtubule sliding behaviour (Nakano *et al.*, 2003) hence Ca^{2+} may be involved in the transport of vesicles to the membrane.

In summary, there are several events in the process of adhesion in *Ulva* zoospores where $[Ca^{2+}]_{cyt}$ could play a role directly or indirectly (illustrated in Figure 1-4):

1. Entry of Ca^{2+} through ion channels in the membrane due to a favourable surface signal causing a signal transduction pathway leading to the release of adhesive vesicles. *Ulva* zoospores have been shown through molecular studies

to contain Ca^{2+} signalling pathway components such as protein kinases and Ca^{2+}-regulated enzymes (Stanley *et al.*, 2005).

2. Act as a second messenger in the cytosol transducing the original signal.

3. Regulate the transport of vesicles by microfilaments/microtubules from the Golgi body to the plasma membrane.

4. Regulate the fusion of vesicles with the plasma membrane via Ca^{2+} binding proteins such as annexins (Carroll *et al.*, 1998).

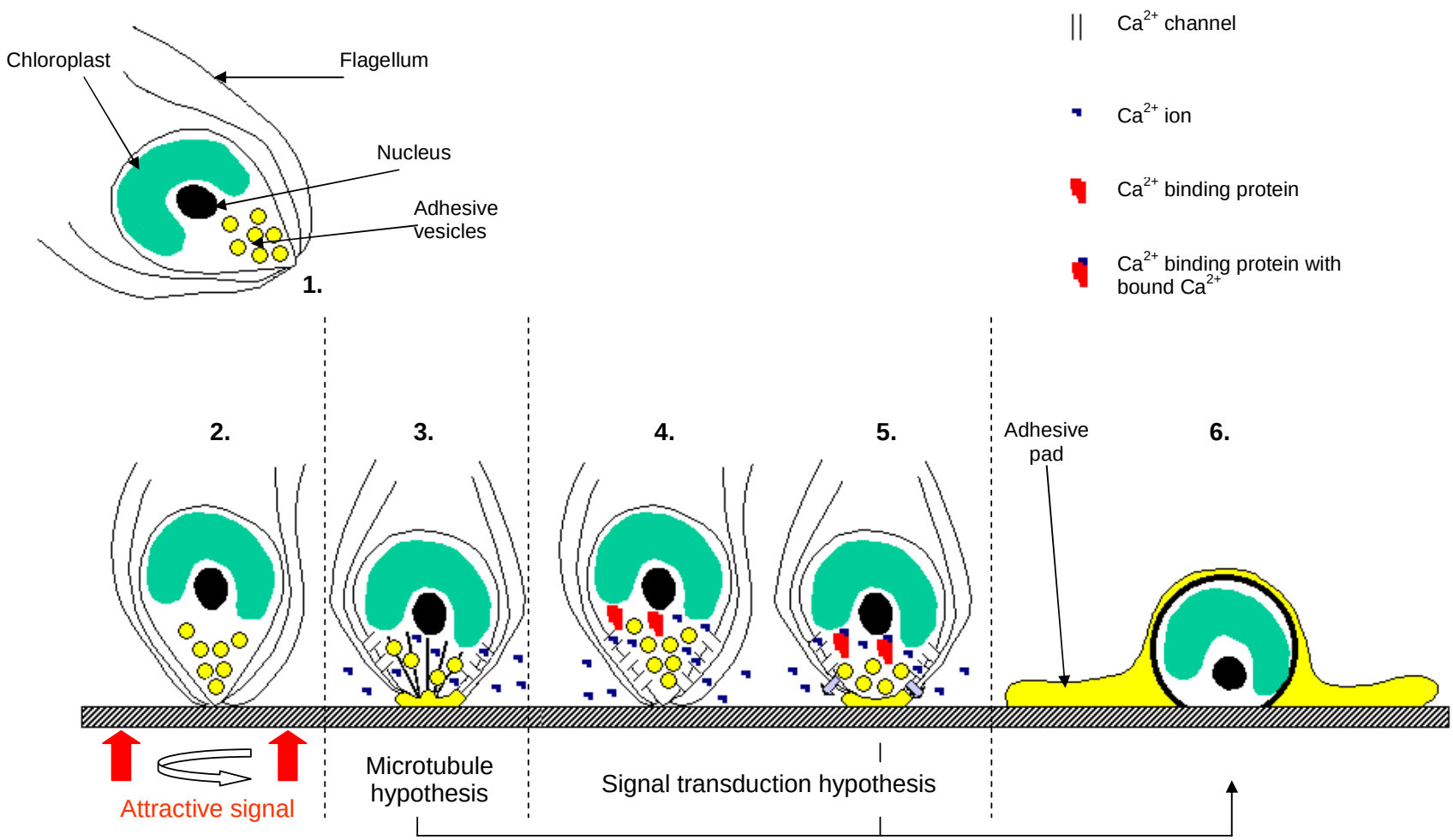
Chloroplast
Flagellum
Nucleus
Adhesive vesicles
1.
Ca2+ channel
Ca2+ ion
Ca2+ binding protein
Ca2+ binding protein with bound Ca2+
2.
3.
4.
5.
Adhesive pad
6.
Attractive signal
Microtubule hypothesis
Signal transduction hypothesis

Figure 1-4 Proposed hypothesis for investigation. 1) The swimming zoospore is attracted to a surface by several cues. 2) The zoospore temporarily binds and explores the surface rotating on a detachable pad on its apical papilla. The favourable signals cause Ca^{2+} channels to open in the plasma membrane allowing Ca^{2+} to flood in. 3) Following the microtubule hypothesis, Ca^{2+} acts directly to activate the transport of the adhesive vesicles possibly along microtubules/microfilaments and allows fusion of vesicles with the plasma membrane resulting in the formation of the adhesive pad (6). 4) Following the signal transduction hypothesis, Ca^{2+} acts indirectly by binding with a Ca^{2+} binding protein such as calmodulin. 5) The Ca^{2+} binding protein activates protein kinases to start a signalling cascade resulting in the release of adhesive vesicles to form an adhesive pad (6).

1.5.5 Possible role of extracellular Ca^{2+} in the hydration of the adhesive

Extracellular Ca^{2+} levels may also play a role in the hydration of the adhesive as it has been shown that Ca^{2+} affects adhesion of human cervical cells (Espinosa *et al.*, 2002). Mucins originate in secretory granules that are released via exocytosis and then swell to form a glycoprotein-type hydrogel. Elevated [Ca^{2+}] reduces the hydration and therefore swelling of the mucins. The adhesive in *Ulva* is also condensed into secretory vesicles which are then exocytosed to become a swollen gel-like glycoprotein-type adhesive pad (Callow *et al.*, 2003) (Figure 1-2c). The adhesive swells by a factor of 300-fold upon extrusion from the vesicles (Callow *et al.*, 2000a). The *Ulva* adhesive shows rapid hydration and swelling possibly in response to changes in extracellular [Ca^{2+}], as is the case with human cervical mucins. Ca^{2+} is thought to neutralise the negative charges of the mucins and hence reduce repellance leading to inhibition of swelling. The swelling of mucins occurs explosively indicating that as Ca^{2+} is released from the granule the negative charges of the mucins are no longer shielded and therefore repel each other leading to the expansion and release of the secretory product (Espinosa *et al.*, 2002).

In the marine environment, extracellular Ca^{2+} is involved in the cross-linking of marine biopolymer mucilages such as alginate (Kohn, 1975), diatom extracellular polymeric substances (EPS) (Cooksey & Cooksey, 1986) and the tube cement of sabellariid polychaetes (Stewart *et al.*, 2004). Alginates from algae are hydrocolloids with a helical structure held together by Ca^{2+} or H^{+} ions to provide rigidity (Verdugo *et al.*, 2004). Calcium is also thought to decrease electrostatic repulsion by neutralisation of the electrical double layer during bacterial cell adhesion to a negatively charged substratum such as a hydrophobic surface (Geesey *et al.* 2000).

1.6 Calcium entry into the cell and measuring cytosolic calcium

1.6.1 Ion channels

Ion channels are membrane proteins that form transmembrane pores across cell membranes and allow the downhill transport of ions from high to low concentration. Channels exist in various states of activity – open, closed and partially conductant. There are specific stimuli that can promote either the open or closed state. Depending on which stimuli the channel responds to, ion channels can be classified into three categories (Ghazi *et al.*, 1998):

1. Voltage-dependent channels – channels that are sensitive to a change of voltage across the membrane.

2. Ligand-dependent channels – channels that are sensitive to the binding of a ligand.

3. Mechanosensitive channels – channels that are sensitive to mechanical stress on the membrane.

1.6.2 Calcium channels

Plant cells appear to differ from animal cells in that Ca^{2+}-permeable channels rather than Ca^{2+}-selective are predominant (Hetherington & Brownlee, 2004). Using molecular data plant plasma membrane Ca^{2+} channels have been broadly classified as nonselective cation channels (Hetherington & Brownlee, 2004), that is they show little selectivity between different cations. The most well characterised channels are:

1. Depolarisation-activated – transduce general stress-regulated signals.

2. Hyperpolarisation-activated – appear to be stretch-activated and hence transduce mechanical stresses. Involved in polarised cell growth and cell signalling (White, 2000).

Characterisation of Ca^{2+} channels has been made in the green unicellular alga *Chlamydomonas* which is closely related to *Ulva*. This organism possesses a visual system that can respond to light via its absorption by the photoreceptor rhodopsin which in turn signals to the flagella to modify the beating pattern (Harz *et al.*, 1992). The photoreceptor signal transduction pathway in *Chlamydomonas* is illustrated below (Harz & Hegemann, 1991):

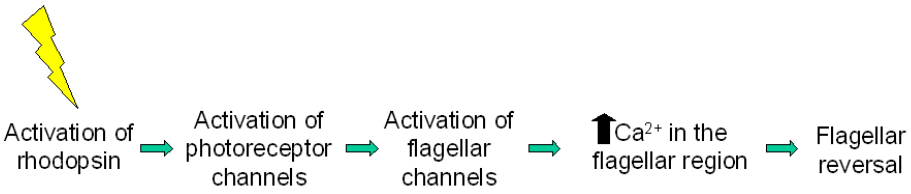

Using the suction pipette technique where a cell is loosely held in a patch pipette with a seal resistance of ~250 MΩ, three specific photocurrents were detected upon light stimulation (Holland *et al.*, 1996) that are largely carried by Ca^{2+} (Nonnengässer *et al.*, 1996).

1) A transient current localised in the eyespot termed the photoreceptor current (P).

2) A transient current localised in the flagella termed the fast flagellar current (F_F).

3) A slow flagellar current (F_S).

Three Ca^{2+} channel populations have been discovered that carry the three types of photocurrent (Nonnengässer *et al.*, 1996).

1) P channel – closely coupled to and activated by the light receptor chlamyrhodopsin. This Ca^{2+} channel is unspecific as it also carries K^+, NH^{4+} and Na^+. At high light intensity the P current activates the voltage-activated F_F channels.

2) F_F channel – voltage-activated and the current is carried purely by Ca^{2+}.

3) F_S channel – voltage-activated and carries K^+ in addition to Ca^{2+}. The Ca^{2+} influx that leads to the F_S current is accompanied by an efflux of K^+ which controls the membrane potential. The low amplitude of the F_S current is a result of Ca^{2+} induced down-regulation of the flagellar Ca^{2+} channels.

There are many Ca^{2+} channel inhibitors and Ca^{2+} chelators such as BAPTA (1,2-bis(o-aminophenoxy)ethane-N,N,N', N'-tetraacetic acid) that buffer changes in $[Ca^{2+}]_{cyt}$ which have been used successfully in plants and algae. However their use in the *Ulva* zoospore when investigating settlement requires caution, as the flagella require Ca^{2+} to move hence by stopping Ca^{2+} entering the flagella the zoospore will be unable to swim and therefore cannot settle.

1.6.3 Mechanosensitive channels

As sensing of the substratum and physical contact of the spore with the surface is an important process in settlement (Callow *et al.*, 1997; Callow & Callow, 2000; Callow *et al.*, 2002) it is possible that mechanosensitive channels may be involved in triggering settlement.

Mechanosensitive (MS) channels are ion channels that are activated by mechanical stress at the cell membrane allowing various ions including Ca^{2+} to enter the cell. In plants, the displacement of the MS channel due to membrane deformation is thought to cause it to be open or closed (Cosgrove & Hedrich, 1991). MS channels can be activated when separated from the membrane hence activation is not dependent on cytosolic messengers or insertion of channels from the cytoplasm (Ghazi *et al.*, 1998). MS channels allow the regulation of $[Ca^{2+}]_{cyt}$ in response to varied mechanical and osmotic stimuli (Taylor *et al.*, 1996) such as the detection of touch, proprioception (the ability to sense position, location, orientation and movement), gravitropism and thigmomorphogenesis (the effects of mechanical stress) (Ghazi *et al.*, 1998).

MS channels appear to be widespread in flagellate algae with *Chlamydomonas* (Yoshimura, 1998) and *Spermatozopsis similis* (Kreimer & Witman, 1994) possessing MS channels in the plasma membrane and flagella. There is a lack of highly specific inhibitors of MS channels (Ghazi *et al.*, 1998). Gadolinium (Gd^{3+}) is said to be a general non-competitive inhibitor of MS channels shortening the opening time and hence preventing elevation of localised $[Ca^{2+}]_{cyt}$ (Ohata *et al.*, 2001). Gadolinium has been used in *Chlamydomonas* to block MS channels activated by applying negative pressure to the cell whilst held in a loose patch-clamp configuration (Yoshimura, 1996; Yoshimura, 1998).

1.6.4 Measuring cytosolic calcium using fluorescent indicators

There are three main categories of techniques used to measure submicromolar levels of $[Ca^{2+}]$ in living cells: Ca^{2+}-sensitive microelectrodes, fluorescent dyes and

luminescent proteins (Read *et al.*, 1993). Each method has its advantages and disadvantages and the choice depends on the biological application.

There is a range of fluorescent dyes available that are highly selective for free Ca^{2+} but vary according to their *viz.*, excitation and emission spectra, quantum yields (ratio of photons absorbed to photons emitted through fluorescence), affinity for free Ca^{2+} and cell permeability. Calcium dyes exhibit an increase in fluorescence emission intensity upon binding Ca^{2+} and some also show a shift in emission spectra (Haughland, 2002). Acetoxymethyl (AM) esters can load directly into a cell by incubation in the dye medium and become active when processed intracellularly to liberate the Ca^{2+} sensitive indicator (Figure 1-5). This feature can also be a disadvantage as dye can be compartmentalised where it is sequestered into membrane-bound organelles or vacuoles and hence is unavailable to respond to changes in $[Ca^{2+}]_{cyt}$ (Bush & Jones, 1987; Brownlee & Pulsford, 1988).

To avoid compartmentalisation dextran-conjugated dyes are used, as they are membrane impermeant. Being impermeant to the membrane however meant until recently that these dyes had to be microinjected into individual cells. Fortunately, in the later stages of this project a new biolistic technique had become available for delivery of dextran dyes where plant or algal cells are loaded with sub-micron pellets coated in dye (Bothwell *et al.*, 2006). In the present study both AM-ester and dextran Ca^{2+} indicators are evaluated for use in *Ulva* zoospores in Chapter 4.

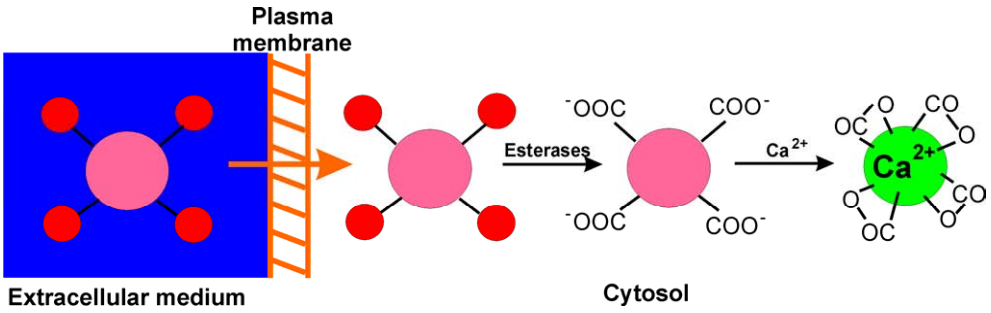

Figure 1-5 Activation of acetoxymethyl-esters. The AM-ester is inactive when in the extracellular medium. The dye is highly lipophilic hence it can pass through the plasma membrane into the cell. Inside the cell the dye is hydrolysed by intracellular esterases trapping it in the cell and making it active to bind Ca^{2+} resulting in an increase in dye fluorescence. The red circles in the figure represent the AM protecting groups and the large central circle represents the fluorescent dye core. Adapted from http://www.sct.ub.es:802/Tutorial/dyes/fluorescentdyes3.htm.

1.7 Diatoms as a system for studying detection of a substratum

Diatoms are unicellular algae that are omnipresent in aquatic environments. They consist of a protoplast surrounded by an elaborately ornamented silica cell wall termed the frustule. Diatoms are a group of great diversity (as many as 100,000 species are thought to exist (Round *et al.*, 1990)) and ecological significance because of their key role in the food web in aquatic environments. They are thought to be responsible for nearly 40% of marine primary productivity (Falkowski *et al.*, 1998). In addition to their important role in the environment they are also of important economic interest due to their role in biofouling. Diatoms are the most frequent and successful microalgal foulers of submerged artificial structures (Wetherbee *et al.*, 1998).

Raphid diatoms are the most common early algal colonisers of substrata in seawater (Wetherbee *et al.*, 1998) where they form the primary biofilm together with bacteria and other algae. Raphid diatoms lack flagella and move and adhere to a surface only through the secretion of EPS from a slit called the raphe. Initial adhesion is an active process requiring adhesion mechanisms to be activated to allow binding to the substratum (Wetherbee *et al.*, 1998). Initial adhesion differs from permanent adhesive structures such as pads, stalks and films in that energy is not continually required to maintain permanent attachment. Diatoms with permanent adhesive structures however are still able to release if environmental conditions degenerate (Wetherbee *et al.*, 1998). Once attached to a surface, the cells divide rapidly and the colony forms a biofilm that can reach a thickness of 0.5 mm.

The raphid diatoms *Seminavis robusta* Danielidis & D. G. Mann[2] and *Craspedostauros australis* Cox[3] (Figure 1-6) are used in this project. Both species look quite different when they are lying on their girdle from when they are lying on their raphe (see Figure 1-6). The cells can only move when their raphe side is in contact with the surface. If a cell lands on its girdle it is able to reorientate itself onto its raphe within 1-2 min by rocking itself on tethers produced from the raphe that connect the cell and the substratum (Higgins *et al.*, 2003). The structure of a diatom is analogous to that of a petri dish with two overlapping valves – one larger than the other – connected by girdle bands (Figure 1-6). The epitheca is the larger, older valve and the hypovalve is the smaller, younger valve. The frustule (cell wall) is composed of silica (SiO_2). The chloroplasts in the two cells studied occur as bands occupying a significant volume of the protoplast.

[2] *Seminavis robusta* was recently reclassified after previously being assigned to the genus *Amphora* as *A. ventricosa* (DANIELIDIS, D. B., MANN, D. G. (2002). The systematics of *Seminavis* (Bacillariophyta): the lost identities of *Amphora angusta*, *A. ventricosa* and *A. macilenta*. *Eur. J. Phycol.* **37**: 429-448.)

[3] *Craspedostauros australis* was recently reclassified after previously being assigned to the genus *Stauroneis* Ehrenberg (COX, E. J. (1999). *Craspedostauros* gen. nov., a new diatom genus for some unusual marine raphid species previously placed in *Stauroneis* Ehrenberg and *Stauronella* Mereschkowsky. *Eur. J. Phycol.* **34**: 131-147.)

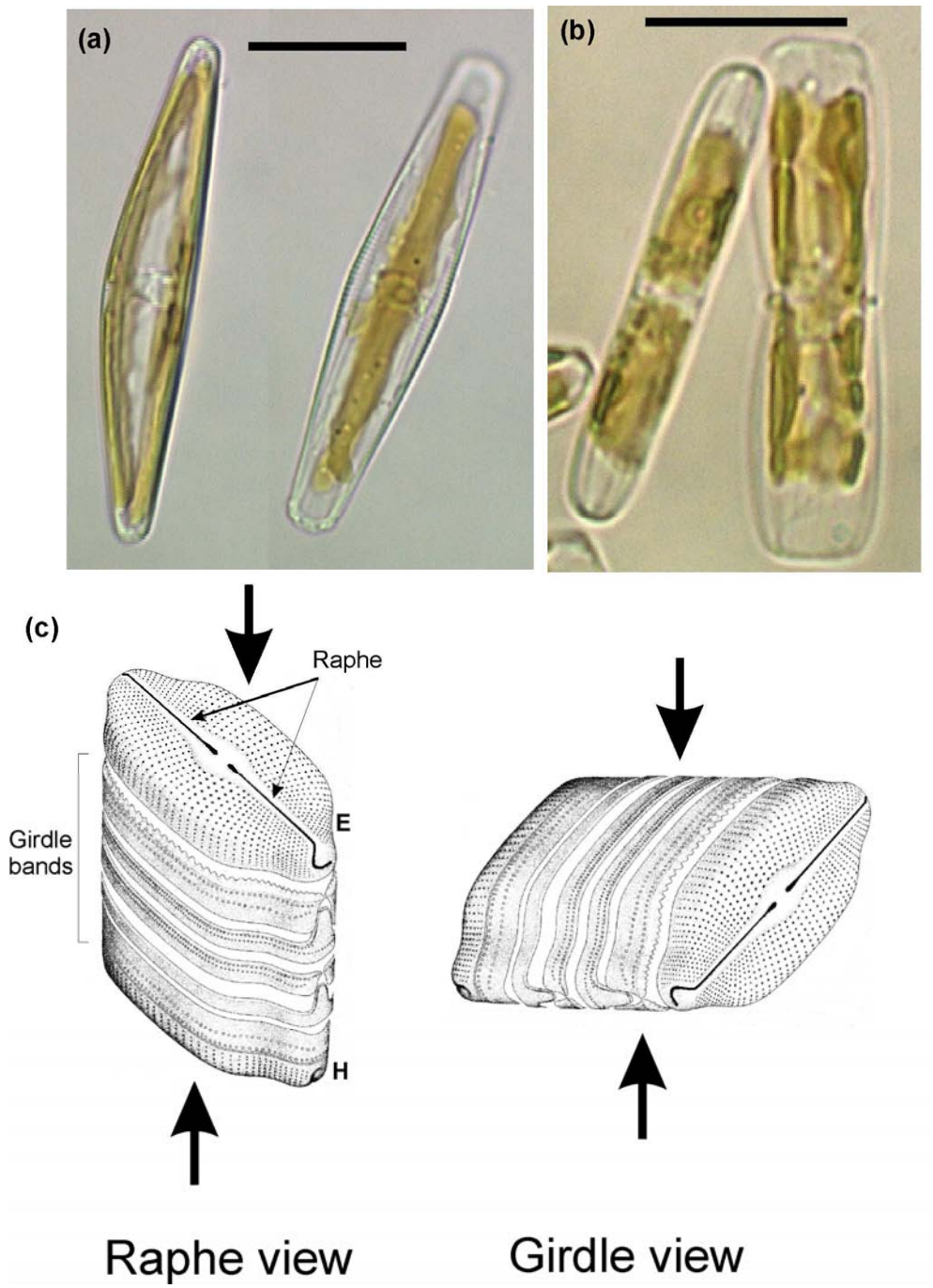

Figure 1-6 Raphe (valve) and girdle views in diatoms. (a) *Seminavis robusta* in raphe (left) and girdle (right) views. **(b)** *Craspedostauros australis* in raphe (left) and girdle (right) views. Bar = 20 µm. **(c)** Exploded view of the frustule of a naviculoid diatom illustrating which part of the cell is seen in raphe (valve) and girdle view. Only in raphe view is the raphe in contact with the substratum and hence able to move. E = epivalve, H = hypovalve. (c) is adapted from Round *et al*. (1990).

1.7.1 Cell and molecular biology in diatoms

Until recently, diatom cell biology has been relatively little studied despite their ecological importance in the oceans of the world. Research has concentrated on ecological aspects and the process of silica cell wall formation hence the techniques required for cellular biology in diatoms remain undeveloped (Scala & Bowler, 2001).

The complete genome sequence of the diatom *Phaeodactylum tricornutum* will become available soon (Lopez *et al.*, 2005) hence it can be used as a model diatom species for functional genomics in addition to the centric diatom *Thalassiosira pseudonana* – the genome of which is already available (Armbrust *et al.*, 2004). Any hypotheses on the existence and function of cell signalling pathways in raphid diatoms made through this project can be tested by the use of knockout genes (the production of deletion alleles at specified gene targets) or overexpression of genes to create transgenic *P. tricornutum. P. tricornutum* has been transformed with nonselectable reporter genes already (Falciatore *et al.*, 1999) as well as the Ca^{2+}-sensitive photoprotein Aequorin (Vardi *et al.*, 2006).

Ideally *P. tricornutum* would have been used for the current studies but the variation in morphotypes and adhesion (Abdullahi *et al.*, 2006) and most importantly its small size (5 µm) do not favour its use as a model for these studies. Hence the significantly larger (50 µm) raphid diatom *S. robusta* was predominantly used for this study.

Wigglesworth-Cooksey & Cooksey (1992) suggest that extracellular signals are responsible for the control of metabolism that leads to cellular adhesion. It has been shown that diatoms possess sensing mechanisms based on changes in $[Ca^{2+}]_{cyt}$ that allow them to perceive changes in the environment such as turbulence, osmotic stress

and dissolved iron levels (Falciatore *et al.*, 2000). With their ability to sense surfaces we hypothesized that diatoms would be able to detect the relative adhesiveness of a substratum. Sensing mechanisms in diatoms have also been shown to involve the production of nitric oxide (Vardi *et al.*, 2006).

1.8 Nitric oxide – a multifunctional molecule

Nitric oxide (NO) is an important molecule in plants and animals with diverse physiological functions. Plants possess the necessary enzymes to produce the freely diffusible NO and it is used as a signalling molecule to mediate plant defence responses against pathogens (Huang *et al.*, 2002). Nitric oxide can have both beneficial and harmful effects on plant cells which is dependent on direct interactions with reactive oxygen species (Van Breusegem *et al.*, 2001). Nitric oxide possesses an unpaired electron that readily interacts with $O_2^{\bullet -}$ to form peroxynitrite ($ONOO^-$) that can oxidize DNA, lipids and proteins damaging enzyme activity and the cell. However, NO also inhibits pathways causing oxidative damage (Van Breusegem *et al.*, 2001). Studies into NO signalling in plants are in their infancy and there is currently debate over the possible source of production of NO in plants and algae (Crawford *et al.*, 2006; Zemojtel *et al.*, 2006).

Nitric oxide production has been shown to be a common response to stress in plants. However, in addition to this NO has recently been found to transmit a wide range of information in plants, playing a crucial role in growth, reproduction and germination (Delledonne, 2005). The production of NO may be through the enzyme nitric oxide synthase (NOS) (Beligni & Lamattina, 2001). Nitric oxide synthases structurally different from mammalian-type NOS have been reported in several plant species (del Río *et al.*, 2004) although their presence has been debated (Crawford *et al.*, 2006;

Zemojtel *et al.*, 2006). Analysis of the genome sequences of *T. pseudonana* and *P. tricornutum* has revealed a diatom ortholog of the plant NOS (Allen *et al.*, 2006). Another route for the production of NO is through the reduction of nitrite (Beligni & Lamattina, 2001) which has been shown to precede via the enzyme nitrate reductase in *Chlamydomonas* (Sakihama *et al.*, 2002).

A role for NO production has been proposed in *P. tricornutum.* Diatoms can control the population size of their predators by producing anti-proliferative aldehydes such as decadienal when wounded that reduce the hatching success of the eggs of copepods (Miralto *et al.*, 1999). *P. tricornutum* can detect the production of decadienal to induce either cell death to control its own population size or convey immunity to subsequent doses. The second messengers involved in decadienal perception and resistance are NO and Ca^{2+}. Therefore sophisticated systems are found in diatoms for detecting stress using NO.

The production of NO can be monitored using specific fluorescent reporter systems to investigate whether NO is involved in the adhesive mechanism in diatoms. DAF-FM (4-amino-5-methylamino-2',7'-difluorofluorescein diacetate) is a cell-permeant reagent for quantifying low concentrations of NO. The dye is essentially nonfluorescent until reaction with NO to form a fluorescent benzotriazole upon which there is a 160-fold fluorescence increase (Haughland, 2002).

1.9 Aims, hypotheses and objectives of the project

Due to the seasonality of *Ulva* it is necessary to use another alga that can be cultured throughout the autumn and winter. Therefore the project is divided so that Ca^{2+} and membrane dynamics are investigated in *Ulva* zoospores and NO signalling is

investigated in diatoms. *Ulva* was used because both its cell biology and adhesion processes have been well studied.

The first part of the work presented focuses on the cellular activities that occur during the settlement of *Ulva* zoospores. The process of settlement is very rapid and membrane dynamics during this time are of interest – the mass exocytosis of adhesive at settlement must be accompanied by membrane recycling otherwise the plasma membrane will expand. Of particular interest at settlement is whether secretion of the adhesive is Ca^{2+}-regulated. Calcium-regulated secretion has been found in *Fucus* during formation of the cell wall after fertilisation – a similar process to secretion of adhesive in *Ulva*. Another area of interest at settlement is whether cross-linking oxidisable agents are released from spores to cure the adhesive.

The second part of the work presented focuses on the cellular processes that occur when a diatom detects a surface. The strength of attachment in diatoms is related to surface wettability. The detection of environmental changes has been shown to occur in diatoms with NO acting as a messenger. Therefore we decided to investigate whether a signalling response involving NO is triggered in relation to the wettability of the substratum and whether changes in NO production could lead to changes in the strength of adhesion in cells.

Therefore the major objectives of this study are:

1. To investigate membrane dynamics during the settlement process (Chapter 3).
2. To evaluate AM-ester and dextran Ca^{2+} indicators for use in *Ulva* zoospores (Chapter 4).

3. To determine whether changes in cytosolic calcium are involved in zoospore settlement and adhesion (Chapter 4).

4. To investigate whether oxidisable products are released to cure the adhesive and if so, over what timescale after settlement (Chapter 5).

5. To determine if there is any difference in NO production by diatoms showing differential adhesion to surfaces of different wettability (Chapter 6).

6. To determine if manipulating the levels of NO through the use of inhibitors and promoters of NO production affects adhesion properties (Chapter 6).

Two papers are included in the appendices:

1. Thompson *et al.*, 2007. *Plant, Cell and Environment*, **30**, 733-744. Membrane recycling and calcium dynamics during settlement and adhesion of zoospores of the green alga *Ulva linza*.

2. Thompson *et al.* (to be submitted). The role of nitric oxide in diatom adhesion in relation to substratum properties.

2: GENERAL METHODS

2.1 Methods used with *Ulva*

2.1.1 Zoospore release

Ulva linza was obtained from Wembury beach, Devon, England (50º18' N; 4º02' W). Reproductive thalli were collected at the beginning of each week independent of the tidal cycle between March and October of each year. The material was gently squeezed to remove excess water, wrapped in absorbent paper and then kept at 4ºC. Twenty-four hours after collection reproductive white tipped thalli were selected and zoospores released into 0.2 µm filtered seawater (collected offshore by boat, pH 8). Concentration of zoospores was obtained by transferring the suspension onto ice where zoospores gravitated to the bottom of the container (Callow *et al.*, 1997). For all imaging experiments cells were stored on ice to prevent settlement and used within 30 min of release.

2.1.2 Visualising individual zoospores during settlement

The onset of settlement was defined as the point at which the cell stopped moving, appeared more spherical and/or the flagella sheaths were discarded and the axonemes absorbed into the cell (Callow *et al.*, 1997). Two approaches were used in order to monitor fluorescent signals during zoospore settlement. Firstly, zoospores tended to undergo settlement preferentially at the air-water interface of small air bubbles attached to the coverslip. This provided a convenient method for monitoring settlement of many cells in the same orientation and plane of focus. Small air bubbles were formed on the base of the viewing dish by applying positive pressure to an air-filled micropipette with the tip close to the base of the dish. On addition of zoospores,

the edge of the bubble became rapidly populated with zoospores as they explored and settled around the air-water interface (see Figure 3-1c). Zoospores were also observed to settle spontaneously on the glass coverslip albeit with a lower frequency than around an air bubble.

In the second approach, groups of cells were stimulated to undergo simultaneous settlement at the gelling temperature (24-28^{o}C) of 2% low melting point agarose (RESolve, Geneflow Ltd. UK) prepared in filtered seawater (seawater at 24-28^{o}C alone, had no effect on settlement). Reize and Melkonian (1989) embedded various flagellated species in ultra-low gelling agarose and cellular function was preserved for days. The agarose does not interfere with fluorescence microscopy as it does not exhibit autofluorescence (Reize & Melkonian, 1989). Twenty µl of molten agarose were added to 40 µl of cells (resulting in a 1% agarose solution) loaded either with FM 1-43 or Ca^{2+} indicator dye.

In both approaches described above, individuals and groups of zoospores were imaged with a BioRad 1024 confocal laser scanning inverted microscope equipped with a krypton/argon laser and a x60 (NA 1.4) oil immersion objective (Nikon, Kingston upon Thames, UK) or a BioRad Radiance 2100 confocal laser scanning upright microscope. For imaging cells on an inverted microscope, cells were placed in small Petri dishes with a glass coverslip base. For imaging with an upright microscope, cells were either placed in Petri dishes for viewing with a water-immersion x40 (NA 0.8) objective (Nikon), or placed in a cavity slide with a coverslip (allowing cells to swim freely) when an oil objective was used. Sequences of images were acquired using TIMECOURSE software (BioRad).

2.2 Extraction of chlorophyll a using DMSO

To determine chlorophyll a concentration of diatoms, chlorophyll was extracted in DMSO (Shoaf & Lium, 1976) and quantified using the equations of Jeffrey and Humphrey (1975). 5 ml aliquots of diatom suspension was filtered through 25 mm diameter cellulose nitrate membrane filters (Whatman, Middlesex, UK) with a pore size of 3 µm. Membranes were immersed in 5 ml of DMSO solvent and placed in the dark for 1 h. The vials were agitated by hand and then left for 5 min to allow debris to settle. Supernatants were transferred to semi-micro cuvettes. The absorbance of the sample was determined at 664 and 630 nm using an LKB Novaspec II spectrophotometer. Chlorophyll a concentrations were calculated using the formulae:

$$[\text{Chl a } \mu g\ ml^{-1}] = 11.47\ (A_{664}) - 0.4\ (A_{630})$$

2.3 Fluorescence and confocal laser scanning microscopy

Fluorescence occurs when a molecule absorbs light which excites electrons into higher energy orbitals. Some energy is lost as these electrons revert to their original energy state and the molecule then emits a photon with lower energy resulting in a shift in wavelength emission. Epifluoresence microscopy separates the wavelengths of the excitation light source and the emitted fluorescence by using a dichroic mirror that allows the longer wavelength emitted light to pass. A limitation of standard fluorescence microscopy is blurring of the fluorescent image as the microscope objective collects light from out-of-focus regions as well as from the plane of interest.

The confocal laser scanning microscope (CLSM) greatly reduces this problem by blocking light from above and below the plane of focus using a confocal aperture so that only light from the region of interest is visible. The field of illumination is limited

to a pinhole of light that scans the specimen. A photomultiplier tube detects the intensity from each point producing a complete image (Figure 2-1). The lack of out-of-focus light results in an increase in contrast and sharpness giving a clearer visualisation of labelled materials (Gilroy *et al.*, 1993). CLSM results in a 60% improvement in horizontal resolution over wide-field microscopy. Using a x60 objective (NA 1.4) lateral resolution of 0.15 µm can be achieved using CLSM (Pawley, 1995). In addition, there is improved vertical resolution i.e. a shorter depth of field due to the CLSM's optical sectioning abilities. Using a x60 objective (NA 1.4) axial resolution of 0.58 µm can be achieved using CLSM (Pawley, 1995).

It is also possible to carry out simultaneous imaging at different emission wavelengths allowing ratio imaging concurrent with the collection of transmitted light bright field images. Simultaneous imaging is essential with motile cells which are difficult to view using conventional epifluorescence microscopy as filter changes are required to move between transmission and fluorescent images resulting in time delays between the images.

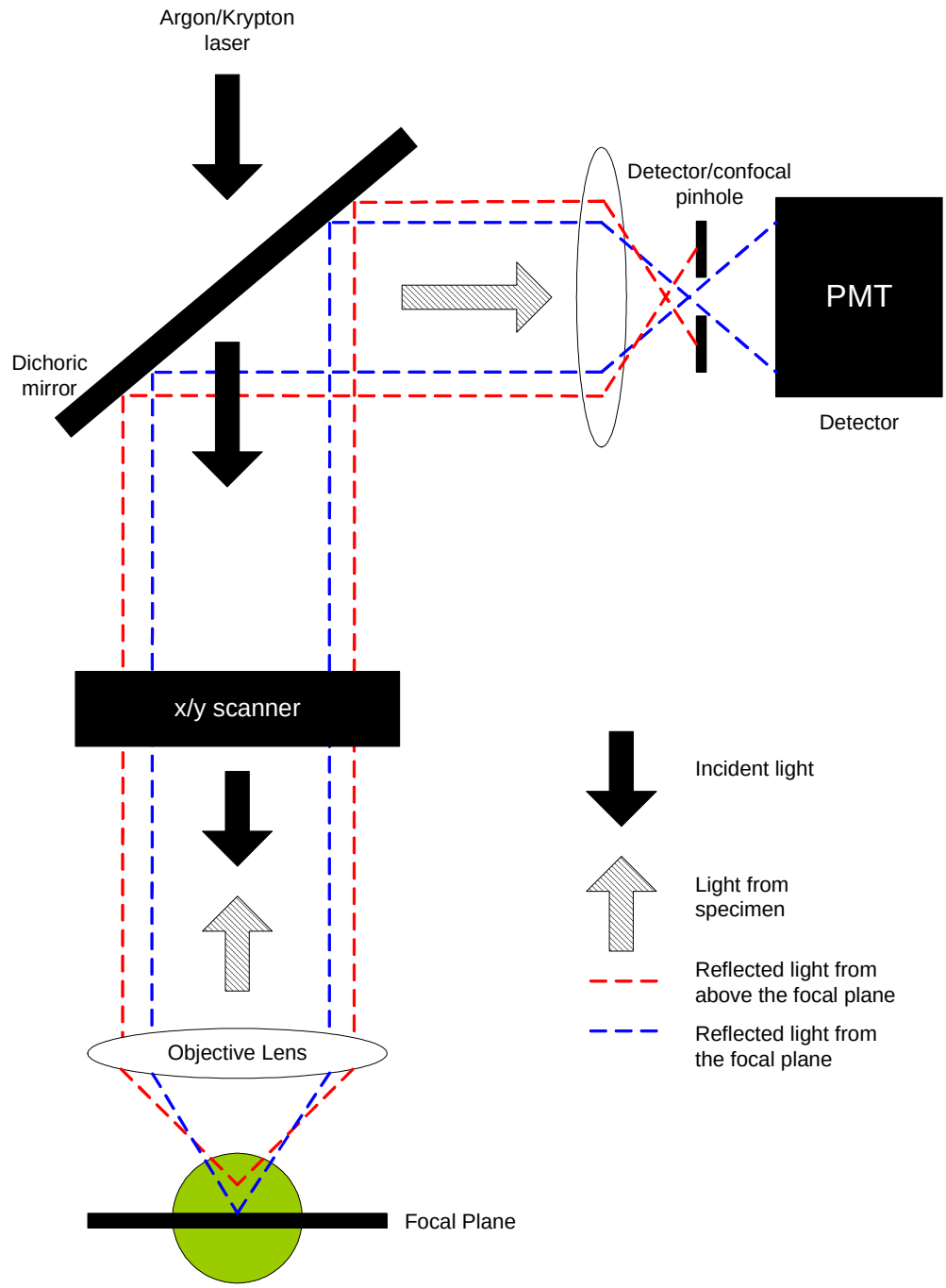

Figure 2-1 Diagram of a confocal laser scanning microscope system. Light from above or below the focal plane is filtered out by the confocal pinhole.

In addition to the major advantages of CLSM given above there are some other benefits:

1. The use of a zoom facility means that variable magnification is possible using the same objective, which aids real-time visual analysis. This is especially important when imaging such small objects as spores. The x60 (NA 1.4) oil objective offers better resolution than the available x100 (NA 1.3) oil objective but by increasing the zoom, the field of view is reduced and hence the spores appear larger. However, care must be taken as the zoom magnification works by changing the relative pixel size so with a given wavelength and numerical aperture (NA) there will be an optimum zoom setting. Increasing the zoom too much will result in a loss of resolution giving a pixelated image. In addition at higher zoom factors, the same laser intensity is used to illuminate a smaller area hence the rate of photobleaching will be greater.

2. CLSM produces a digitised image that can be processed by a computer allowing the measurement of fluorescence intensity. Brightness is recorded as 256 grey levels and hence comparison of fluorescence intensity can be made. Stable illumination from a laser source is required for accurate measurement of photons – a mercury light source as used in most epifluorescence microscopes will undergo minor fluctuations resulting in inaccurate measurements.

3. The wavelength of illumination can be selected precisely by choosing the correct laser. However, this can also be a disadvantage as the available laser lines can restrict the dyes that can be used.

2.3.1 Depth of field

The most common depth of field used in this project was ~1 µm. The depth of field is defined by the numerical aperture of the objective and the size of the confocal pinhole. It is possible to record at depths of field lower than 1 µm (down to 0.85 µm) using the available confocal and a x60 (NA 1.4) objective at the optimum iris setting which would improve the axial resolution but there were insufficient photons reaching the photon multiplier tube (PMT) and the fluorescence signal became too weak when the pinhole was reduced in size.

In confocal imaging, cells are generally fixed to a coverslip so that changes in time over an area can be measured (Kirkman-Brown *et al.*, 2000). Methods described in section 2.1.2 were used to alleviate issues due to movement. An example of confocal imaging on a non-fixed but attached living organism can be found in Stricker *et al.* (1992). They show that a flatter sea urchin egg exhibits less of a difference in relative fluorescence increase between the cortex and the centre than is seen with a more spherical egg, presumably because there is less difference in path length in a flatter egg. The path length is affected when a spore adheres to a surface as it changes from pear-shaped to spherical (Callow *et al.*, 1997). Consequently an important issue for Ca^{2+} imaging was being able to use ratio imaging to prevent changes in shape resulting in changes in fluorescence (see Chapter 4).

2.4 Image acquisition and processing

Three digital images could be collected simultaneously. These were 1) fluorescence emission of dye, 2) autofluorescence from the chloroplast, and 3) transmitted light. In cases where two dyes were imaged simultaneously such as with Texas Red-dextran

and Oregon Green BAPTA-1 dextran (Chapter 4) the dye emissions were collected plus the transmission image.

There is a trade-off between image quality and the scanning speed. Motile cells can be captured more easily with a higher imaging speed but the resulting resolution will be poorer and laser damage to the specimen will be greater the more often a field of view is scanned. For diatom cells, which were less motile, images were captured at 50 lines per second to provide resolution suitable for data analysis. For imaging *Ulva* spores a higher rate of scanning speed was required, however, illuminating the sample too frequently prevented settlement. Faster scanning is achieved by reducing the box size hence reducing the number of lines that have to be scanned to produce each image. Images were generally captured as 512 x 512 pixels as this was determined to be the optimum setting for image storage and quality for the size of the field of view scanned. The images generated by a confocal microscope are in .pic format. This format is unreadable by most image analysis programs and therefore pic files were converted to bitmap format using Thumbsplus Pro v7 (Cerious Software Inc., Charlotte, USA).

To enable subtle variations in signal intensity to be detected (such as those seen in Ca^{2+} imaging), greyscale images were converted to false colour using a user-defined look up table (LUT) in Scion Image (Scion Corporation, Frederick, USA). Pseudo-colour results in an increased visible difference between similar pixels (Russ, 1990). Where images showed a poor signal-to-noise ratio spatial smoothing was applied (using Scion Image), which reduced pixelation by replacing the value of each pixel with the weighted average of the surrounding 3 x 3 neighbouring pixels.

3: MEMBRANE RECYCLING DURING SETTLEMENT AND ADHESION OF ZOOSPORES OF THE GREEN ALGA *ULVA LINZA*

3.1 Introduction

Although there is a broad understanding of the cellular events involved in *Ulva* zoospore settlement (Callow *et al.*, 1997; Stanley *et al.*, 1999), detailed information on the cellular mechanisms linking the detection of a suitable substrate and the secretory process is lacking. This chapter presents a study of the dynamics of membrane recycling during the settlement process.

In all eukaryotes, endocytosis of plasma membrane balances exocytosis and is important in regulating cell size, membrane recycling and repair (Marcote *et al.*, 2000). Settlement of *Ulva* zoospores involves rapid and dramatic secretion by exocytosis of adhesive-containing secretory vesicles (Evans & Christie, 1970; Callow *et al.*, 1997). Plasma membrane recycling is required in order to balance this exocytosis. Membrane recycling can be monitored either through optical or electrochemical methods (see Chapter 5). Fluorescent styryl dyes such as FM 1-43 can be used to view exocytosis and endocytosis of single vesicles using Total Internal Reflection Fluorescence microscopy (see Chapter 1, section 1.4.2) or can be used to view membrane recycling at a whole cell level. For this study, FM 1-43 was used to visualise membrane dynamics in zoospores undergoing settlement. This lipophilic dye partitions strongly into plasma membranes from the external solution, resulting in fluorescent labelling of the plasma membrane (Cousin & Robinson, 1999). Moreover, it does not partition into the cytosol or diffuse across the plasma membrane due to its

Field Code Changed

two highly charged nitrogen atoms (Betz & Bewick, 1992). Appearance of dye fluorescence in the cell interior is therefore a robust marker for the internalisation of plasma membrane via endocytosis (Emans *et al.*, 2002). It has found widespread use in a wide range of cell types (Carroll *et al.*, 1998; Parton *et al.*, 2001; Atkinson *et al.*, 2002) and has recently been successfully used in diatoms to visualise the dynamics of membrane internalisation (Kühn & Brownlee, 2005).

3.1.1 Objective

To investigate membrane dynamics during the settlement process in *Ulva* zoospores using the styryl dye FM 1-43.

3.2 Methods

Zoospores were incubated either continuously or for specific times (see below) at 18ºC in the presence of 2 µM FM 1-43 (Molecular Probes, Invitrogen Ltd, Paisley, UK) dissolved in seawater from a 1 mM stock solution in distilled water. For pulse-chase experiments, zoospores were washed twice by centrifugation (400 g for 1 min) in 1 ml of seawater after incubation for 3 min in FM 1-43. FM 1-43 was excited at 488 nm and emission monitored at 522 nm (± 17.5 nm).

To show that intracellular FM 1-43 accumulation was an active process, zoospores were killed by exposure to 4% osmium tetroxide vapour for 5 min and then incubated for 15 min in 2 µM FM 1-43. The relationship between FM 1-43 uptake and cell wall formation (a marker for settlement) was determined by incubating zoospores in both 2 µM FM 1-43 and 0.4 mM Calcofluor White. Calcofluor and FM 1-43 fluorescence was monitored by simultaneous excitation at 405 and 488 nm respectively using the blue diode and argon lasers of a BioRad Radiance 2100 confocal microscope.

Calcofluor emission was monitored at 440 nm. The nucleus was visualised by loading zoospores on ice (to prevent settlement) in 75 µM DAPI (Sigma, Gillingham, UK) prepared from a 30 mM stock solution in artificial seawater. After 15 min DAPI incubation 2 µM FM 1-43 was added to the mixture and zoospores were allowed to settle on a cavity slide. Zoospores were excited simultaneously at 405 and 488 nm with DAPI emission collected at 460 nm using a Nikon x40 oil objective (NA 1.0).

3.3 Results

3.3.1 Membrane labelling in the presence of FM 1-43

When 2 µM FM 1-43 was added to swimming zoospores, labelling of the plasma membrane alone was observed within 3 min, with little evidence of dye internalization (Figure 3-1a). At higher concentrations of FM 1-43, labelling of the flagellar sheath could also be seen (Figure 3-1b). In settling spores, rapid membrane internalisation of labelled plasma membrane occurred resulting in a discrete localized intracellular accumulation of dye within 1 min of commitment to settlement (Figure 3-1b-d, see also Figure 3-2). Loss of flagella in Figure 3-1b indicates that the cell has committed to settlement and this coincides with the intracellular accumulation of labelled plasma membrane. The internalised dye was located in the anterior region of the cell from where the adhesive vesicles are released (Figure 3-1d). Incubation in Calcofluor White (CFW) used as a marker for cell wall formation confirmed that spores exhibiting rapid membrane internalisation had all undergone settlement. After 30 min incubation with CFW all spores that had internalised spots of FM 1-43 fluorescence (n = 37) were co-labelled with CFW (Figure 3-1e). To exclude the possibility that FM 1-43 was labelling the cell nucleus, which is a similar size to the FM 1-43-positive spot, cells were loaded with the nuclear dye DAPI. No co-

localisation of DAPI and FM 1-43 was observed in settled zoospores (n = 12, Figure 3-1f). Control experiments using spores inactivated by fixation with osmium vapour showed no chlorophyll fluorescence and no membrane labelling by FM 1-43 (data not shown).

Settling cells exhibited higher FM 1-43 fluorescence at the anterior end of the spore just prior to rapid membrane internalisation (Figure 3-2 and Figure 3-3). This was apparent within 15 s of the cell beginning to change from elongated to a more spherical shape. Within 30 s a spot of FM 1-43 fluorescence was visible in the cell interior (Figure 3-2), reaching maximum size and intensity around 75 s after the initial cell shape change. Immobilization of cells in low melting point agarose induced a slower settlement response – 3-4 min for complete rounding up of the cells compared to 1 min in free swimming cells. As the settlement response proceeded, formation of the internal FM 1-43 spot could be visualised simultaneously in many cells in one field of view over several minutes (Figure 3-3).

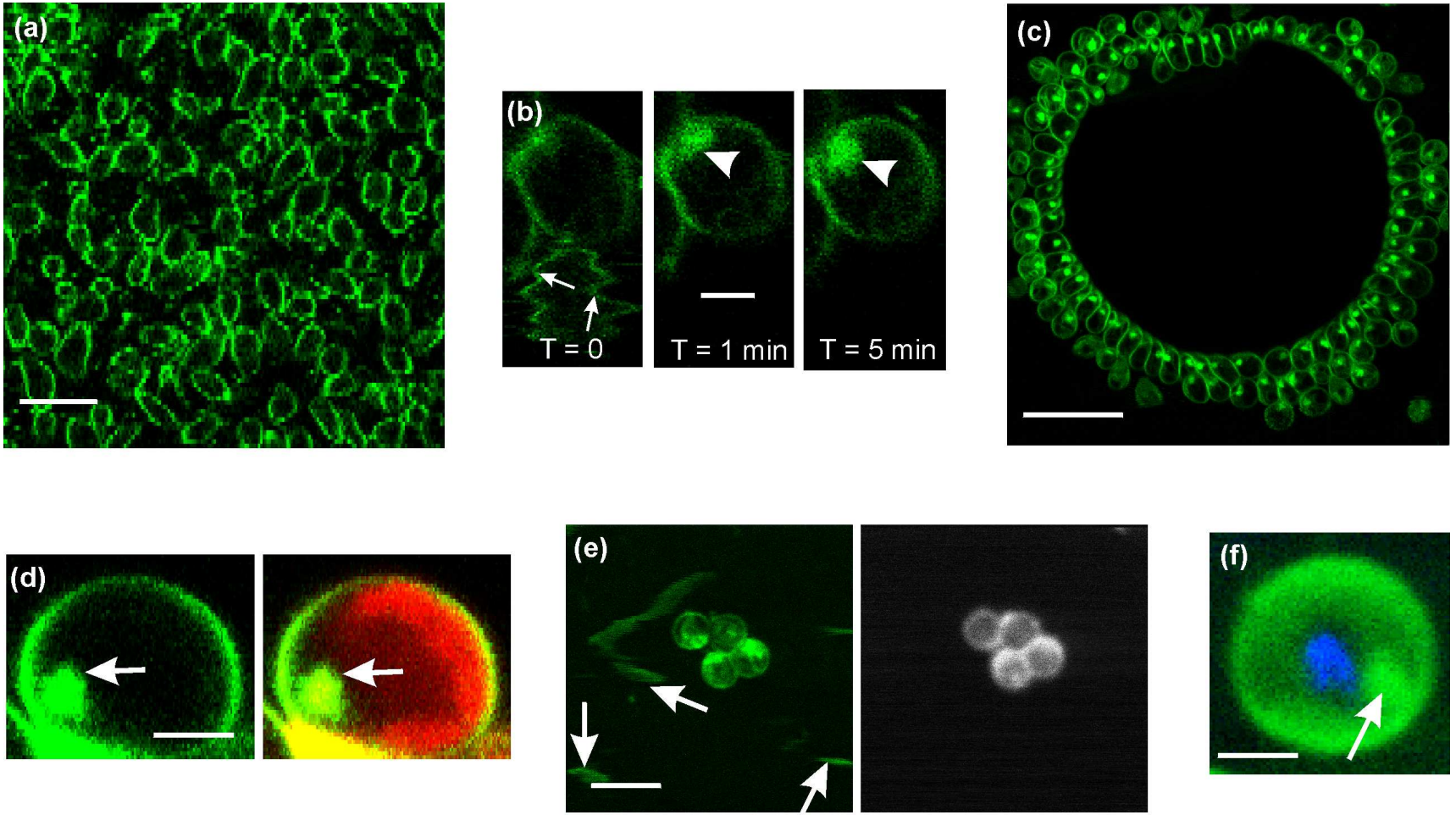
(a)
(b)
T = 0
T = 1 min
T = 5 min
(c)
(d)
(e)
(f)

Figure 3-1 Localisation of FM 1-43 labelling in swimming and settled zoospores. (a) Confocal images of swimming zoospores incubated in the presence of FM 1-43 for 3 min. The distorted lines indicate that the cells are moving. Only the plasma membrane is labelled with FM 1-43. Bar = 10 µm. **(b)** A settling zoospore incubated with 4 µM FM 1-43 in which the flagella are labelled at t = 0 (arrows). One minute later the flagella have been lost and a spot of internalised dye (arrowheads) has formed at the anterior region becoming more pronounced after 5 min. Bar = 2 µm. **(c)** Zoospores incubated in the presence of FM 1-43 for 15 min that have settled around an air bubble. All settled zoospores have an interior cytoplasmic spot of FM 1-43 fluorescence. Bar = 20 µm. **(d)** The dual-colour image (right) of the same cell shown in Figure 3 shows chlorophyll autofluorescence (red) and FM 1-43 fluorescence (green). It can be seen from the position of the chloroplast (red) that the spot of internalised dye (arrows) is situated at the anterior of the cell. **(e)** Calcofluor White (CFW) loading of spores (left: FM 1-43, right: CFW). CFW only labels settled cells with a cell wall and only cells that are immobile with internalised dye are labelled with CFW. Swimming cells can be seen (moving fast) labelled with FM 1-43 (arrows) but are not labelled with CFW. Bar = 10 µm. **(f)** Dual labelling of a settled zoospore with DAPI (blue) and FM 1-43 (green) shows the separate location of internalised FM 1-43 (arrow) and the nucleus. Bar = 2 µm.

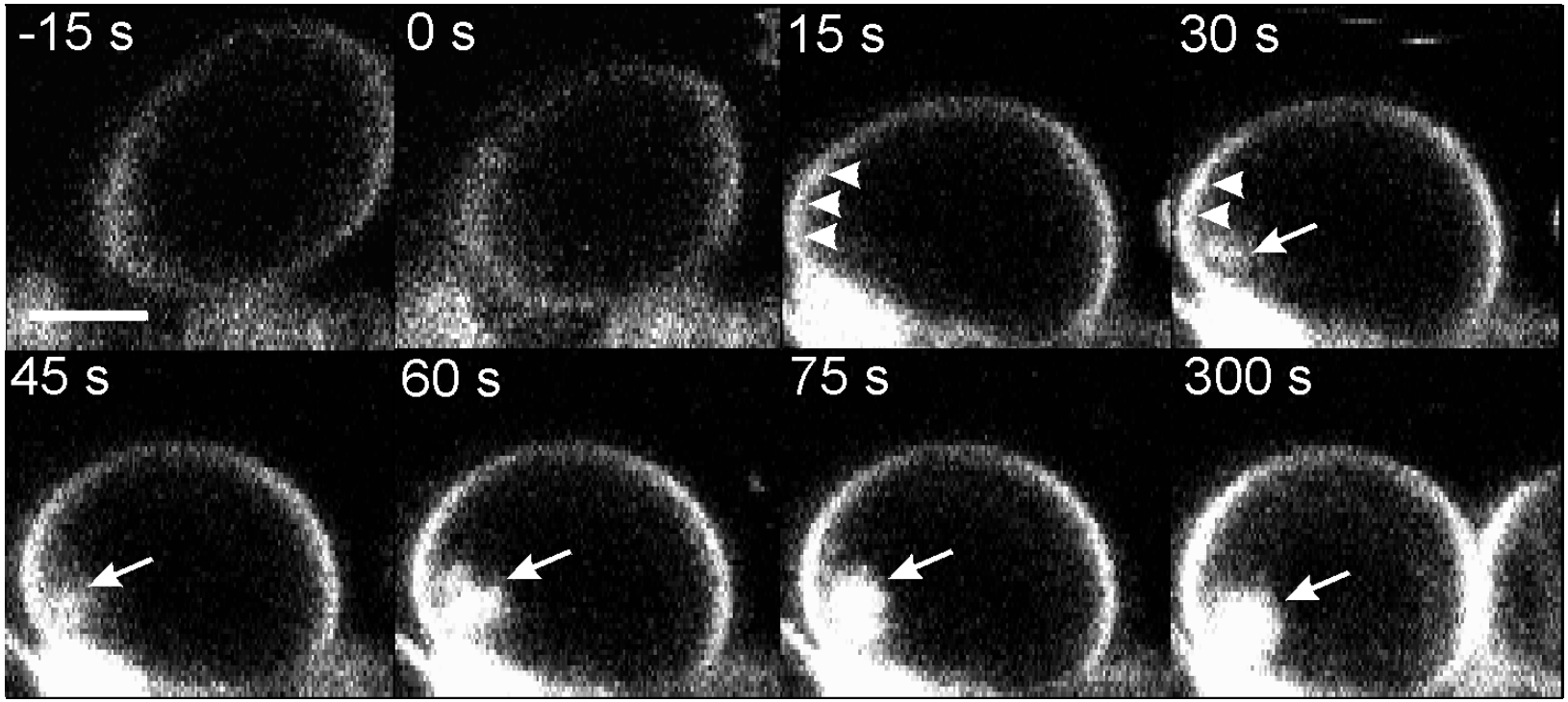

Figure 3-2 Time course of confocal images of an FM 1-43 labelled zoospore undergoing spontaneous settlement. The initial image shows the zoospore 15 s prior to commitment to permanent adhesion at 0 s as seen by the spore beginning to round up and the lack of movement. The development of a spot of FM 1-43 fluorescence (arrows) to full size was apparent 75 s after permanent adhesion. Increased fluorescence was also apparent at the cell anterior at 15 and 30 s (arrowheads). The bright fluorescence seen below the cell from 15 s onwards and adjacent to the cell at 300 s is due to the presence of adjacent spores moving into view. Bar = 2 µm.

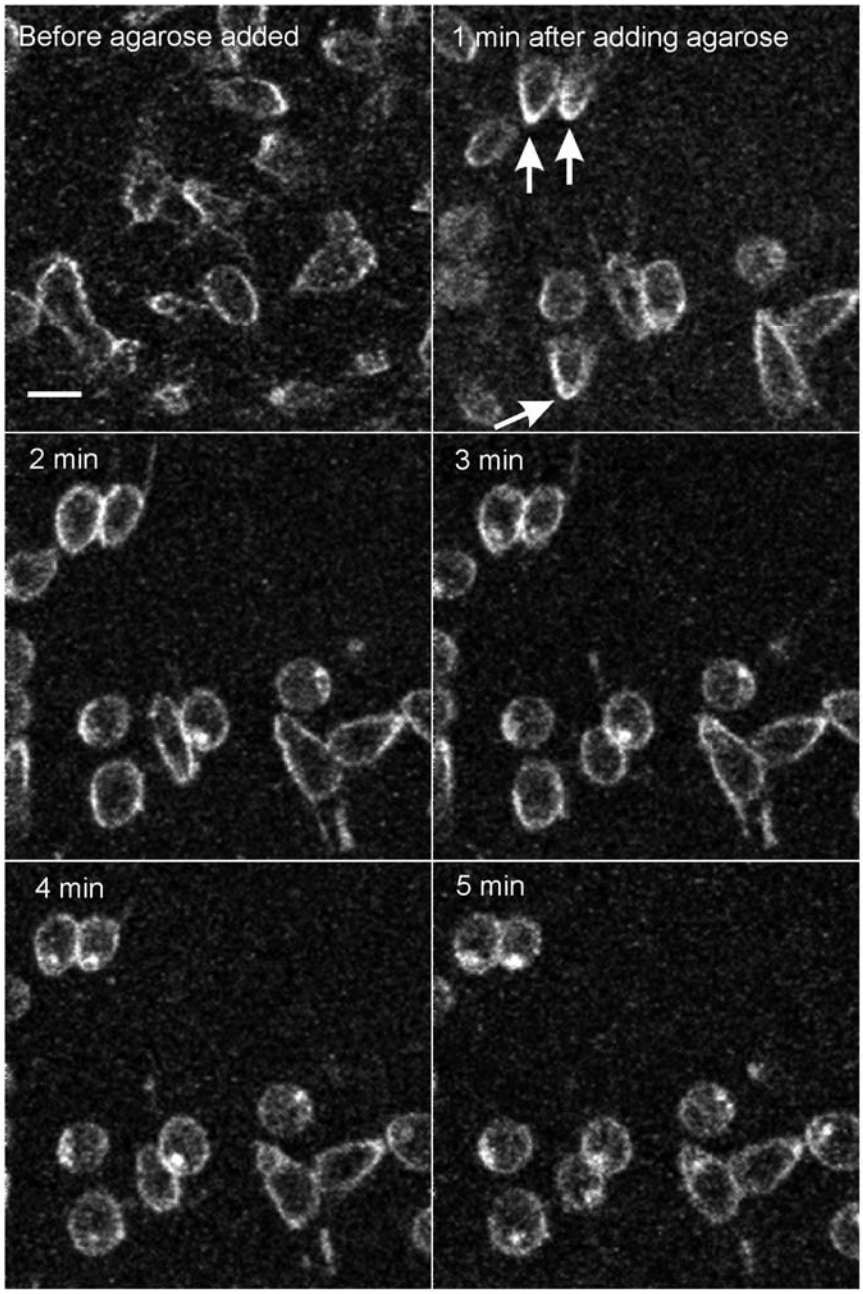

Figure 3-3 Time series of cells settling after addition of low melting point agarose to zoospores loaded with FM 1-43. Before the agarose was added the cells were all swimming with no settled spores visible in the field of view. 1 min after agarose addition the cells are immobilised and 80% of cells have undergone a settlement response after 5 min (as indicated by spot of interior FM 1-43 fluorescence). The pre-settlement increased fluorescence at the cell anterior was particularly apparent at 1 min in three cells (arrows). Note in the subsequent images the typical dye internalisation on settlement in these three cells. Bar = 5 µm.

3.3.2 Membrane labelling in pulse-chase experiments

Because the binding of FM 1-43 to a membrane is reversible, the dye can be rapidly removed from the plasma membrane by washing cells (Ryan *et al.*, 1996) and without the presence of FM 1-43 in the external medium, internalised labelled plasma membrane is replaced by new unlabelled membrane. This allows internalised membrane to be visualised in the absence of the strong signal from the plasma membrane. Cells were therefore pulse-labelled with FM 1-43 for 3 min before removal of the dye and incubation in unlabelled filtered seawater for 15 min. Following this procedure, the intracellular distribution of FM 1-43 revealed general labelling of internal membranes in both swimming and settled cells (Figure 3-4a and b).

Unlike the rapid dye internalisation observed at zoospore settlement in the presence of external FM 1-43, only gradual accumulation of label inside the cell after the removal of FM 1-43 was observed. The intracellular uptake of FM 1-43 label in the pulse-chase experiments suggests constant steady-state turnover of plasma membrane. The intense rapid FM 1-43 labelled spot observed in the anterior region of settled cells could arise either from redistribution of previously labelled intracellular membrane or direct cycling from the plasma membrane. However, in previously pulse labelled zoospores a bright spot of FM 1-43 was not observed on settlement in the absence of external FM 1-43. The bright internalised FM 1-43 spot was only ever observed in pulse labelled zoospores after the re-addition of FM 1-43 (Figure 3-4c).

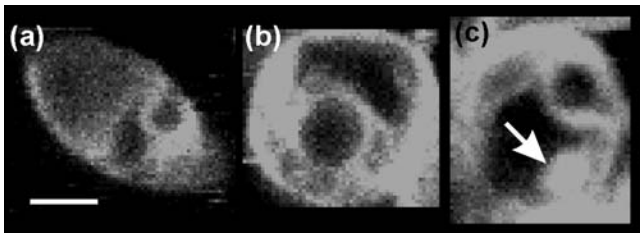

Figure 3-4 Confocal images of membrane recycling in *Ulva* zoospores after a brief incubation with FM 1-43 followed by 15 min incubation in unlabelled seawater. (a) When swimming zoospores were exposed to a 3 min pulse of FM 1-43 and then washed, diffuse internal labelling of membranes was seen after 15 min. **(b)** When cells were subsequently followed undergoing settlement in the absence of FM 1-43, the diffuse internal labelling was still present as in the swimming zoospore but the localised spot characteristic of settlement in cells that settled in the presence of external FM 1-43 (Figure 3-1 to 3-3) was not seen. **(c)** When FM 1-43 was re-added to the medium, cells that had previously been given a pulse of FM 1-43 showed both labelling of internal membranes and developed a localised spot of FM 1-43 (arrow) upon settlement. Bar = 2 µm.

3.4 Discussion

In the absence of cell size increase, mass vesicle release must be balanced by mass membrane retrieval during zoospore settlement otherwise the plasma membrane will expand (Samuels & Bisalputra, 1990). In this study, the styryl dye FM 1-43 was used to investigate membrane recycling during settlement. This approach showed that the plasma membrane is dynamically recycled to a specific intracellular region as evident from the concentrated spot of intracellular FM 1-43 staining seen in settled spores. A number of studies have used FM-dyes to follow endocytosis in plant cells (Carroll *et al.*, 1998; Kubitscheck *et al.*, 2000; Ueda *et al.*, 2001; Emans *et al.*, 2002; Meckel *et al.*, 2004) and less commonly in algal cells (Belanger & Quatrano, 2000; Kühn & Brownlee, 2005). Intracellular FM 1-43 labelling indicates that internalisation of the plasma membrane occurred both in swimming and settling zoospores. However, while slow label internalisation occurred over long periods in swimming zoospores, the lack of rapid localized FM 1-43 internalisation indicates that mass endocytosis does not occur during swimming. Hence the localised rapid FM 1-43 labelling of settled spores means that it can be used as a fluorescent marker for settlement. The possibility that the internalised spot of FM 1-43 fluorescence represents flagella retracted during settlement can be eliminated since although the flagella sheaths are labelled with FM 1-43 it is only the axoneme that is withdrawn into the cell, the flagella membranes being shed into the extracellular medium during settlement (Callow *et al.*, 1997).

It is proposed that the initial increase in FM 1-43 fluorescence at the anterior of the cell (see Figure 3-2 & Figure 3-3) is a result of rapid secretion. Such localised brightening may reflect transient increase in membrane that is accessible to dye

labelling as the rate of vesicle fusion locally increases the membrane surface area prior to the onset of membrane retrieval.

Experiments in which zoospores were observed to settle in the presence or absence of external FM 1-43 revealed that the localized internalisation of FM 1-43 label typical of settling spores was only seen when FM 1-43 was continually present in the medium and thus represents dynamic accumulation of FM 1-43 in an endomembrane compartment. In non-settling spores there was only a gradual accumulation of label inside the cell after the removal of FM 1-43. There are two possible reasons why only cells that are undergoing settlement show localised intracellular accumulation: 1) there may be a specialised pathway for membrane retrieval during settlement where recycled membrane is taken to an endosomal compartment; or 2) there may be an accumulation of (labelled) plasma membrane resulting in a "bottleneck" in the membrane recycling pathway. It is proposed that on removal of FM 1-43 from the bath the constant replenishment of FM 1-43 to the plasma membrane is prevented and the rapid plasma membrane internalisation on settlement therefore remains undetected.

The discrete spot of FM 1-43 internalisation indicates that recycled membrane is targeted to an intracellular structure not previously shown in published electron micrographs (Evans & Christie, 1970). It is proposed that this compartment is a form of endosome. The existence of endosomes in animals and plants is well documented (González-Gaitán, 2003; Meckel *et al.*, 2004), however their presence in algae has hitherto not been shown. Endosomes are membranous compartments formed as a result of receptor-mediated endocytosis involving coated pits and vesicles. Clathrin forms the protein coat in coated pits and vesicles and facilitates plasma membrane

recovery and vesicle cycling in the endomembrane system (Battey *et al.*, 1999). Endocytosis involving coated pits has been shown to occur in the giant unicellular alga *Ventricaria ventricosa* in response to mechanical wounding (Shepherd *et al.*, 2004). Recent molecular studies of sporulating tissue of *Ulva linza* have revealed expressed sequence tags for a clathrin vesicle coat protein (Stanley *et al.*, 2005). The expression of clathrin genes in tissue containing zoospores is consistent with the evidence given here that targeted membrane retrieval is occurring.

Adhesive secretion occurs in less than 1 min following the onset of zoospore settlement (Callow *et al.*, 1997) coinciding with the development of localized FM 1-43 accumulation within the cell. Membrane internalisation in *Ulva* spores is very rapid in comparison to most other studies of higher plant and algal cells. For example significant FM 1-43 internalisation was apparent only after approximately 30 min in non-secretory cells (see Emans *et al.* (2002); Kubitscheck *et al.* (2000); Kühn & Brownlee (2005); Ueda *et al.* (2001)). Non-secretory maize root cap protoplasts showed much less internalisation of FM 1-43 than actively secreting protoplasts (Carroll *et al.*, 1998). While germinating fungal spores of *Magnaporthe grisea* which are also highly active secretory cells show a similar speed of FM-dye internalisation, showing accumulation of FM 4-64 into small structures ~ 0.4 µm in diameter within 2-4 min of labelling (Atkinson *et al.*, 2002). *Lilium longifluorum* pollen tubes also show high rates of FM-dye internalisation with labelling of small spherical structures at the apex within 1-2 min of staining, presumed to be early endosomes (Parton *et al.*, 2001). The only other published example of plasma membrane recycling at a similar speed in algae is in *Fucus serratus* embryos where hypoosmotic treatment resulted in rapid internalisation of FM 1-43 within 20 s of the shock (Battey *et al.*, 1999). It is

therefore likely that the rapid internalisation in *Ulva* zoospores is closely associated with the rapid secretory characteristics of this cell during settlement.

3.5 Conclusions

This study has identified a robust cellular marker for settlement in *Ulva* zoospores that arises as a result of rapid membrane turnover associated with mass exocytosis and targeted membrane retrieval involving an endosomal-like compartment. This appears to be one of the most rapid membrane dynamics observed to date in a plant or algal cell.

4: CALCIUM DYNAMICS DURING SETTLEMENT AND ADHESION OF ZOOSPORES OF *ULVA LINZA*

4.1 Introduction

In order to improve understanding of the signalling processes involved in the commitment of zoospores to settlement, and the associated secretory processes, the work described in this chapter investigates the potential role of changes in cytosolic calcium ($[Ca^{2+}]_{cyt}$) during settlement.

The regulation of membrane cycling involving the endomembrane system, cytoskeleton and plasma membrane is Ca^{2+}-dependent in plants and animals (Steer, 1988; Battey & Blackbourn, 1993; Barclay *et al.*, 2005). In algae an increase in $[Ca^{2+}]_{cyt}$ is thought to be responsible, at least in part, for inducing cell wall exocytosis in the *Fucus serratus* egg (Roberts *et al.*, 1994) and regulating secretion in *Phaeocystis globosa* (Chin *et al.*, 2004). There are several rapid events in the process of settlement in *Ulva* zoospores where $[Ca^{2+}]_{cyt}$ could play a regulatory role; for example, in secretion of the adhesive, loss of the flagellar sheaths and reorganisation of the cytoskeleton following commitment to settlement.

The use of fluorescent Ca^{2+} indicators has allowed the visualization of $[Ca^{2+}]_{cyt}$ dynamics in a wide range of animal and plant cells. In order to monitor $[Ca^{2+}]_{cyt}$ dynamics associated with zoospore settlement using Ca^{2+} indicators, the Ca^{2+} dyes must be loaded into the cytosol. The most widely used method for introduction of Ca^{2+} dyes in single cells is via incubation with cell-permeant AM-ester forms of the dyes. Until recently this was the only practical way to load Ca^{2+} indicators into such small, delicate and motile cells as *Ulva* zoospores, which are not amenable to

microinjection. Although AM-esters are easy to load into cells this method often results in dye compartmentalisation when the indicator is sequestered into membrane-bound compartments and organelles where it is unavailable to respond to changes in $[Ca^{2+}]_{cyt}$ (Bush & Jones, 1987; Brownlee & Pulsford, 1988). Dextran-conjugated dyes provide an ideal solution to compartmentalisation potentially resulting in more accurate reporting of $[Ca^{2+}]_{cyt}$ (Haughland, 2002). However, dextran dyes cannot be loaded passively and require direct microinjection or microperfusion into the cell. Such approaches are not possible with swimming *Ulva* zoospores. The suitability of a recently developed biolistic approach was therefore assessed where plant or algal cells are shot with sub-micron pellets coated in dye (Bothwell *et al.*, 2006) allowing dextran Ca^{2+} indicators to be loaded into zoospores.

4.1.1 Objectives

1. To evaluate AM-ester and dextran Ca^{2+} indicators for use in *Ulva* zoospores.

2. To determine whether changes in cytosolic calcium are involved in zoospore settlement and adhesion.

4.2 Methods

4.2.1 Loading of AM-ester calcium indicators

The following non-ratiometric AM-ester indicator dyes were evaluated: Fluo-3, Fluo-4, Oregon Green BAPTA-5N, Calcium Crimson and Calcium Orange (Molecular Probes, Invitrogen). 1 mM stock solutions of each AM-ester Ca^{2+} indicator were prepared in DMSO supplemented with 15% (w/v) Pluronic F-127 (Molecular Probes) to facilitate cell loading (Braun & Hegemann, 1999). Zoospores were incubated with

the AM-ester at 4ºC (to prevent settlement) for 30 min and subsequently at ~18ºC for the duration of the experiment. All images were acquired using a BioRad 1024 confocal laser scanning inverted microscope equipped with a krypton/argon laser and a x60 (NA 1.4) oil immersion objective (Nikon). Fluo-3, Fluo-4 and Oregon Green BAPTA-5N were excited at 488 nm (522 nm +/- 10 nm emission). Calcium Crimson and Calcium Orange were excited at 568 nm (605 nm +/- 10 nm emission). Cytosolic loading of the Ca^{2+} indicators was verified using the membrane permeabiliser digitonin (5–50 µM) (Sigma) and the Ca^{2+} ionophore ionomycin (5–50 µM) (Sigma) to impose increases in $[Ca^{2+}]_{cyt}$. The positions of the chloroplasts were monitored by chlorophyll fluorescence excited at 488 nm (>600 nm emission), along with bright field images to monitor cell movement or changes in cell shape.

4.2.2 Biolistic loading of dextran calcium indicators

Fluorescent dextran-conjugated dyes were loaded into zoospores using a modified biolistics-based method previously applied to *Chlamydomonas* cells (Bothwell *et al.*, 2006). Zoospores were released into seawater and concentrated on ice as previously described (Chapter 2, section 2.1.1). 1 ml of concentrated cells (approx. 5 x 10^8 cells ml^{-1}) was centrifuged at 400 g for 1 min. The pellet was resuspended in 30 µl of cytoplasmic buffer (200 mM K^+-glutamate, 10 mM HEPES, 1 mM sorbitol, pH 8.1) and then spread thinly onto the centre of a 35 mm diameter culture dish immediately prior to biolistic bombardment. Cytoplasmic buffer was used to prevent the cells from experiencing a Ca^{2+} and Na^+ shock when loaded. 8 nmol of Oregon Green BAPTA-1 dextran conjugate (10 kDa) and 10 nmol Texas Red dextran conjugate (Molecular Probes, Invitrogen) were mixed with 0.9 mg of 0.6 µm diameter gold microparticles (Bio-Rad Hemel Hempstead, UK) suspended in 60 µl of distilled water and dried onto

a carrier disk (Bio-Rad) (Bothwell *et al.*, 2006). Microparticle delivery was performed using a Bio-Rad PDS-1000 particle delivery system, using a 1350 psi rupture disk. Following bombardment, cells were immediately washed in filtered seawater to remove background dye fluorescence, resuspended in 1 ml of seawater and stored on ice for a maximum of 30 min to prevent settlement prior to imaging. Cells were induced to settle by the addition of low melting point agarose (see Chapter 2, section 2.1.2) and imaged using a BioRad 1024 confocal laser scanning microscope equipped with a Nikon x60 (NA 1.4) oil immersion lens. The excitation/emission wavelengths for Oregon Green and Texas Red dextran were 488/530 nm and 568/605 nm respectively.

Oregon Green-BAPTA-1 exhibits an increase in fluorescence emission when bound to Ca^{2+} hence its fluorescence is dependent on Ca^{2+} concentration. Texas Red fluorescence is independent of Ca^{2+} concentration, hence when Oregon Green and Texas Red are used together, ratiometric measurements of $[Ca^{2+}]_{cyt}$ can be used to reduce optical artefacts due to changes in cell shape or movement.

4.2.3 Data analysis

Sequences of images were acquired using TIMECOURSE software (BioRad). The software produces a .pic file that contains a series of images. For data analysis the file was split into .bmp files using ThumbsPlus. Each individual file was then opened in Scion Image and a stack of images was created. To aid visual interpretation false colour was added by applying a look-up table (LUT) and the stack saved as a .tif file.

For ratio imaging .tif files were created of the time series from both the Oregon Green and Texas Red images. To the Texas Red stack a macro was applied to reduce the

background fluorescence ('Divide 250/255 and add 5' – see Appendix I). Ratio images were obtained from both Oregon Green and Texas Red stacks (Appendix I) to produce a new stack containing the images with the applied ratio. Spatial smoothing was applied to images to reduce pixelation using a filter that replaced the value of each pixel with the weighted average of the surrounding 3 x 3 neighbouring pixels (Appendix I). For measuring Ca^{2+} dye fluorescence in individual cells, a region of interest was selected around the cell to measure the grey level and produce temporal plots of ratio image intensity over a set of images.

4.2.4 Settlement assays

Settlement assays using the membrane marker FM 1-43, were performed by allowing spores (1.5×10^6 ml^{-1}) to spontaneously settle in the dark for 30 minutes in the presence of 2 µM FM 1-43. Ten fields of cells were imaged in each of three replicate dishes. Settlement was scored by the presence of a localised internal accumulation of FM 1-43 (see Figure 3-1 to Figure 3-3). The effect of inhibitors on the ability of zoospores to settle was determined by comparing control dishes with those where zoospores had been exposed to 1, 10, 25 and 50 µM verapamil or 100 µM gadolinium (Gd^{3+}). Cells were incubated with gentle stirring for 30 min. Control cells were incubated with an equivalent amount of the solvent used to make the stock solutions of inhibitor (distilled water).

To determine the effects of inhibitors on swimming rate, zoospores were imaged after 30 min incubation with 25 µM verapamil or 100 µM gadolinium. Bright field images were recorded with a BioRad Radiance confocal microscope at a rate of 10 frames per second. The speed of swimming zoospores was analysed using Image Pro-Plus v5.1 motion tracking software (Media Cybernetics, Silver Spring, MD, USA).

4.3 Results

4.3.1 Evaluation of AM-ester calcium indicators

A range of AM-ester Ca^{2+} indicators were evaluated for cytosolic loading of *Ulva* zoospores. While AM-ester dyes potentially bring the benefit of ease of loading, they can become sequestered into cellular compartments which prevents accurate measurement of $[Ca^{2+}]_{cyt}$. This was the case with zoospores loaded with AM-esters of Fluo-3, Fluo-4 and Calcium Crimson which showed dye accumulation into 2 discrete sub-cellular compartments after only 15 min loading (Figure 4-1a). Moreover, no change in dye fluorescence was seen in response to the membrane permeabiliser digitonin (data not shown). Calcium Orange-AM loaded rapidly with a diffuse appearance (Figure 4-1b) and small transient increases in intracellular dye fluorescence could be elicited with 5 µM of the Ca^{2+}-ionophore ionomycin (n = 9, data not shown). However, 10 min after settlement of Calcium Orange-loaded cells, a halo of external dye fluorescence was visible around cells, indicating secretion of dye that remains associated with the adhesive (Figure 4-1c). The increase in external dye fluorescence was concomitant with a decrease in intracellular fluorescence indicating that dye was rapidly compartmentalised into secretory vesicles during the loading procedure (Figure 4-1b).

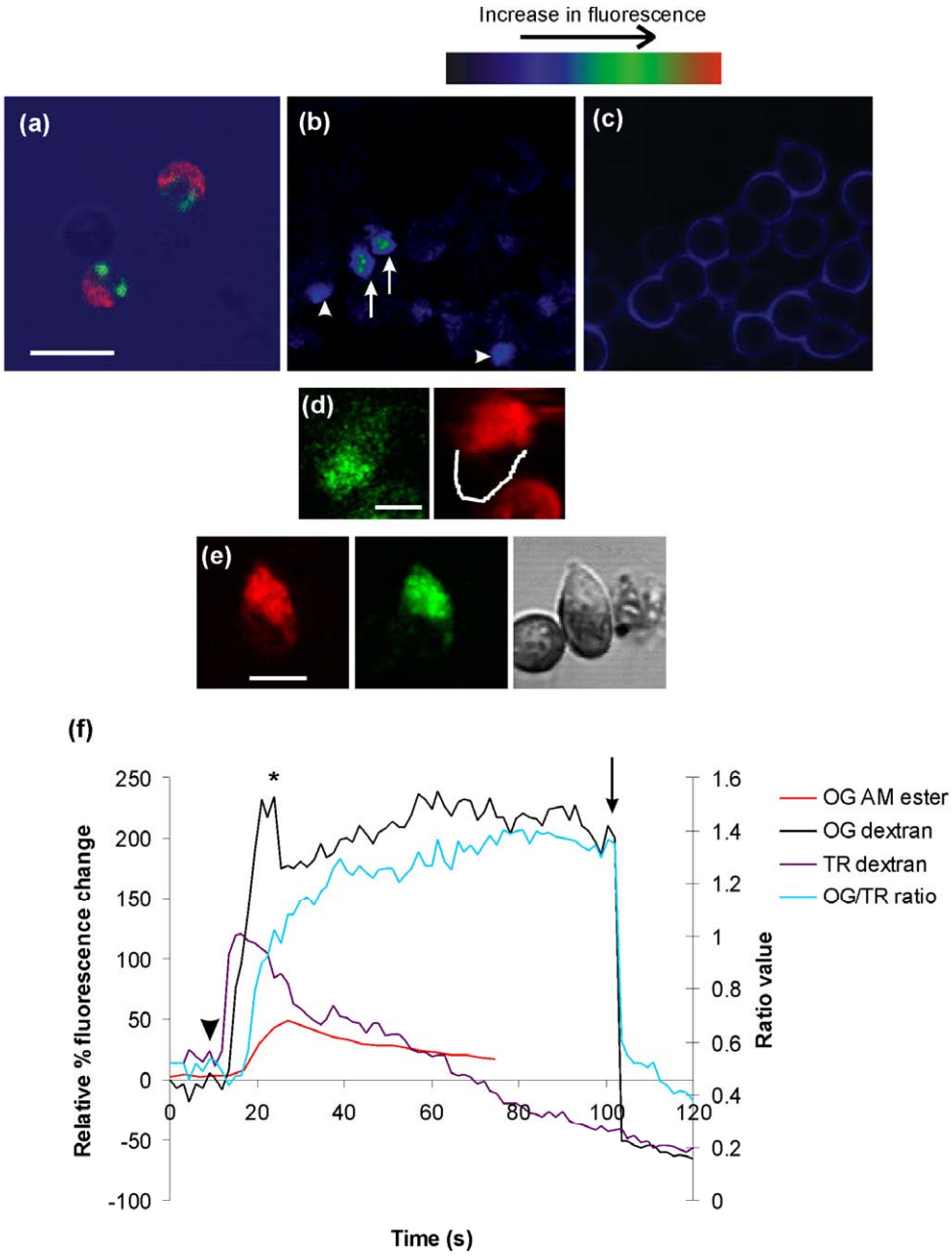
Increase in fluorescence
(a)
(b)
(c)
(d)
(e)
(f)
Relative % fluorescence change
Ratio value
Time (s)
OG AM ester
OG dextran
TR dextran
OG/TR ratio

Figure 4-1 Evaluation of AM-ester and dextran calcium indicators. (a) Fluo-3 (AM-ester) loaded zoospores showed sequestration of dye into two vacuoles (green = Fluo-3 fluorescence, red = chlorophyll fluorescence). **(b)** and **(c)** Calcium Orange (AM-ester) loaded zoospores showed progression of internal to external label due to sequestration of the dye in the adhesive vesicles. **(b)** Swimming cells (arrows) and cells in early settlement (less than 5 min - arrowheads) show internal anterior labelling. **(c)** 10 min after settlement external labelling is apparent. Bar = 10 µm. **(d)** Oregon Green BAPTA-5N AM ester loaded zoospores appeared to show diffuse loading (left: Oregon Green AM-ester, right: chlorophyll autofluorescence with an outline to indicate the anterior part of the spore). Bar = 2 µm. **(e)** Oregon Green BAPTA-1-dextran loaded zoospores showed diffuse cytosolic loading. The cytosol was co-labelled with Texas Red-dextran (left) and Oregon Green-dextran (centre). Right: transmission image. Bar = 5 µm. **(f)** 5 µM ionomycin (added at 10 s – arrowhead) produced a 45% increase in intracellular dye fluorescence after 10 s in cells loaded with Oregon Green BAPTA-5N AM ester (red line). However ionomycin induced a 200% increase in fluorescence in cells loaded biolistically with Oregon Green-dextran (black line). The ratio value of Oregon Green (OG):Texas Red (TR) is given on the secondary y axis (blue line). The transient increase in $[Ca^{2+}]_{cyt}$ seen immediately after the addition of ionomycin (*) is abolished when the Oregon Green-dextran is ratioed against Texas Red dextran (purple line) indicating that at least part of the apparent increase in $[Ca^{2+}]_{cyt}$ seen in the unratioed AM ester values may be due to a change in cell shape. The increase in Texas Red fluorescence seen at the start is thought to be due to a change in cell shape, which is followed by a rapid decrease thought to be due to photobleaching. The sudden decline in fluorescence (arrow) in the dextran-loaded cell is due to loss of dye on ionomycin-induced cell lysis.

Oregon Green BAPTA-5N-AM did not show any obvious compartmentalisation (Figure 4-1d) on loading. However in settled cells, a maximum increase of only 45% in relative dye fluorescence occurred in response to 5 µM ionomycin (n = 10) (Figure 4-1f). The small increase in dye fluorescence in response to Ca^{2+} ionophores suggested there was inadequate reporting of $[Ca^{2+}]_{cyt}$ levels using this AM dye.

Due to these problems with the use of AM-esters, a new method of biolistic loading of zoospores with dextran-conjugated Ca^{2+} indicators was developed based on the method of Bothwell *et al.* (2006). Using this method *Ulva* zoospores were loaded with the Ca^{2+}-sensitive indicator Oregon Green BAPTA-1-dextran (10 kDa) together with the Ca^{2+}-insensitive indicator Texas Red–dextran (10 kDa) to allow ratio imaging and so reduce artefacts due to changes in cell shape and movement. Loading efficiency varied but on average 10% of cells exhibited diffuse cytosolic loading (Figure 4-1e). There was also a marked improvement in the sensitivity of dye with ~200% increase in dye fluorescence after addition of 5 µM ionomycin – 4 times greater than that seen in AM-ester loaded zoospores (Figure 4-1f). In addition, ratiometric analysis of Oregon Green BAPTA-1 and Texas Red images minimized artefacts due to changes in cell shape (Figure 4-1f). Cell shape changes following ionophore treatment caused a transient increase of up to 100% in the Ca^{2+}-independent Texas Red fluorescence (Figure 4-1f), suggesting that the increases in fluorescence induced by ionomycin in the non-ratiometric images of AM-ester loaded spores could be explained purely by a change in shape of the cell rather than an increase in $[Ca^{2+}]_{cyt}$. This transient increase in Texas Red Fluorescence was also reflected in an initial peak in Oregon Green BAPTA-1 fluorescence at around 20 s after addition of ionomycin. However, these transient elevations in fluorescence were removed in the ratiometric images.

4.3.2 Cytosolic calcium elevations in settling zoospores

Zoospores pre-loaded with the AM-ester Oregon Green BAPTA-5N, were observed as they settled around air bubbles. Localised Ca^{2+} dye elevations were seen in spores as they settled (Figure 4-2). The cell in Figure 4-2 exhibited a 3-fold increase in Ca^{2+} dye fluorescence, a proportion of which may be due to cell shape changes, although from observing the chlorophyll images there appears to be little change in cell shape during the period of greatest Ca^{2+} dye elevation. Three other zoospores in the same experiment showed elevations of Ca^{2+} dye fluorescence during settlement, after similar periods of contact with the air bubble. These results were investigated further when the techniques for biolistic delivery of dextran dyes technique became available.

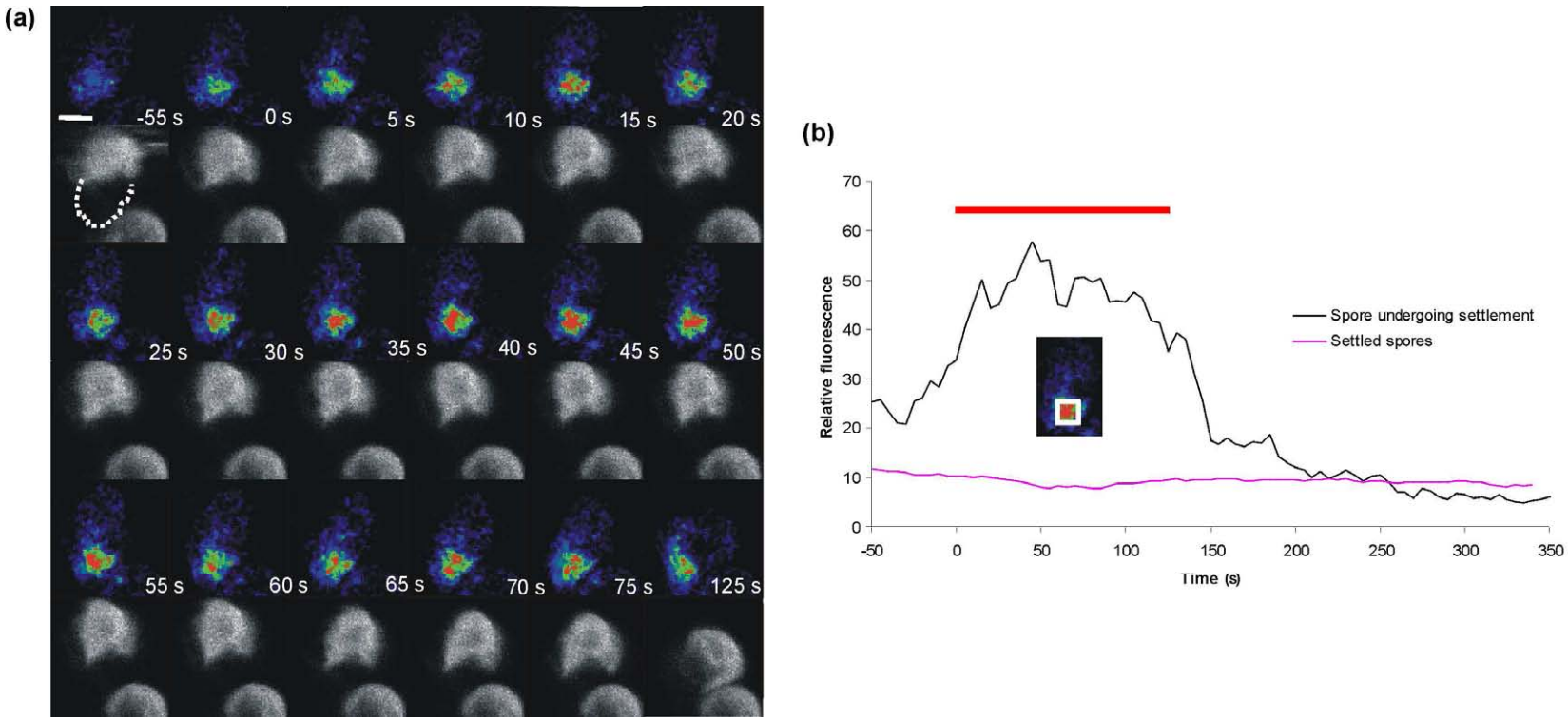
(a)
-55 s
0 s
5 s
10 s
15 s
20 s
25 s
30 s
35 s
40 s
45 s
50 s
55 s
60 s
65 s
70 s
75 s
125 s
(b)
Relative fluorescence
Time (s)
Spore undergoing settlement
Settled spores
0
10
20
30
40
50
60
70
-50
0
50
100
150
200
250
300
350

Figure 4-2 Time series of confocal images of calcium elevations in a zoospore undergoing the settlement response loaded with Oregon Green BAPTA-5N, AM. (a) The false-colour images show Ca^{2+} dye fluorescence and the black and white images below show the corresponding chlorophyll fluorescence to illustrate changes in spore movement and shape as the spore settles. Calcium elevations were seen in the anterior region of the settling cell. The outline of the zoospore is shown in the first image. At -55 s the zoospore has just arrived at the air bubble and at 0 s the cell started to commit to settlement as it stopped swimming and started to round up. There was very little movement between 25 and 50 s when the greatest change in $[Ca^{2+}]_{cyt}$ was seen and the zoospore had completed the rounding up process at 125 s after commitment to settlement. Bar = 2 µm. **(b)** Time-course comparing relative fluorescence (256-grey level value) of the anterior region (see inset) of the settling zoospore in (a) to that of settled spores (mean of 10 spores) recorded in the same field of view during the same time-course. The settling spore showed a peak in fluorescence as it settled which then decreased with time after settlement to a level below that when it was swimming whereas settled spores showed very little change in fluorescence over the same time span. The area highlighted in red is illustrated in (a).

Zoospores loaded with Oregon Green BAPTA dextran by the biolistic method were induced to settle by the addition of low melting point agarose. A small number of loaded cells were captured undergoing settlement after the addition of agarose. Of 10 loaded cells that underwent normal settlement as assessed by reduced length/width ratio and/or loss of flagella, 8 showed increases in $[Ca^{2+}]_{cyt}$. The pattern of $[Ca^{2+}]_{cyt}$ increase that was associated with settlement varied from cell to cell with half of the cells showing transient increases (Figure 4-3 and Figure 4-4) and the other half showing more prolonged increases (Figure 4-5 and Figure 4-6). Localised $[Ca^{2+}]_{cyt}$ elevations at the anterior end of the zoospore coincided with loss of the flagellar sheaths and change in cell shape from elongate to spherical (Figure 4-3 and Figure 4-4a). Cytosolic calcium was seen to decrease to a resting level below that of a swimming zoospore within 60 s of the peak elevation of $[Ca^{2+}]_{cyt}$ (Figure 4-4a). Oregon Green BAPTA/Texas Red fluorescence ratios in swimming zoospores were approximately 2-fold greater than those of post-settled zoospores, suggesting $[Ca^{2+}]_{cyt}$ levels approximately double those of resting cells. Assuming a typical eukaryote resting $[Ca^{2+}]_{cyt}$ of 100 nM in unstimulated cells (Sanders *et al.*, 1999) and that a doubling in ratio values represents a doubling in $[Ca^{2+}]$ this suggests that the average $[Ca^{2+}]_{cyt}$ of swimming zoospores is approximately 200 nM. In cells that showed prolonged increases in $[Ca^{2+}]_{cyt}$ the elevation was less spatially constrained.

The cytosol in the cell in Figure 4-3 does not decrease in size relative to the rest of the cell. However, there is a decrease in the relative size of the cytosol in the cell in Figure 4-5 indicating that the cell may have undergone secretion. It is therefore possible that there are at least two Ca^{2+} signatures at settlement resulting in at least two different responses in the cell. The prolonged diffuse increase in $[Ca^{2+}]_{cyt}$ seen in

Figure 4-5 may result in secretion whereas a transient localised elevation of $[Ca^{2+}]_{cyt}$ seen in Figure 4-3 may result in flagella loss.

Oregon Green BAPTA/Texas Red fluorescence ratio values of settling spores were similar to those reached in spores that were stimulated with Ca^{2+}-ionophore (see Figure 4-1f) indicating that the dye is saturated at these concentrations of $[Ca^{2+}]_{cyt}$. Assuming a Kd of 265 nM (Haughland, 2002), the elevations of fluorescence ratio seen in settling cells most likely correspond to increases in $[Ca^{2+}]_{cyt}$ of at least 2.0 µM.

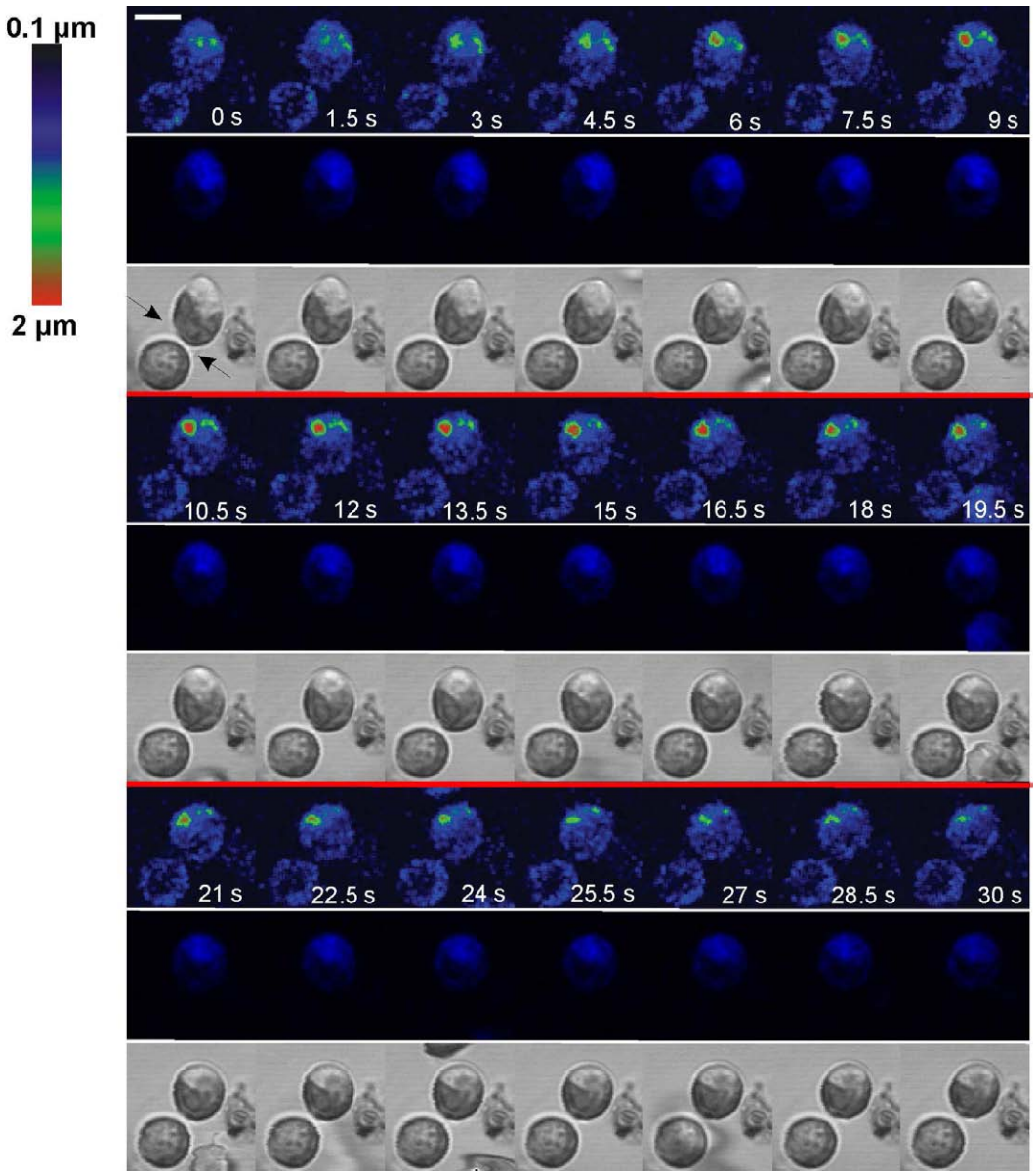
0.1 µm
2 µm
0 s
1.5 s
3 s
4.5 s
6 s
7.5 s
9 s
10.5 s
12 s
13.5 s
15 s
16.5 s
18 s
19.5 s
21 s
22.5 s
24 s
25.5 s
27 s
28.5 s
30 s

Figure 4-3 Time series of confocal ratio images of a localised cytosolic calcium elevation in a zoospore undergoing agar-induced settlement loaded with Oregon Green BAPTA-1 dextran and Texas Red dextran. The false-colour images show relative $[Ca^{2+}]_{cyt}$ (first row) and Texas Red (second row) and the corresponding bright field image is below (third row). Ratio images were obtained from both Oregon Green BAPTA-1 and Texas Red images. The localised elevation in $[Ca^{2+}]_{cyt}$ coincides with the release of the flagella (labelled with an arrow at 0 s and which are not visible after 6 s) and rounding up of the cell both of which indicate the cell is committing to settlement. Only the cell on the right is loaded with dye (as can be seen from the Texas Red images), there is some autofluorescence at the emission peak of Oregon Green BAPTA-1. The Texas Red images clearly indicate where the cytosol is as there is no visible autofluorescence at 605 nm. Bar = 5 µm.

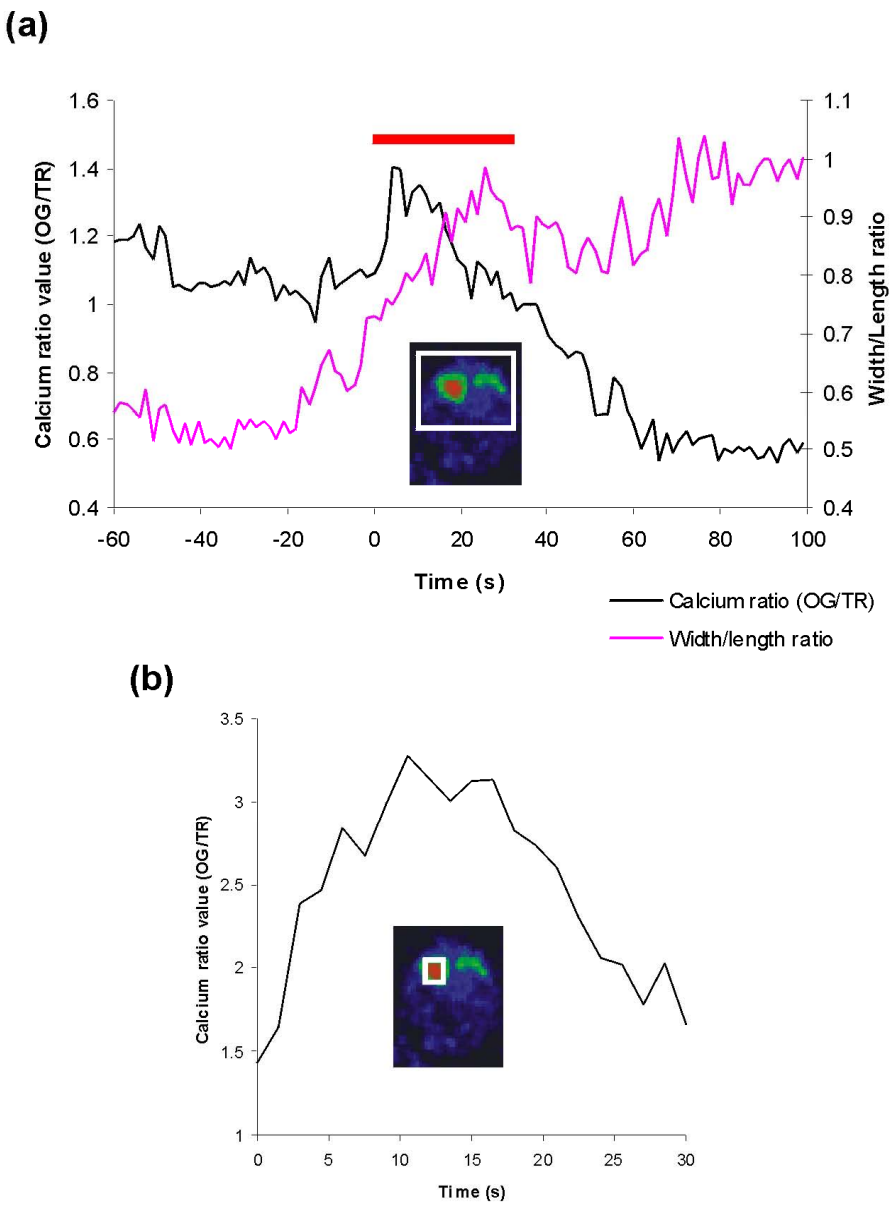

Figure 4-4 Region of interest from the spore in Figure 4-3 showing a transient elevation in cytosolic calcium during settlement. (a) A transient whole cell $[Ca^{2+}]_{cyt}$ increase was seen during zoospore settlement which precedes the cell shape change as defined by its increasing width/length ratio (1 = spherical). The cytosol was identified from Texas Red images and used to define a region of interest (inset) to measure the ratio value of $[Ca^{2+}]_{cyt}$ in the cytosol. 0 s is when the cell had stopped moving. The images in Figure 4-3 are taken from the area of the trace highlighted with the red bar. **(b)** Maximum ratio values for settlement-induced Ca^{2+} elevations determined by the defined region of interest (see inset).

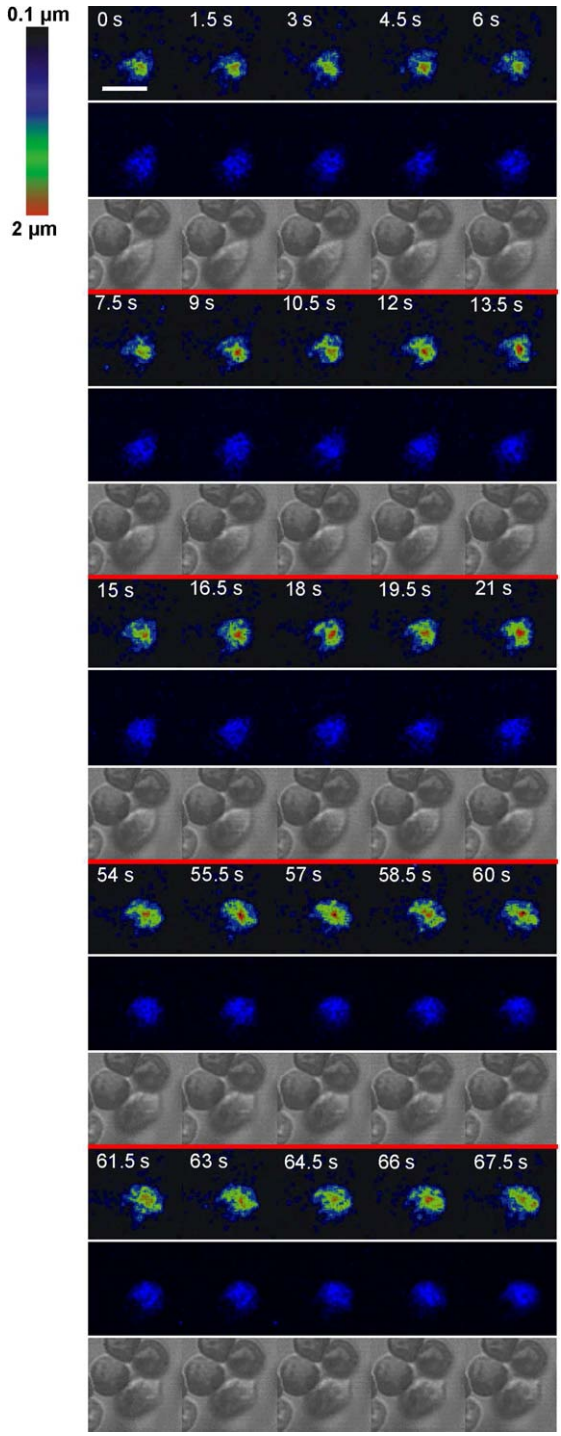

Figure 4-5 Time series of confocal ratio images of a more prolonged and less localised elevation in cytosolic calcium in a zoospore undergoing agar-induced settlement loaded with Oregon Green BAPTA-1 and Texas Red dextran. Similar to the cell shown in Figure 4-3, the elevation in $[Ca^{2+}]_{cyt}$ coincides with the rounding up of the cell and secretion of adhesive starting 20 s after the zoospore had committed to settlement (at 0 s) but in this cell the elevation is more prolonged. Bar = 5 µm.

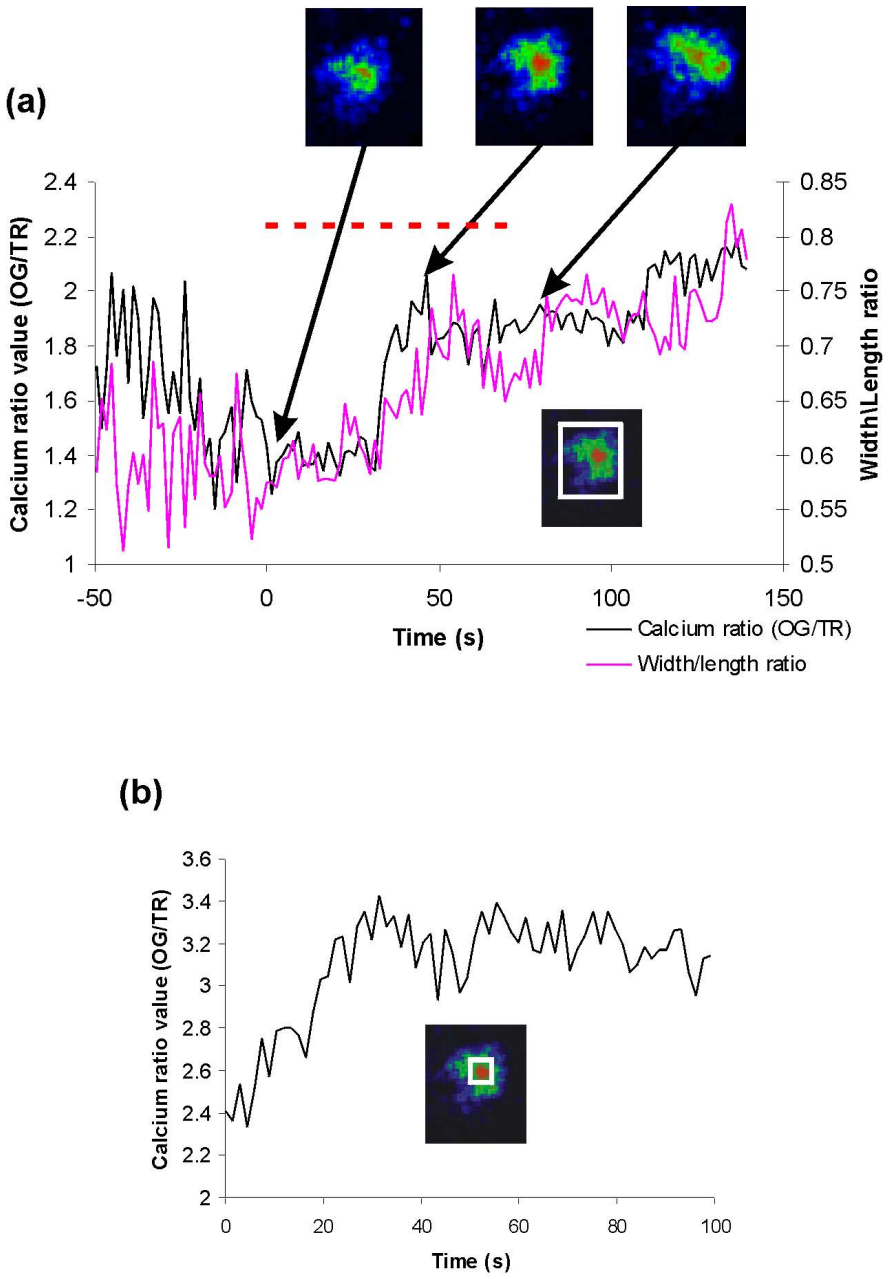

Figure 4-6 Region of interest from the spore in Figure 4-5 showing a prolonged elevation in cytosolic calcium during settlement. (a) A prolonged initial increase in $[Ca^{2+}]_{cyt}$ was seen as the cell underwent settlement followed by a further increase at 110 s. In this cell there was less localisation of the elevated $[Ca^{2+}]_{cyt}$. The cell was swimming rapidly prior to commitment to settlement, hence there is large variability in values preceding 0 s. Imaging was stopped at 140 s after committing to settlement. The cell became more spherical as $[Ca^{2+}]_{cyt}$ increased. Enlargements are shown of the spore before, during and after the $[Ca^{2+}]_{cyt}$ elevation. Parts of the area highlighted in red are illustrated in Figure 4-5. **(b)** Maximum ratio values for settlement-induced Ca^{2+} elevations determined by the defined region of interest (see inset).

4.3.3 Effect of calcium channel inhibitors on settlement

The source of Ca^{2+} underlying elevations in $[Ca^{2+}]_{cyt}$ during spore settlement was investigated using the putative Ca^{2+} channel inhibitors verapamil and gadolinium. Since extracellular Ca^{2+} is required for motility-dependent settlement (M.E. Callow, unpublished observations), inhibitors were used at concentrations that did not cause loss of motility. Verapamil at 25 µM gave statistically significant reductions in spore settlement compared with controls (48.3% reduction) (Table 4-1). The Ca^{2+} channel blocker Gd^{3+} (100 µM) caused a 54.5% reduction in settlement. The experiment was repeated with similar results.

Spore settlement is dependent on spore motility but in neither case was the effect of these inhibitors on settlement due to reduced spore motility since swimming speed was either unaffected (gadolinium), or increased (verapamil) (Table 4-1). Higher concentrations of verapamil caused a reduction of both swimming speed and settlement and using verapamil at concentrations below 25 µM had no effect on settlement (results not shown).

Table 4-1 Effect of calcium channel inhibitors on swimming and settlement of *Ulva* spores. a) Swimming speeds (µm s^{-1}) of zoospores in the presence of 25 µM verapamil and 100 µM gadolinium. Each inhibitor was tested with separate batches of freshly-released zoospores. Mean values presented are from 10 avi files. **b)** Percentage reduction in settlement of zoospores using FM 1-43 as a settlement marker in the presence of 25 µM verapamil and 100 µM gadolinium. Each inhibitor was tested with separate batches of freshly-released zoospores. Mean values presented are from 30 fields of view. ** = significantly different from control at p <0.01, *** = significantly different from control at p <0.001. Swimming data was normally distributed so significance was tested using the 2-sample *t*-test; settlement data was not normally distributed so the Mann-Whitney *U*-test was used.

a)

		Swimming speed (µm s^{-1})
Verapamil	Treatment	19.3***
	Control	11.4
Gadolinium	Treatment	20.0
	Control	20.0

b)

		Spore settlement mm^{-2} +/- SE	% reduction in settlement compared with control
Verapamil	Treatment	78.3+/- 12.1**	48.3
	Control	151 +/- 20.5	/
Gadolinium	Treatment	77.3 +/- 9.22***	54.5
	Control	170 +/- 23.1	/

4.4 Discussion

Evaluation of AM-ester Ca^{2+} indicators strongly suggests that they are not suitable for monitoring changes in $[Ca^{2+}]_{cyt}$ in *Ulva* zoospores. Despite an apparently diffuse pattern of loading of Calcium Orange-AM and Oregon Green BAPTA-5N the changes in dye fluorescence seen after the addition of Ca^{2+}-ionophore were small and could be accounted for by Ca^{2+}-independent changes in dye fluorescence, such as changes in cell shape (see Figure 1f). Cells of the dinoflagellate *Crypthecodinum cohnii* loaded with Calcium Orange-AM (Lam *et al.*, 2005) showed a similar, approximately 50% increase in Ca^{2+} dye fluorescence, suggesting that significant dye compartmentalisation was occurring.

Biolistic loading of dextran dyes proved to be the most successful approach to monitor $[Ca^{2+}]_{cyt}$ in the highly motile zoospores. Moreover, ratio imaging of biolistically delivered dextran dyes minimised artefacts due to changes in cell shape and movement associated with settlement. Using this approach zoospores were shown to exhibit significant elevations of $[Ca^{2+}]_{cyt}$ during settlement. Calcium-regulated secretion has been shown in other algae such as *Fucus* (Roberts *et al.*, 1994) and *Phaeocystis* (Chin *et al.*, 2004). It is therefore proposed that a major role of elevated $[Ca^{2+}]_{cyt}$ during *Ulva* zoospore settlement is in the regulation of exocytosis of the adhesive vesicles.

In addition to the onset of secretion, the elevations in $[Ca^{2+}]_{cyt}$ coincided with loss of the flagellar sheaths and settlement-associated changes in cell shape. The localised elevations in $[Ca^{2+}]_{cyt}$ which occur near the base of the flagella during settlement (see Figure 4-3), may have a role in the deflagellation response. In motile *Chlamydomonas* cells, deflagellation in response to elevated external Ca^{2+} is associated with a localised

elevation in $[Ca^{2+}]_{cyt}$ at the base of the flagella (Quarmby, 1996; Bothwell *et al.*, 2006). In *Chlamydomonas*, deflagellation occurs by flagellar excision whereas in *Ulva* zoospores, only the sheath is discarded and the axoneme is reabsorbed (Callow *et al.* 1997). Nevertheless, the results presented here are consistent with the hypothesis that deflagellation in *Ulva* is a Ca^{2+}-dependent process. Cytosolic calcium elevations also accompanied the change to a more spherical cell shape which is an indicator of settlement (Callow *et al.*, 1997). The specific $[Ca^{2+}]_{cyt}$ requirements for each of these processes (i.e. secretion, deflagellation and change in cell shape) are currently unknown – whether a single common elevation in $[Ca^{2+}]_{cyt}$ underlies the triggering of all of these processes, or whether there are more subtle spatio-temporal patterns of elevated $[Ca^{2+}]_{cyt}$ that regulate each separate process, remains to be determined.

Verapamil and Gd^{3+} have been used to show the Ca^{2+}-dependence of chemotaxis (Ermilova *et al.*, 1998) and deflagellation (Quarmby, 1996) in *Chlamydomonas*. The reduction in settlement of *Ulva* zoospores in the presence of Gd^{3+} and verapamil at concentrations that did not reduce swimming speed indicates that an influx of extracellular Ca^{2+} is required for settlement and that a rise in $[Ca^{2+}]_{cyt}$ is needed to allow settlement to proceed, presumably through triggering the exocytosis of the adhesive vesicles.

The use of Gd^{3+} in inferring a role for Ca^{2+} channels should however be treated with caution due to the wide range of effects it can have on cells as a result of its high positive charge (Taylor *et al.*, 1996). Gd^{3+} has been shown to facilitate non-specific adhesion (Dunina-Barkovskaya *et al.*, 2004) and hence it is possible that it may cause zoospores to adhere to glass more strongly countering any inhibitory effects mediated via Ca^{2+} signalling. Pimozide, another inhibitor similar to verapamil in that it is a

selective inhibitor of L-type Ca^{2+} channels in higher animals (Glossmann & Striessnig, 1988), has been used in *Chlamydomonas* to block Ca^{2+} currents (Harz & Hegemann, 1991) and could also be used in *Ulva* zoospores.

Calcium channel inhibitor experiments suggest that extracellular Ca^{2+} is required for settlement, but internal release of Ca^{2+} from stores such as the ER and vacuole may also be important and may be induced by Ca^{2+} influx through the plasma membrane (Sanders *et al.*, 1999). Internal release of Ca^{2+} can be tested through the use of inhibitors such as the aminosteroid U73122 which blocks phospholipase C-mediated intracellular Ca^{2+} release (Lee & Shen, 1998) and has been used in *Fucus* to block release of Ca^{2+} from intracellular stores (Coelho *et al.*, 2002).

4.5 Conclusions

By using a novel dye delivery method, sensitive and accurate measurements of $[Ca^{2+}]_{cyt}$ were obtained that provided evidence that elevations in $[Ca^{2+}]_{cyt}$ accompany the settlement response. The reduction in settlement using Ca^{2+} channel inhibitors provided further evidence that Ca^{2+} is required for settlement. The *Ulva* zoospore is a highly dynamic system that undergoes secretion, loss of flagella and changes in cell shape during the rapid settlement processes. The active detection of a suitable surface and mass secretion at settlement provides a unique system for unravelling the intracellular signalling pathways that give rise to the different responses induced by contact-mediated stimuli.

5: ELECTROCHEMICAL DETECTION OF SECRETION BY ZOOSPORES OF *ULVA LINZA*

5.1 Introduction

Exocytosis is an important event in *Ulva* zoospore settlement as the polymers required for adhesion to the substratum and formation of the cell wall are both secreted from the cell (Evans & Christie, 1970; Stanley *et al.*, 1999; Callow & Callow, 2006). Studies described in Chapter 3 using the styryl dye FM 1-43, showed significant endocytosis following settlement, indicating retrieval of excess membrane due to the massive secretory event during settlement. Imaging the actual release of the adhesive vesicles is difficult (Callow *et al.*, 1997), their small size (45-300 nm) makes the use of Total Internal Fluorescence (TIRF) microscopy difficult (see Zenisek et al. (2000)) and prevents the use of other techniques such as video microscopy to visualise them directly.

Micro-amperometry offers an alternative, non-optical approach to monitor secretion. If the secreted product is redox-active then this sensitive electrochemical technique has the potential to provide high spatio-temporal resolution of individual exocytotic events (Travis & Wightman, 1998). This resolution is accomplished using carbon-fibre microelectrodes (CFME) that have an active detection surface of just a few microns and which can be used to non-invasively measure individual vesicle release events over time (Chow *et al.*, 1992). This technique depends on the contents of the released vesicles being readily oxidised; alternatively vesicles can be artificially loaded with a redox-active substrate (Kim *et al.*, 2000). In most cases the released compound is a reduced natural product of metabolism that, on release, is oxidised at

the surface of the CFME, which is positioned against the plasma membrane. The oxidation of the released molecules generates an oxidation current that represents the flow of electrons from the molecule to the electrode surface (Figure 5-1). These oxidation currents are readily recorded and can be analysed to provide information on the quantity of molecule released and fusion dynamics of the vesicle with high temporal resolution (Travis & Wightman, 1998).

Recent studies have provided support for oxidisable products being released to consolidate the cell wall in *Ulva* spores (Stanley *et al.*, 1999; Humphrey *et al.*, 2005). Stanley *et al.* (1999) produced monoclonal antibody probes that labelled the contents of the adhesive vesicles. One of the antigens identified was Ent6, which strongly labelled the anterior region of unsettled zoospores where the adhesive vesicles reside. Western blotting demonstrated that after settlement, the amounts of soluble Ent6 antigen that could be extracted were inversely related to time. It was proposed that this was due to extensive cross-linking during curing of the adhesive (Stanley *et al.*, 1999). Moreover, cross-linking was shown to be inhibited by the SH-reducing agent dithiothreitol and the SH-capping Ellman's Reagent (Humphrey *et al.*, 2005) implying that cell wall cross-linking involves S-S bond formation. Disulphide bond formation is an oxidative process between two cysteine residues. Treatment with either of the two reagents resulted in reduced adhesion of spores implying that cross-linking is important in development of the adhesive strength during settlement of spores (Humphrey *et al.*, 2005).

Other oxidisable products that may be released by zoospores during settlement include polyphenols. Circumstantial evidence by Vreeland *et al.* (1998) indicates that a common mechanism of adhesion in diverse taxa of marine algae involves a

polyphenol-carbohydrate fibre glue that is activated through extracellular polymerisation by a haloperoxidase. A similar mechanism of secretion of polyphenols to that which occurs in *Fucus* eggs during adhesion and cell wall formation (Vreeland *et al.*, 1998) can therefore not be ruled out in *Ulva* zoospores. Release of oxidisable substrates from vesicles of *Fucus* eggs is readily detected by amperometry (Taylor, A.R. pers. comm.).

If there is vesicular secretion of products that cross-link the zoospore adhesive then such vesicles may be present in the zoospores prior to settlement. Electron microscopy studies by Evans and Christie (1970) describe 3 major types of vesicles present in *Ulva* zoospores. The least abundant and smallest vesicles (45-65 nm in diameter) are found at the apical dome just beneath the plasma membrane and it was postulated that these may be involved in initial attachment. The most abundant and largest vesicles (150-300 nm) fill the anterior half of the zoospore. These large vesicles are Golgi-derived and contain the glycoprotein adhesive (Callow & Evans, 1974; Callow & Evans, 1977; Stanley *et al.*, 1999) which is secreted at settlement. A third class of vesicles (~55 nm) surrounding the Golgi bodies are actively produced by both swimming and settled cells leading to the hypothesis that they contain cell-wall precursors (Evans & Christie, 1970). The work described in this Chapter tests the hypothesis that vesicles containing redox-active compounds are present and involved in settlement/adhesion processes.

5.1.1 Objective

To investigate whether oxidisable products are released to cure the adhesive and if so, over what timescale after settlement.

5.2 Methods

Ulva plants were collected and zoospores released as described in Chapter 2 section 2.1.1. The medium used for all experiments was 0.2 µm filtered natural seawater.

5.2.1 Electrode fabrication

CMFEs were manufactured according to Schulte and Chow (1998) and Taylor and Chow (2001). Sections of carbon fibre (2 cm long, ~5 µm in diameter – gift from Dr R. Chow, University of Southern California) were attached to a straightened piece of ~8 cm length of 0.5 mm thick copper wire with carbon paste. The carbon paste was made by mixing carbon powder (Sigma) with N-Butyl acetate (Sigma) and allowing to evaporate in a fume hood until the constituency resembled 'thick slurry'. After attaching the carbon fibre to the wire it was left to dry for at least 30 min in a draught-free place. Once the carbon paste was set, the fibre and wire were cannulated in a glass capillary (GC200-10; Harvard Instruments, Pangbourne, UK) and secured with a drop of Araldite epoxy glue. The assembly was left for several hours to dry before pulling the capillary to a fine point around the carbon fibre using a conventional patch clamp electrode puller (PP-83, Narashige, Japan). The join between the glass tip and carbon fibre was sealed with Sylgard (Corning, New York, USA) and the remaining exposed fibre insulated with electro-deposition paint (BASF, Germany – gift from Dr R. Chow) by applying a voltage of 4 mV for 1-2 min and then baking at 190 ºC for 2-3 min (Schulte & Chow, 1996). Using a dissection microscope, electrodes were cut with a new scalpel blade to reveal a fresh electro-active surface before calibration and use in experiments.

5.2.2 Amperometric measurements

The CFMEs were connected to the headstage of a voltammetry amplifier (VA-10, NPI electronic, Tamm, Germany) directly to the folded end of the protruding copper wire and currents were recorded with reference to a silver-silver chloride pellet (Harvard Instruments). To determine the response and sensitivity of the electrode, CFMEs were dipped into the calibration solution comprising 1 mM potassium ferricyanide in a 0.5 M KCl solution at pH 3.0 (Taylor & Chow, 2001) and a ramped voltage protocol was applied using Clampex 9.0 software (Axon Instruments, Foster City, CA, USA). If the observed response was noisy or did not follow the symmetrical ramp profile shown in Figure 5-2, the CFME was recut and retested.

For recording amperometric currents from cells a command overpotential of +800 mV was applied to the electrode to ensure rapid and complete oxidation of secreted products. The headstage was mounted on a micromanipulator (Leica, Bensheim, Germany), which enabled the tip of the electrode to be positioned so that it was just touching an *Ulva* spore.

5.2.3 Testing for secretion of oxidisable products

5.2.3.1 Release of oxidisable products by populations of zoospores

To examine bulk secretion of oxidisable products by populations of spores as they settle, cells at a concentration of ~3 x 10^6 ml^{-1} were left to settle in a glass vial for 30 min. After recording a baseline oxidation current in fresh seawater, the supernatant from above settled cells was then added (which will still contain some swimming spores and bacteria) and the oxidation current recorded to test for the presence of

oxidisable substances that may have been secreted into the bulk medium by the settling zoospores.

5.2.3.2 Spontaneous secretion

To investigate whether spontaneous secretion of redox-active compounds occurred in cells as they underwent settlement, the CFME was held next to a group of settled spores until a spore started settling in the vicinity. The CFME was then moved if necessary so that it was touching the settling spore and continuous recording was initiated. To investigate amperometric currents generated from swimming cells, micropipettes were fabricated from 1.5 mm filamented borosilicate glass to give a 1-2 µm tip and suction was applied to catch swimming zoospores. The micropipette was held using a motorised micromanipulator (MP-285; Sutter Instruments, Novato, CA, USA) and the CFME positioned so that it was just touching the zoospore.

5.2.3.3 Ionomycin

To test whether the secretion of oxidisable products could be stimulated by Ca^{2+}, the Ca^{2+}-ionophore ionomycin (Sigma) was added to cells. It has already been shown using Ca^{2+} indicators that 5 µM ionomycin added to spores causes $[Ca^{2+}]_{cyt}$ to increase rapidly in the first minute before the cell ruptures (see Chapter 4). Cells were left to settle in the viewing dish for 30 min. Swimming cells were then washed off and 1 ml of seawater was added to provide a bath solution. The tip of the CFME was positioned just touching a settled spore before adding 5 µM ionomycin.

5.2.3.4 Mechano-stimulated secretion

Settled cells were stimulated to secrete by gently pushing the tip of the CFME against the cell. It was noted if a cell ruptured upon contact.

5.2.4 Data analysis

Oxidation currents were filtered to 500 Hz using a low-pass filter before sampling at 4 KHz (Digidata 1322A, Axon Instruments). Amperometric spikes were analysed off-line using threshold analysis of the resultant current trace (Clampfit 9.0, Axon Instruments). Data were digitally filtered with a Bessel 8 pole filter and manually adjusted for any baseline drift during the experiment. For accurate estimates of single vesicle size and kinetics, only events occurring immediately at the electrode surface should be analysed. Event detection by the software was therefore monitored and events rejected if they were smaller than 5 pA and if there were multiple events occurring. In order to exclude artifactual oxidation peaks due to cell rupture from the analysis, subjective thresholds were applied based on the rise time, peak height and peak length (see Figure 5-1 for explanation of these measurements). These thresholds were determined by analysing known rupture events and subsequently rejecting events that had a rise time greater than the mean +25%, a peak height >100 pA and peak length of more than twice the mean value. The rise time is important in determining true events because it represents the distance that the event is occurring from the active surface. If the rise time is too slow it implies then the event occurred at a distance from the active surface meaning that there will be diffusion losses and the event kinetics will not represent the true release dynamics. Parameters of interest obtained in the analysis were event peak (pA); charge (pC) – an indication of how many electrons were transferred during the event; rise time 10-90% (ms); half-width (ms); length of peak (ms) and percentage of events with a foot signal (Figure 5-1).

Because the charge transferred in the redox reaction at the CFME surface is directly proportional to the quantity of oxidisable substrate released, this parameter can be

used to estimate the number of molecules released in a single exocytotic event using the following equation:

$$M = Q/ze$$

Where M is the number of reactant molecules, Q is charge in the redox transfer (C), z is the number of electrons transferred per molecule, assuming that z = 1 (i.e. 1 electron is transferred per molecule) and e is the charge per electron (1.6×10^{-19} C).

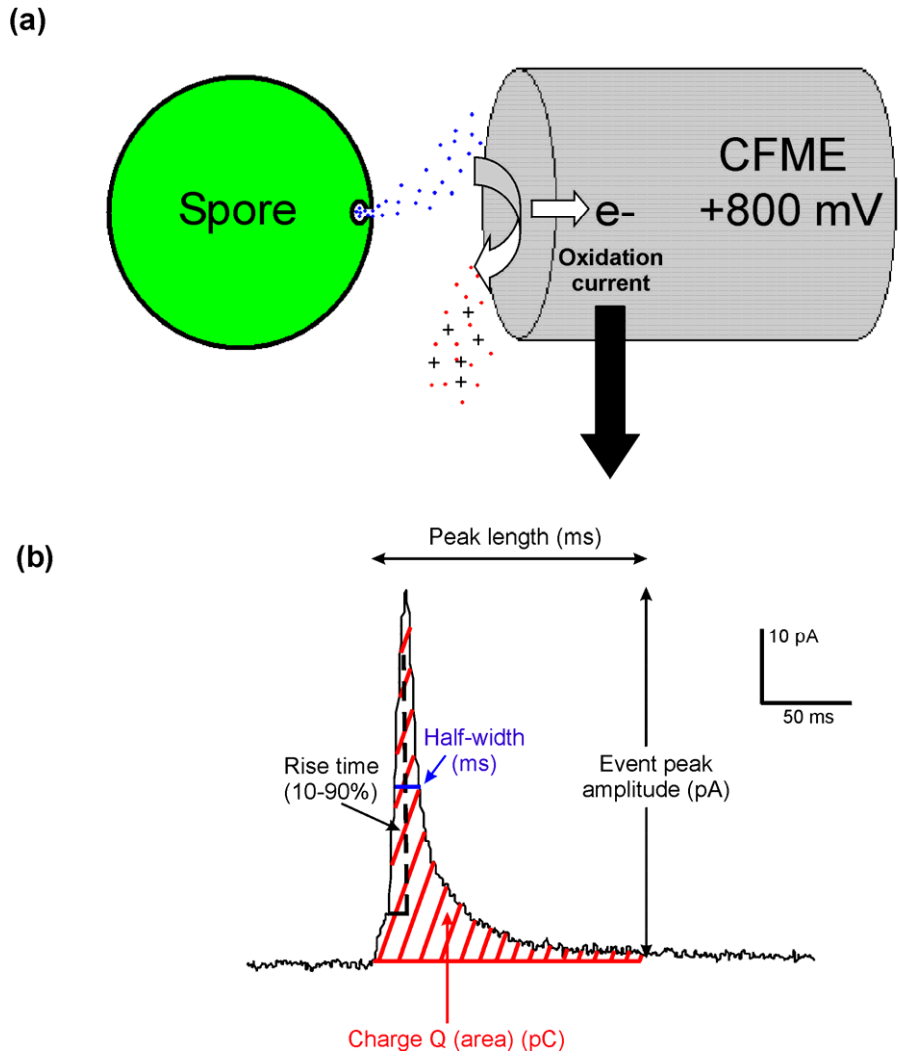

Figure 5-1 Detection of secretion of redox-active substances and analysis of secretory events using CFMEs. (a) A vesicle is secreted from the *Ulva* spore containing a readily oxidisable substance. The product is oxidised at the surface of the CFME, generating an oxidation current representing the flow of electrons from the substrate to the electrode. The resultant oxidation leaves the substrate molecule positively charged. **(b)** A typical oxidation current event is illustrated with the main features that are recorded. The event peak is measured as the maximum height the event reaches from the baseline. The peak length is the duration of the event. The charge is the area under the peak and indicates the amount of molecules released. The rise time is the time between the trace crossing 10% and 90% of the rising stage of the peak. The rise time for the whole spike is not used to avoid temporal artefacts due to foot signals (see later) and filtering at the base and peak of the event. The half-width is the width measured at 50% of the maximum peak amplitude.

5.3 Results

5.3.1 Calibration of CFMEs

Figure 5-2 shows a typical calibration of a good CFME in 1 mM potassium ferricyanide in a 0.5 M KCl solution. When applying a ramp protocol, a symmetrical, noise-free recording should be obtained (Figure 5-2). When the voltage is positive, there is little current as ferricyanide is not reduced. When the redox potential of ferricyanide (E^0 = 358 mV) is reached there is a large increase in current as ferricyanide is converted to ferrocyanide. A plateau in the current is reached when the reduction of ferricyanide at the tip of the CFME becomes diffusion-limited.

5.3.2 Release of oxidisable products by populations of zoospores

A slow increase in the background oxidation current representing bulk release of oxidisable products into the medium was often seen during experiments to monitor zoospore secretion. This baseline drift was not seen when electrodes were put in filtered seawater indicating that there was secretion of oxidisable products by the population of cells. This was further investigated by examining whether or not this was due to the cells secreting oxidisable products as they are settling and producing a cell wall. Cells were left to settle in a glass vial for 30 min. 0 ml, 0.5 ml or 1 ml of the supernatant from above these cells was then added to the recording chamber containing 0.5 ml of fresh filtered seawater. When no supernatant was added and the electrode was left in seawater there was no measurable increase in background when recorded over 25-30 min (Figure 5-3a). The mean increase in background when adding 0.5 ml of supernatant was 3.7 pA (three experiments), and when adding 1 ml a

mean increase of 7.9 pA (two experiments) was seen (Figure 5-3b). These results indicate that the spores release oxidisable products as they undergo settlement.

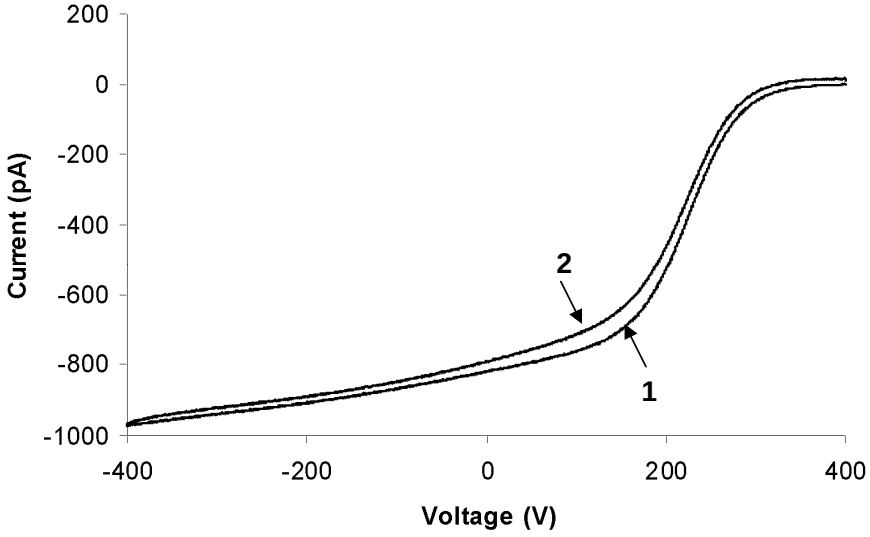

Figure 5-2 Characteristics of a typical reliable CFME. Current/voltage calibration curve for a 5 µm carbon fibre microelectrode coated with electrodeposition paint. The solution contained 1 mM potassium ferricyanide in 0.5 M KCl at pH 3. Electrode voltage was ramped from +400 mV to -400 mV (1) and then back to +400 mV (2) at 100 mV s^{-1}. A good CFME will show a symmetrical, stable and noise-free recording with a rapid decline in current when the redox potential of ferricyanide is reached. The reaction then becomes diffusion limited resulting in a plateau at the more negative potentials.

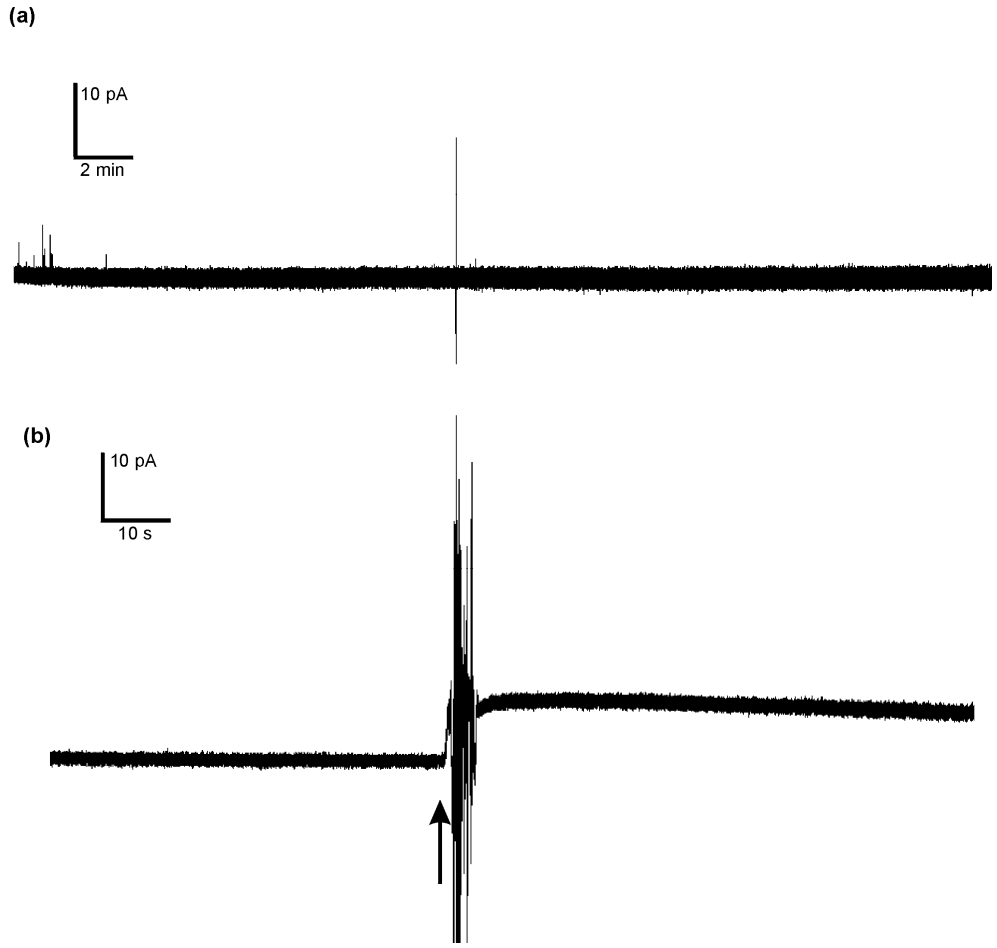

Figure 5-3 Release of oxidisable products by populations of settling zoospores. (a) When an electrode was held in seawater with no spores for 30 min there was no noticeable background drift in the current but a slight increase in noise possibly indicating deterioration of the electrode deposition paint (data shown is representative of three experiments). **(b)** An increase in the background current was seen when 1 ml supernatant from cells settled for 30 min was added to seawater (arrow) (data shown is representative of two experiments), which is consistent with the release of oxidisable products as cells settle and form the cell wall.

5.3.3 Spontaneous secretion

Zoospores settle gregariously (Callow *et al.*, 1997) hence there is more chance of a cell settling in a pre-existing group than on its own. Therefore, to test for spontaneous secretion on settlement, the CFME was placed near to a group of settled spores with just enough space for a cell to settle in between the group and the tip of the CFME (Figure 5-4ai). This technique was successful with many cells (>12) settling very close if not on the tip of the CFME. In initial experiments the electrode was only left recording for 10-15 minutes after a cell had settled (6 experiments) but later experiments recorded for 20-25 min after settlement (6 experiments). In both cases, when cells settled at the tip there were no detectable oxidation currents seen. The only release of oxidisable products occurred when the electrode was pulled away from the group of settled spores (Figure 5-4aii and b). In this case, spores remained attached to the tip of the CFME. Recordings for more than 30 min were not possible because background noise of the CFME became too great. Therefore, if the secretion of oxidisable substances occurs more than 30 min after settlement then these events cannot be captured.

Because spontaneous settlement and subsequent vesicle release from groups of cells may not occur close enough to the active electrode surface to be detected, the approach was adapted to examine isolated single cells. Zoospores were held using a suction pipette and the CFME electrode was placed touching the spore to induce settlement. However, despite many attempts on only two occasions did a cell appear to round up on the end of the micropipette in a typical settlement response. On all occasions when the electrode was held close to a spore on the tip of the pipette there were no secretory events detected. Together with the experiments monitoring

zoospores settling close to groups of previously settled cells, it was concluded that there is no detectable secretion of oxidisable products from individual cells during the immediate settlement process and up to 30 min after.

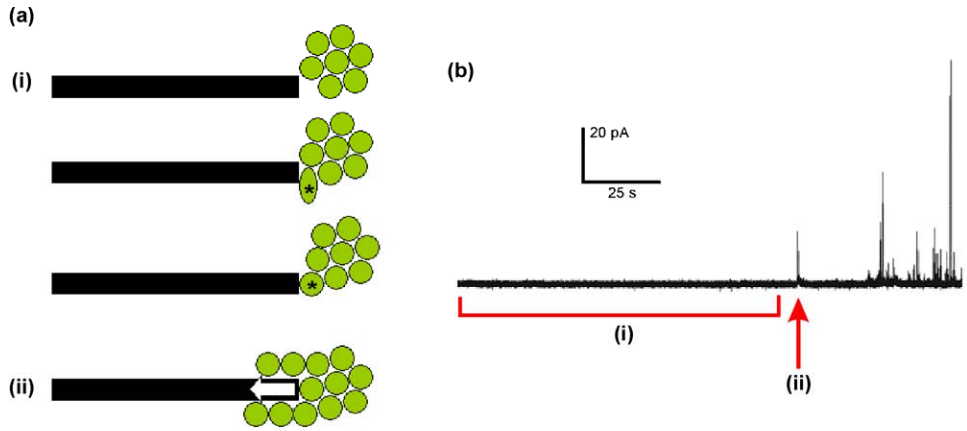

Figure 5-4 Testing for spontaneous secretion. (a) The CFME was positioned next to a group of previously settled spores. A swimming spore then came along (marked with an asterisk) and settled adjacent to the tip of the CFME. **(b)** No secretory activity was seen as the cell was settling (i). The only activity seen was when the CFME was pulled away from the group of cells (at arrow) (see aii) (data shown is representative of 5 experiments).

5.3.4 Ionomycin

To test for Ca^{2+}-dependent exocytosis of oxidisable products, the Ca^{2+}-ionophore ionomycin was added. When 5 µM ionomycin was added to cells loaded with a Ca^{2+} indicator, $[Ca^{2+}]_{cyt}$ increased rapidly in the first minute then the cell tended to rupture (Chapter 4). Therefore any secretory events would be expected in the first minute after addition of ionomycin. After placing the CFME within 5 µm of a settled spore, a baseline was recorded for 2 min before ionomycin was added to a final concentration of 1-5 µM (9 experiments). When ionomycin was added at a concentration of 1-2 µM there was no response (4 experiments). Upon addition of 5 µM ionomycin there was a large peak in current that rapidly decreased to a new baseline after 2-3 min, on average 46 pA above the starting baseline (5 experiments) (Figure 5-5). There were no visible secretory peaks after the addition of ionomycin. The cells were seen to have broken up so the increase in the baseline is presumably due to cells rupturing and releasing redox-active metabolites from the cytosol.

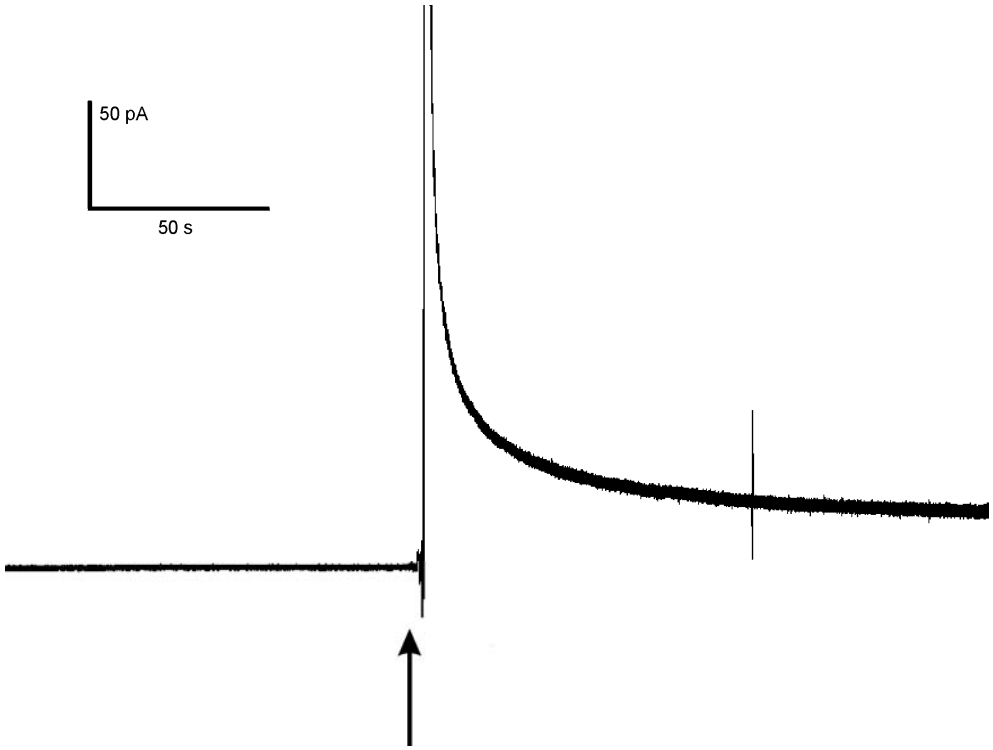

Figure 5-5 Addition of ionomycin to test for calcium-regulated secretion of oxidisable products. A CFME was held next to a settled spore. When 5 µM ionomycin was added (arrow) there were no secretory peaks from the cell where the electrode was close to but cells did rupture resulting in a single massive peak in oxidation current and an increase in the background current (data shown is representative of 5 experiments).

5.3.5 Mechano-stimulated secretion

Despite the lack of detectable secretory events in settling cells, it was possible to mechanically induce the release of oxidisable products in settled spores. Secretory events were detected when settled cells were prodded (Figure 5-6a and b) such that they detached from the surface and adhered to the electrode.

The larger the group that was detached the larger the spike. However, secretory events were not seen when cells that had only recently settled (less than 10 min beforehand) were prodded. Spikes were also not seen when settled spores were prodded gently so that they did not detach from the surface. When cells were attached to the electrode, spikes were only seen if the CFME was moved and not when it was kept stationary.

Two types of events could be distinguished when mechanically stimulating settled spores. Events typically exhibiting peaks between 8-76 pA and of a short (<280 ms) duration resulted from individual exocytotic secretory events (Figure 5-6c and d). Of these events 8.5% exhibited a foot signal preceding the main oxidation current peak (Figure 5-6d and Table 5-1). When a cell ruptured, large sustained oxidation currents were detected (Figure 5-6e and f) that indicate mass release of reduced equivalents of the cytoplasm. In order to distinguish between genuine secretory events and leakage of intracellular redox-active compounds due to cell injury, the kinetic characteristics of secretory and rupture events were compared (Table 5-1). Secretory events from single exocytotic vesicle fusion and release are short in duration and small in amplitude, whereas spikes from a cell rupturing are comparatively long in duration and large in amplitude. Thresholds were then applied to remove any events that may be due to cell rupturing. After applying thresholds to the data (see Methods, section 5.2.4) to exclude mechanically induced cell rupture events, the average charge per

secretory event was estimated to be 1.13 pC (Table 5-1). The histogram in Figure 5-7 illustrates the distribution of charge events for individual mechanically stimulated secretory spikes. *Ulva* spores released on average 7.06×10^6 molecules per event.

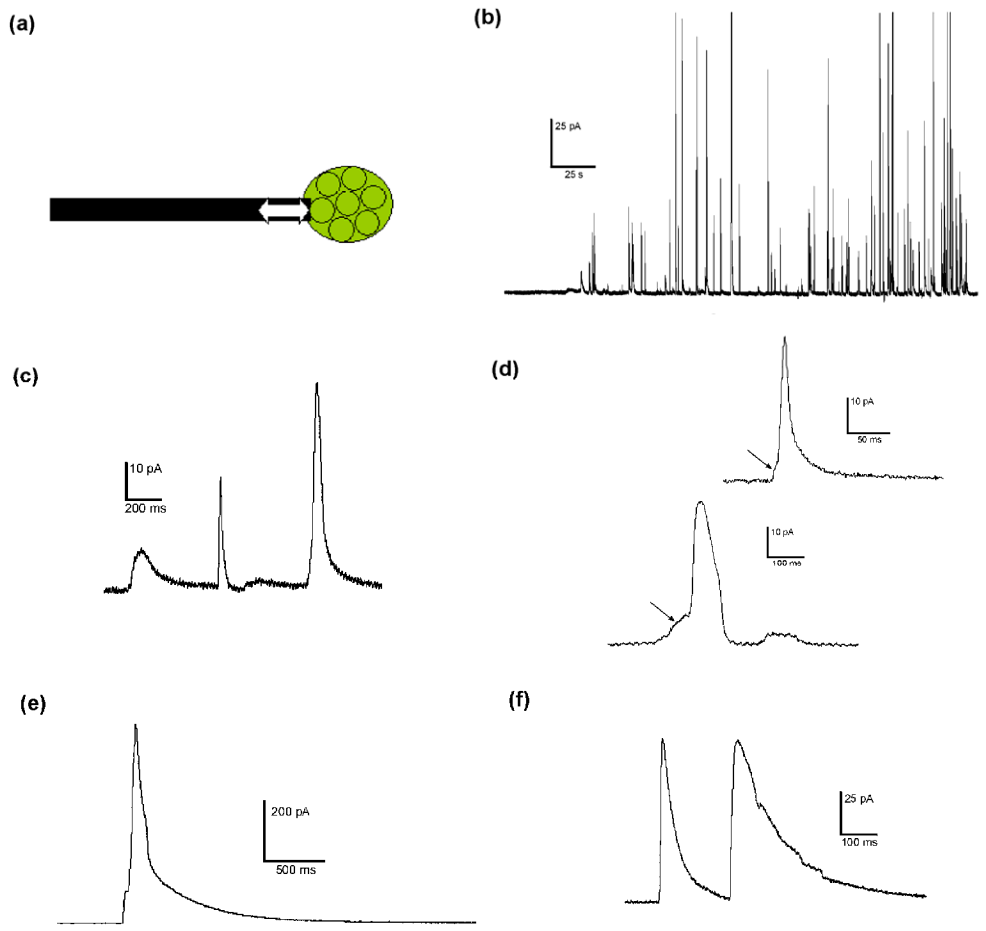

Figure 5-6 Testing for mechano-stimulated secretion. (a) When a CFME was pushed against groups of spores that had been settled for at least 10 min, secretory spikes were seen **(b)**. The trace shows repeated mechanical stimulation of different groups of settled cells. Typical secretory spikes are shown in **(c). (d)** "Foot" signals (arrowed) were sometimes seen preceding a larger spike. **(e)** and **(f)** Examples of spikes that were seen as cells ruptured. Characteristics of these events were a large amplitude (e) and large charge (f).

Table 5-1 Characteristics of *Ulva* zoospore secretory and rupture events. Known events when cells were seen to rupture were analysed and compared to genuine single vesicle secretory events. Rupture peaks were of larger amplitude, higher charge and the half-width was 4x longer. The characteristics of rupture peaks were subsequently used to reject these artefacts from traces of mechanically stimulated secretion by applying thresholds as described in the methods. Values given are means +/- standard error from 5 experiments.

	Number of spikes	Average spike peak pA	Average charge pC	Average rise time (ms)	Average half-width ms	Spikes with foot %
Secretion	103	37.8 +/- 2.80	1.78 +/- 0.15	14.5 +/- 1.45	41.1 +/- 2.85	12.2
Ruptured	10	144 +/- 61.8	19.3 +/- 6.22	33.6 +/- 13.3	198 +/- 71.1	/
Secretion with thresholds applied	47	35.2 +/- 2.45	1.13 +/- 0.08	8.79 +/- 0.63	26.0 +/- 2.03	8.5

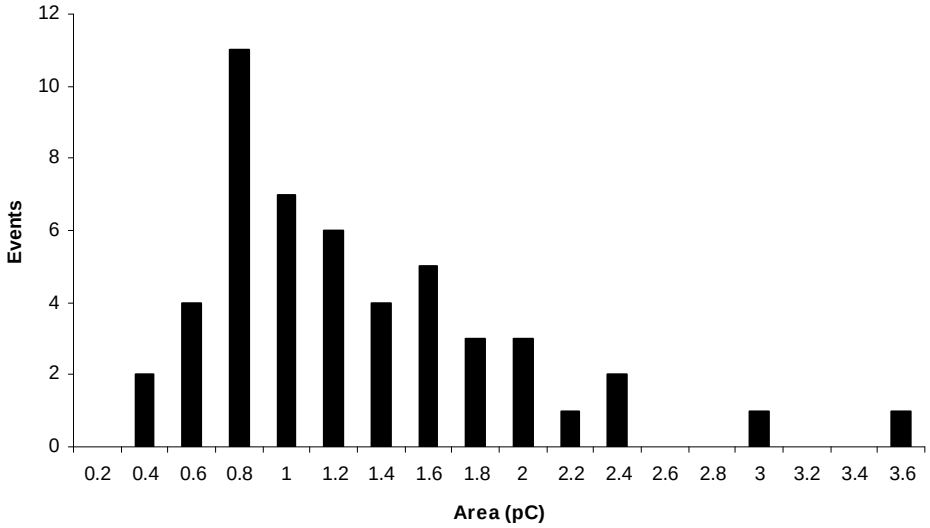

Figure 5-7 Distribution of individual spike areas (pC) released from mechano-stimulated *Ulva* spores. The spike area represents how much material was released in each secretory event. The bins are divided into 0.2 pC intervals.

5.4 Discussion

Previous experiments using the membrane dye FM 1-43 showed very rapid membrane recycling occurring at settlement, providing indirect evidence of mass exocytosis required to release adhesive and cell wall precursors (Chapter 3). The aim of the work described in this Chapter was therefore to directly detect individual exocytotic events before, during and after settlement using amperometric detection of the putative redox-active cross-linking agents (Humphrey *et al.*, 2005) needed for cell-wall consolidation.

Release of oxidisable substrates during settlement was supported by the preliminary experiments examining the accumulation of oxidisable compounds in the bulk medium of settling populations of cells. However, in individual cells, amperometric spikes that represent spontaneous exocytotic release events were not detected during settlement and up to 30 min after. The lack of detectable events is inconsistent with the bulk release of oxidisable products by settling spores. It is possible that secretion of redox-active substrates was not detected because it may be that the kinetics of spontaneous release of oxidisable products at settlement cannot be measured using amperometry – perhaps the amount per cell released is too small to be recordable above the noise (2-5 pA). However the recorded range of vesicle size is 45-300 nm in *Ulva* zoospores (Evans & Christie, 1970) and release of vesicles of size 200 nm from chromaffin cells is easily detected using amperometry (Wightman *et al.*, 1991). In spite of increasing background noise of the CFME over time (possibly due to deterioration of the electrodeposition paint coating), detection of spontaneous individual secretory events would have been expected under these conditions. An additional reason for the lack of detection may be reduced sensitivity of the CFME

active surface due to contamination with zoospore adhesive. Reduced sensitivity of the CFME would not have been an issue for the bulk secretion experiment as no secretion took place at the CFME active surface.

The presence of vesicles containing redox-active molecules was confirmed in settled zoospores. However, secretory events were only detected when the cell was settled and was mechanically stimulated either by touch or physical movement once cells were attached to the CFME. Gentle stimulation of the cells resulted in secretion. If cells were stimulated too forcefully then the cell ruptured which was accompanied by the release of oxidisable products. This presumably cytoplasmic release could be distinguished from exocytotic secretion by analysis of the shape of the spikes. It is not possible to determine what chemical is being released using amperometry alone (cyclic voltammetry is required) so it is not possible to say whether the chemical released upon rupturing is the same as seen when mechano-stimulated. Release of oxidisable products from photosynthesis such as NADPH would be expected when an algal cell ruptures.

The stimulated release of redox-active molecules may be due to a mechanosensitive activation pathway. Mechanosensitive (MS) channels are ion channels that are activated by mechanical stress at the cell membrane allowing various ions including Ca^{2+} to enter the cell. MS channels appear to be widespread in flagellate algae with the unicellular green algae – *Chlamydomonas* (Yoshimura, 1998) and *Spermatozopsis similis* (Kreimer & Witman, 1994) possessing MS channels in the plasma membrane and flagella. When bovine chromaffin cells were mechanically stimulated by non-destructive but forceful contact using amperometry, they too showed secretion (of catecholamines) with the initial response being a burst of spikes, after which the spike

frequency diminished (Wightman *et al.*, 1991). The charge distribution seen was very similar to that seen with *Ulva* spores (Figure 5-7) with the average area being 1.03 +/- 0.08 pC (cf. 1.13 +/- 0.08 in *Ulva*).

When comparing characteristics of mechanically stimulated amperometric-recordings of secretion in *Ulva* spores to bovine chromaffin cells, the events appear similar in their duration with the mean half-width being 26 ms in *Ulva* and 25 ms in bovine chromaffin cells (Moser *et al.*, 1995). *Ulva* spores also show a similar charge per secretory event with 7.06 x 10^6 molecules detected per event compared to mean values of 2.8 x 10^6 (Chow *et al.*, 1992) to 6.9 x 10^6 molecules of catecholamine in bovine chromaffin cells (Wightman *et al.*, 1991). There are no published examples of algal secretory events recorded using amperometry yet, but recent work (Taylor, A.R. in prep.) has shown that *Fucus* eggs secrete oxidisable products presumed to be phenolic in nature, with a slower half-width (3x slower) and larger charge (4x) than *Ulva*. The secretory characteristics of *Ulva* however, seem to be remarkably similar to those of animal cells than to those of the brown alga *Fucus*, which probably reflects the similarity in size of the intracellular secretory vesicles in these smaller cells. In Fucoid zygotes, physode vesicles range in size from 0.1 µm to 2 µm in *Acrocarpia paniculata* and *Hormosira banksii* (Clayton & Ashburner, 1994) and 0.57-0.71 µm in *Durvillaea potatorum* (Schoenwaelder & Clayton, 1998) whereas the mean vesicle diameter in adrenal chromaffin cells is <200 nm (Coupland, 1968), which is similar to the maximum vesicle size of 300 nm seen in *Ulva* zoospores.

With *Fucus* eggs mechano-stimulation was not necessary to see secretion of oxidisable products as it spontaneously occurred preceding and during fertilisation (Taylor, A.R. in prep). The lack of spontaneous secretion of oxidisable products in

Ulva zoospores does not support the hypothesis of a similar mechanism of adhesion in brown and green algae involving a polyphenol-carbohydrate fibre glue as proposed by Vreeland *et al.* (1998).

The lack of detectable single vesicle secretory events in settling zoospores cannot be easily reconciled with the fact that oxidisable substrates are detected in the bulk medium over a 30 min settling period. Moreover, oxidative events were frequently detected during mechanical stimulation confirming the presence of a population of vesicles with a redox-active cargo in settled zoospores. Detection of single exocytotic events relies on a close contact between the cell surface and active CFME surface. It is possible that detachment of spores from the surface during mechanical stimulation results in closer contact of the CFME and cell plasma membrane hence improving detection. In addition, oxidative events were only detected from cells that had been settled for a minimum of 10 min. At 0-10 min after settlement the cell is only weakly attached to the surface resulting in minimal contact between the cell and CFME (personal observation) thus reducing the potential to resolve single secretory events.

Regulation of secretion in *Ulva* zoospores by $[Ca^{2+}]_{cyt}$ has already been shown for secretion of the adhesive (Chapter 4). Use of the Ca^{2+}-ionophore ionomycin suggested that secretion of oxidisable products cannot be stimulated by an influx of extracellular Ca^{2+} and subsequent rise in $[Ca^{2+}]_{cyt}$ alone. The preliminary data therefore suggests that the vesicles containing redox-active substances are not secreted through Ca^{2+}-regulated secretion which is in contrast to results from *Fucus* eggs which show Ca^{2+}-dependent secretion of phenolic vesicles (Taylor, A.R. in prep.). Nevertheless, Ca^{2+}-independent exocytotic pathways are found in plants, for instance in barley aleurone protoplasts thought to be involved in cell expansion (Homann & Tester, 1997) and in

maize coleoptile protoplasts, Ca^{2+}-independent exocytosis is mechanosensitive as it is driven by changes in osmotic potential that result in a change in membrane tension (Thiel *et al.*, 2000).

The foot signal seen preceding the main peak of current may represent leakage of molecules out of a narrow 'fusion pore' before full fusion of the vesicle with the plasma membrane (Chow *et al.*, 1992; Monck & Fernandez, 1992). Fusion pores occur in the early stages of exocytosis, when a channel forms between the vesicle and plasma membrane so that the lumen of the secretory vesicle is connected to the exterior of the cell. They have been shown to have a universal presence in secretory cells (Anderson, 2006) and the data presented here is consistent with this. Atomic force microscopy and transmission electron microscopy studies have revealed the fusion pore to be a cup-shaped lipoprotein structure with the base containing the membrane protein t-SNARE which allows the docking of vesicles and the release of secretory products (Cho *et al.*, 2002; Jena *et al.*, 2003).

Foot signals have also been recorded in *Fucus* eggs (Taylor, A.R. in prep) but with a greater frequency of occurrence. In chromaffin cells, 20-50% of secretory events are preceded by foot signals (Zhou *et al.*, 1996) compared to only 8.5% of events recorded in *Ulva* spores. The low frequency of foot events compared to chromaffin and *Fucus* cells may signify that the kinetics of fusion pores in the release of the redox-active substance in *Ulva* spores differ from other cells in that they dilate at a greater rate so that there is little leakage of vesicle contents before full fusion with the plasma membrane.

5.5 Conclusions

Amperometry has demonstrated the presence of a population of vesicles containing redox-active molecules in *Ulva* zoospores. The redox-active secretory events detected in *Ulva* spores are one of the first demonstrations of single secretory events in an alga or a higher plant. These vesicles were readily detected on mechanical stimulation of settled spores. The kinetics of vesicle release were very similar to those described in animal cells and the presence of a foot signal in some mechano-stimulated secretory events indicates that release of the vesicles may involve a fusion pore. It is proposed that the cell produces vesicles containing an oxidisable product that is used in consolidation of the cell wall. It is not possible to spontaneously detect secretion of the product from individual cells undergoing settlement, possibly because the CFME active tip becomes obstructed with adhesive, but when a settled cell is prodded the CMFE tip may be wiped clean allowing closer access to the plasma membrane.

It may not be possible to record spontaneous release of redox-active substrates if they occur at settlement and shortly after, if the CMFE active surface becomes blocked with adhesive. Possible future ways to look for spontaneous secretion are to test for release in cells that have already settled before putting the CFME tip close to the cell. In addition, more frequent cutting of the electro-active surface to expose a fresh surface may enable spontaneous secretion to be detected.

6: THE ROLE OF NITRIC OXIDE IN DIATOM ADHESION IN RELATION TO SUBSTRATUM PROPERTIES

6.1 Introduction

Biofouling is the undesirable accumulation of microorganisms, plants and animals on artificial submerged structures. Diatoms are the most frequent and successful microalgal foulers of illuminated submerged artificial structures (Wetherbee *et al.*, 1998) and with increasingly stringent regulations governing the use of biocidal antifouling paints, there is a need for non-biocidal, environmentally friendly coatings (Yebra *et al.*, 2004). The most common non-biocidal coating for ship hulls, effective in reducing fouling by macroalgae and invertebrates, is based on polydimethyl siloxane (PDMSE). These hydrophobic, elastomeric coatings do not prevent colonisation by fouling organisms, but are designed as 'fouling-release' coatings, i.e. they 'release' adhered organisms by the hydrodynamic forces generated when a ship moves through the water. Paradoxically, and in contrast to macroalgae such as *Ulva*, diatoms adhere more strongly to these hydrophobic coatings, and conversely, adhere more weakly to hydrophilic surfaces such as glass (Holland *et al.*, 2004; Statz *et al.*, 2006; Cassé *et al.*, 2007). Similar trends in adhesion were noted in comparisons between surfaces formed from hydrophobic fluorinated, and hydrophilic, PEG-ylated block copolymers (Krishnan *et al.*, 2006). Diatoms also adhere more strongly to hydrophobic model surfaces such as self-assembled monolayers of methyl-terminated alkanethiols, compared to OH-terminated alkanethiols (Finlay *et al.*, 2002a). It is

therefore relevant to know how diatoms detect the properties of a substratum as this may provide insight into the improved design of antifouling surfaces.

At present, little is known about the strategies diatoms use for responding to environmental changes. Falciatore *et al*. (2000) have shown that diatoms possess sensing mechanisms based on changes in $[Ca^{2+}]_{cyt}$ that allow them to perceive changes in the environment such as turbulence, osmotic stress and dissolved iron levels. Environmental stress has been shown to lead to increased production of EPS and a change in its composition in the diatom *Phaeodactylum tricornutum* (Abdullahi *et al.*, 2006). If diatoms can detect their environment in this way then it is possible that detection of an unfavourable surface i.e. one that they do not stick to well, could trigger a stress response. Nitric oxide is a multifunctional messenger molecule commonly produced in stress responses (Beligni & Lamattina, 2001; del Río *et al.*, 2004). Therefore it was decided to investigate whether a signalling response involving NO is triggered in relation to the wettability of the substratum and whether changes in NO production could lead to changes in the strength of adhesion of cells.

In algae, research into NO signalling is in its infancy. General production of NO in algae such as *Chlamydomonas* (Sakihama *et al.*, 2002), Antarctic *Chlorella* (Estevez & Puntarulo, 2005), *Scenedesmus* (Mallick *et al.*, 2002), dinoflagellates (Zhang *et al.*, 2006) as well as in the diatom *Skeletonema* (Zhang *et al.*, 2006) has been shown. In diatoms there are examples of both NO acting as a stress response causing cell death and also being essential for growth. In *P. tricornutum*, recent work has found that a stress response based on NO is triggered by diatom-derived reactive aldehydes leading to cell death (Vardi *et al.*, 2006). In the planktonic diatom *Skeletonema*

costatum, low concentrations of NO were produced during conditions of normal growth (Zhang *et al.*, 2006) where NO is thought to act as a growth factor.

Nitric oxide production can be readily followed in real time and with good temporal and spatial resolution, by imaging in the confocal laser scanning microscope with the fluorescent probe 4-amino-5-methylamino-2',7'-difluorofluorescein diacetate (DAF-FM DA) (Foissner *et al.*, 2000). DAF-FM allows measurement of NO over a wider range of pH values than previous generation dyes such as DAF-2 and greater sensitivity with a detection limit for NO of 3 nM (Kojima *et al.*, 1999).

6.1.1 Objectives

1. To determine if there is any difference in NO production by diatoms showing differential adhesion to surfaces of different wettability.

2. To determine if manipulating the levels of NO through the use of inhibitors and promoters of NO production affects adhesion properties.

6.2 Methods

6.2.1 Cell cultures

Diatoms were cultured in natural seawater supplemented with nutrients to form Guillard's F/2 medium (Guillard & Ryther, 1962) (Appendix II). *Seminavis robusta* (strain F3-61B) was kindly provided by Victor Chepurnov (Ghent University, Belgium). Cultures of *S. robusta* were grown in 250 ml Pyrex conical flasks under static conditions inside a growth cabinet at 18ºC with a 16:8 light:dark cycle (photon flux density 15 µmol m^{-2} s^{-1}). Cultures of *Craspedostauros australis* were grown on a shaker incubator in 250 ml Pyrex conical flasks at 18ºC with a 16:8 light:dark cycle

(photon flux density 25 µmol m^{-2} s^{-1}). Both cultures were subcultured weekly. If clumps of cells were present, the culture was filtered to produce a suspension of mostly single cells. For imaging experiments diatom cultures were diluted with fresh F2 medium to produce a chlorophyll a content of between 0.9 and 1.2 µg ml^{-1}.

6.2.2 Test surfaces

Glass microscope slides were degreased in Decon detergent, soaked in 1 M HCl for 24 h and then all traces of acid were removed using distilled water. Slides were rinsed in seawater before addition of diatoms. The resulting water contact angle of a small droplet of deionised water on the acid-washed slides was <15º measured using a goniometer (transverse mounted microscope). The polydimethyl siloxane elastomer (PDMSE) used was Silastic® T-2 (Dow-Corning Corporation) and these coatings were provided on glass microscope slides by Prof. AS Brennan (University of Florida, Gainesville, Florida, USA). The water contact angle of the T-2 PDMSE was 109 ± 3.5º, a full description of the method of fabrication is presented in Holland *et al*. (2004). The PDMSE slides were leached in seawater for 1 h before adding the diatom culture.

6.2.3 Adhesion strength assays

To prepare cultures for adhesion assays, the medium from log phase cells was removed and replaced with fresh medium. Cells were dislodged from the bottom of the flask and resuspended using a pipette. Diatom cultures were diluted to produce a chlorophyll a content of between 0.3 and 0.4 µg ml^{-1}, the precise value being verified after the experiment was set up.

Methods described in Holland *et al*. (2004) were followed. Briefly, slides were placed in quadriperm culture dishes (Greiner Bio-One, Germany) and 10 ml of diatom suspension added. Three replicates were used for each treatment. The cells were allowed to settle for 1 h before the slides were rinsed gently in F/2 medium to remove unattached cells. Slides were then incubated for a further 1 h.

Cells were then exposed to shear stresses comparable to those experienced around the hull of a typical ship (Schultz *et al.*, 2000). Slides were placed in a calibrated flow channel as described in Finlay *et al*. (2002a) and were exposed to the fully-developed turbulent flow for 5 min at a range of wall shear stresses up to the maximum of 53 Pa.

All slides exposed to the flow channel (three per shear stress) and three replicate slides not exposed to the flow channel were fixed in 2.5% glutaraldehyde in seawater, washed thoroughly in distilled water then dried before counting. Cells were counted in 30 fields of view of 0.1 mm^2 from each of three replicate slides. Data are given as percentage removal and 95% confidence intervals from arcsine-transformed data.

6.2.4 Measuring production of nitric oxide on surfaces

6.2.4.1 Exposure to air

In preliminary investigations with the diatom *Craspedostauros*, several experiments had to be abandoned due to cells being briefly exposed to air, leading to cell death. Exposure to air occurred when slides were removed from the settlement dishes so that a coverslip could be put on and slides imaged using an oil objective.

In order to quantify the damage caused by exposure to air two experiments with *Craspedostauros* were undertaken concurrently. One experiment used Evans Blue (Sigma) to test cell viability after exposure to air for 0 s (nominally, in practice the

minimum exposure possible), 30 s, 60 s and 120 s. The other experiment used DAF-FM to assess NO production after exposure to air for the same time periods.

Evans Blue is a non-permeating dye that leaks through ruptured membranes and stains the contents of dead cells blue. *Craspedostauros* cells (10 ml of culture at 1 µg chl a ml^{-1}) were added to a conical flask. DMSO (50 µl) was added to the flask (to replace the addition of DAF-FM) which was then put in a shaking incubator for 1 h (at 18ºC with a 16:8 light:dark cycle at 100 rpm). After removal from the incubator the cells were settled on 3 cm^2 pieces of PDMSE for 1 h, exposed to air by allowing water to run off the surface, then stained with 0.05% Evans Blue. After 10 min staining, the surfaces were rinsed in ASW and mounted on slides. Evans Blue staining was imaged on an Olympus (Hamburg, Germany) light microscope.

DAF-FM DA (4-amino-5-methylamino-2',7'-difluorofluorescein diacetate) was obtained from Molecular Probes (Invitrogen) and a stock solution of 1 mM was prepared in DMSO. *Craspedostauros* cells (10 ml of culture at 1 µg chl a ml^{-1}) were added to two conical flasks. DMSO (50 µl) (the solvent for DAF-FM) was added to the control flask and 50 µl DAF-FM added to the other flask to give a concentration of 5 µM and then put in a shaker incubator for 1 h. After removal from the incubator, separation from the dye and resuspension in fresh F2, the cells were settled on 3 cm^2 pieces of PDMSE for 1 h, exposed to air and then mounted on slides. Cells were imaged with a BioRad Radiance 2100 confocal laser scanning microscope equipped with a Nikon x60 (NA 1.4) oil objective. Cells were excited at 488 nm and emission collected at 500-530 nm.

6.2.4.2 Methods developed for preventing exposure to air

Diatom cultures were diluted to produce a chlorophyll a content of ~1 µg ml^{-1}. Slides were placed in individual compartments of quadriperm dishes and 10 ml of diatom suspension added. Cells were settled on acid-washed glass slides and PDMSE slides for 1, 2 or 3 h. Slides were washed *in situ* to remove unattached cells by exchanging old medium for new without exposing the cells to air and a water-immersion lens was used so that cells remained covered with medium whilst being imaged.

DAF-FM was added to each quadriperm section to give a final concentration of 5 µM and left for 1 h. An equivalent amount of the solvent (DMSO) was added to the control. The dye was then washed off by replacing old for new medium (at least 100 ml) and left for 15 min to allow de-esterification of the intracellular diacetates. Cells were imaged in the quadriperm dishes with a Nikon x60 (NA 1.0) water-immersion lens.

6.2.4.3 Labelling the cytosol and nucleus

To label the cytosol of *Seminavis*, cells were incubated with 2 µM of the general cell stain fluorescein diacetate (Sigma) prepared from a 1 mM stock in DMSO. Cells were excited at 488 nm and emission collected at 500-530 nm. Nuclear localization in *Seminavis* was achieved by loading with 75 µM of the nucleic acid dye DAPI (Sigma) prepared from a 30 mM stock in artificial seawater. DAPI was imaged with a Zeiss (Jena, Germany) Axioskop epifluorescent microscope equipped with a Zeiss x20 (NA 0.5) lens. Cells were excited at 365 nm and emission collected at 420 nm.

6.2.5 Image Analysis

Diatoms show some autofluorescence at 500-530 nm which was the wavelength where DAF-FM fluorescence was collected. To remove autofluorescence from DAF-FM measurements, fluorescence was measured in control cells which had not been incubated with dye. The average fluorescence of control cells was then subtracted from the total fluorescence recorded from cells loaded with DAF-FM in each experiment.

All images used for comparison of DAF-FM fluorescence were generated under the same microscope settings. Images were taken at the plane of focus where DAF-FM fluorescence was maximal. At least 10 fields of view were recorded for each slide. Raw files from the computer were in .pic format and were converted to .bmp using ThumbsPlus. Scion Image was used to convert greyscale images into false colour using a 256 colour LUT. A rectangular 'region-of-interest' (ROI) was drawn around each healthy looking cell that was lying on its raphe side (see Figure 6-1) and hence was in contact with the surface (as determined from looking at the transmission image) to measure the mean grey level for that cell. The grey level value was averaged for the number of cells in each field of view. Means were compared using a *t*-test if the data was normally distributed or the Mann-Whitney *U* test if not normally distributed as determined by using the Anderson-Darling test of normality.

6.2.6 Nitric oxide donor and inhibitor assays

The NO donor S-nitroso-N-acetylpenicillamine (SNAP) (Molecular Probes, Invitrogen) was used to verify the reliability of DAF-FM as a probe for NO detection in *Seminavis* cells. *N*G-monomethyl-L-arginine (NMMA) (Sigma) was used as a

general inhibitor of NOS. SNAP was prepared as a stock solution of 100 mM in DMSO. NMMA was prepared as a 100 mM stock in distilled water. Cells were mixed with either 0.5 mM SNAP or 0.5 mM NMMA prior to settlement on acid-washed glass slides or PDMSE for 1 h. Control cells were mixed with an equivalent amount of the solute (DMSO for SNAP and distilled water for NMMA). Slides were then washed *in situ* to remove unattached cells and DAF-FM was added to give a final concentration of 5 µM. Cells were then left for a further 1 h before again washing *in situ* to remove the dye.

To test whether elevated or reduced NO levels caused by addition of SNAP or NMMA respectively resulted in a difference in growth, cells settled on acid-washed glass were incubated with either SNAP or NMMA (0.5 mM) and control slides were incubated with either DMSO or distilled water (equivalent amount) for 1 h. Slides were then washed with F/2 *in situ*. Cell counts were made from 10 fields of view (0.1 mm^2) over 48 h (SNAP) or 72 h (NMMA). Relative growth rates were calculated using the equation given in Wood *et al*. (2005)

$$r = \frac{\ln(N_t/N_0)}{\Delta t} = \frac{\ln N_t - \ln N_t}{\Delta t}$$

where r is the specific growth rate, N_0 is the population size at the beginning of the time interval, N_t is the population size at the end of the time interval, and Δt is the length of the time interval in days.

Evans Blue was used to test viability of cells after exposure to SNAP or NMMA. Cells settled on acid-washed glass that had been exposed to 0.5 mM SNAP or 0.5 mM NMMA were stained with 0.05% Evans Blue (dissolved in ASW) for 10 min.

Slides were then rinsed with ASW. Cells that were stained blue were identified as being dead (measured over 10 fields of view [0.1 mm^2] per slide).

For adhesion assays in the presence of SNAP or NMMA the methods given in section 6.2.3 were followed but prior to settlement on surfaces cells were mixed thoroughly with either SNAP or NMMA (0.5 mM) and control cells were mixed with either DMSO or distilled water. Cells settled on acid-washed glass were exposed to a shear stress of 2 Pa in the flow channel and cells settled on PDMSE were exposed to 21 Pa.

6.3 Results

The diatom *Seminavis robusta* was predominantly used for this study, as it is a large raphid diatom and a member of the *Naviculaceae* – a family of raphid diatoms that is commonly found on fouled hulls. *Seminavis* was used rather than other species commonly used in fouling research, viz. *Navicula perminuta* or *Craspedostauros australis*, because the large cell size (~50 µm in length) facilitates separation of the different regions of the cell in imaging. *Seminavis* is shown in raphe and girdle views in Figure 6-1. The cell possesses two bar-like chloroplasts, a central nucleus, two large vacuoles and a small amount of cytosol at the ends and sides of the cell (Chepurnov *et al.*, 2002). In addition, for preliminary studies involving exposure to air, the raphid diatom *Craspedostauros australis* was used (see Figure 1-6b). For all graphs shown, one typical set of data is presented.

6.3.1 Adhesion strength

In studies on cell adhesion strength, like *Navicula perminuta* (Holland *et al.*, 2004) cells of *Seminavis* adhered very strongly to PDMSE with only a small proportion being removed with increasing shear stress up to the maximum 50 Pa developed by the flow channel (Figure 6-2). In contrast, the detachment curve from the glass surface showed that cells adhered to the hydrophilic glass much less strongly; 50% removal of cells was obtained at only 3 Pa and at higher shear stresses the removal was almost total.

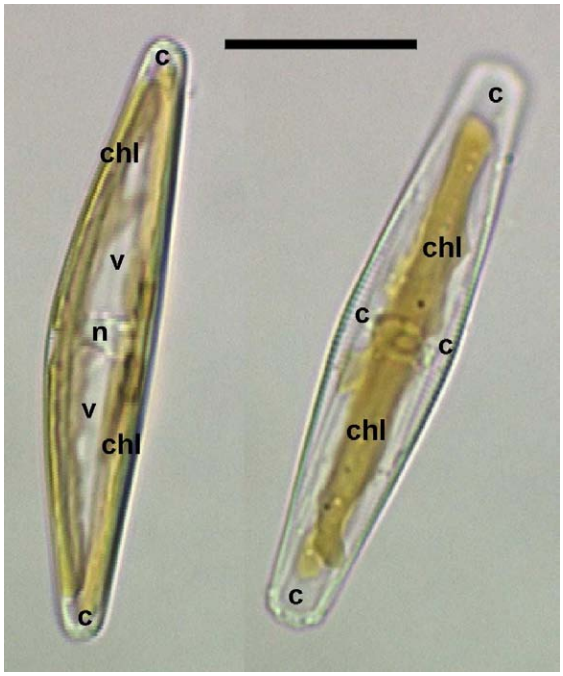

Figure 6-1 Light microscopy of *Seminavis* in raphe (left) and girdle (right) views. c = cytosol; chl = chloroplast; v = vacuole; n = nucleus. Scale bar = 20 µm.

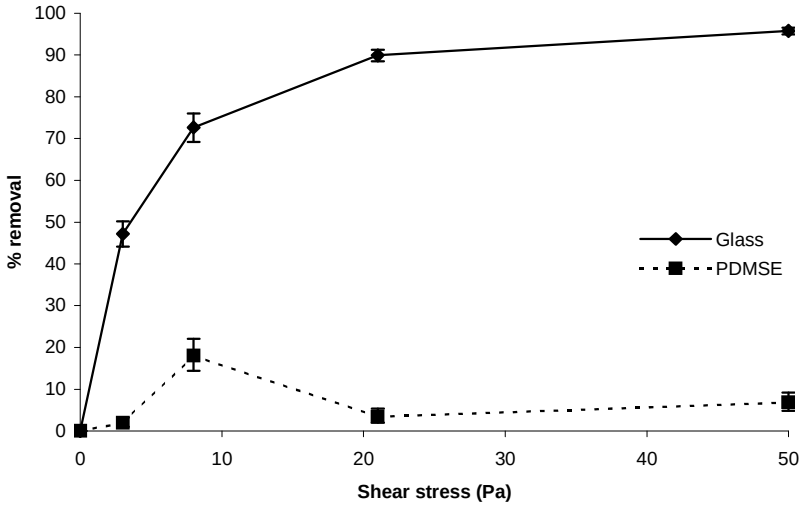

Figure 6-2 Adhesion strength of *Seminavis* to glass and PDMSE. The mean percentage removal of *Seminavis* from glass and PDMSE at various shear stresses generated in the flow channel. Data shown is representative of two experiments. The error bars are 95% confidence intervals from arcsine-transformed data.

6.3.2 Production of nitric oxide

The NO probe DAF-FM DA was used to measure intracellular NO production. Once DAF-FM DA passes through the cell membrane into the cell it is deacetylated by intracellular esterases to become active (Kojima *et al.*, 1999). When NO reacts with the compound it forms a fluorescent benzotriazole, the quantum yield of which is 160-fold higher than the inactive form (Kojima *et al.*, 1999). DAF-FM is highly specific for NO and does not react with reactive oxygen species (Foissner *et al.*, 2000). Hence an increase in fluorescence between 500-530 nm, after removal of autofluorescence, was attributed to an increase in NO emission.

6.3.2.1 Exposure to air

An important aspect of this study was the development of appropriate methods for the accurate detection of NO production in response to surfaces. As NO is produced as a stress response in many organisms including diatoms (Vardi *et al.*, 2006), it was essential to keep stress to a minimum to observe any NO production in response to the surface the diatom is adhered to. Whilst exposure to air is not a problem for cells on glass, as a layer of seawater will still surround the cells, on the hydrophobic PDMSE surface seawater is rapidly drawn off once the slide is removed from the medium.

Initial experiments performed with *Craspedostauros* led to stress-induced production of NO of cells settled on PDMSE, due to the cells being taken through the air-water interface. With increased exposure to air, *Craspedostauros* cells showed higher NO production and higher cell mortality (Figure 6-3). After only 60 s exposure to air over 90% of cells were dead.

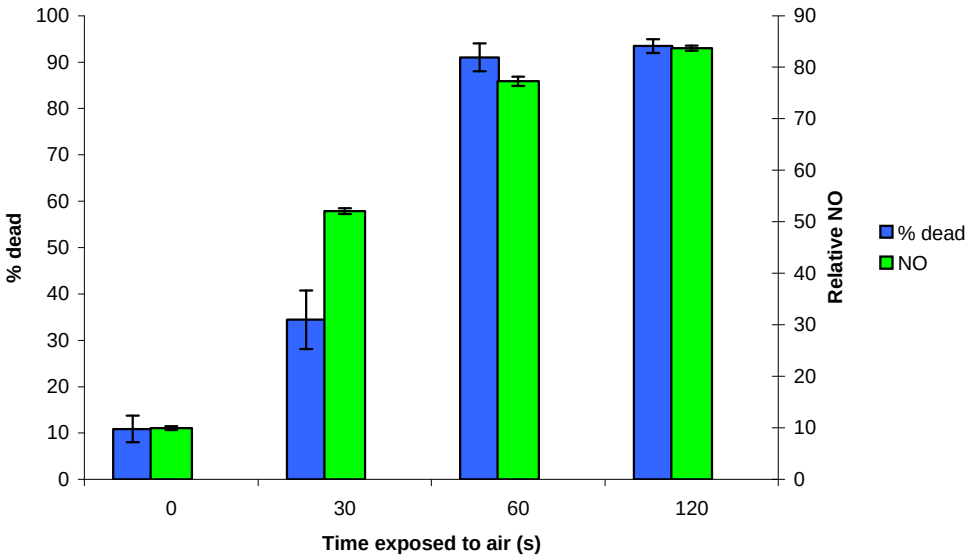

Figure 6-3 Nitric oxide production and cell death in cells exposed to air. Percentage of dead cells measured using DAF-FM in *Craspedostauros* cells after varying lengths of exposure to air. Increasing length of exposure to air significantly increased NO levels (F = 9.92; p <0.001; ANOVA) and the percentage of dead cells (F = 119; p <0.001; ANOVA). Data shown is representative of two experiments. Error bars are +/- standard error.

Statistically significant differences (Tukey test) were obtained between all levels of exposure except between 60 and 120 s, indicating that the greatest damage is done in the first minute of exposure to air when cells are settled on PDMSE.

Exposure to air could therefore lead to artificially high readings of NO in cells on PDMSE. Hence for experiments comparing the effect of different substrates, techniques were developed so that cells were not removed from the seawater for the duration of the experiment. All washing was done *in situ* by replacing old for new medium without exposing cells to air, and cells were imaged using a water-immersion lens.

6.3.2.2 Location of nitric oxide production

Using methods involving no exposure to air, NO production was apparent in *Seminavis* cells. In order to ascertain whether NO was being produced in the cytosol Fluorescein diacetate (FDA) was used as a general cell stain. Fluorescein labelling revealed cytosol is present surrounding the nucleus in the centre of the cell, along the sides and at the tips of the cell (Figure 6-4a and b). DAPI labelling confirmed the presence of the nucleus in the centre of the cell (Figure 6-4c). Nitric oxide production in response to surfaces was predominantly in the cytosol adjacent to the raphe as well as at the tips and sides of the cell (Figure 6-4d and e) and in some cells in the nucleus (Figure 6-4d) and chloroplast (Figure 6-4f). When NO levels were elevated due to incubation with the NO donor SNAP, NO emission was predominantly seen in the chloroplasts, vacuoles and cytosol at the tips of the cell (Figure 6-4g).

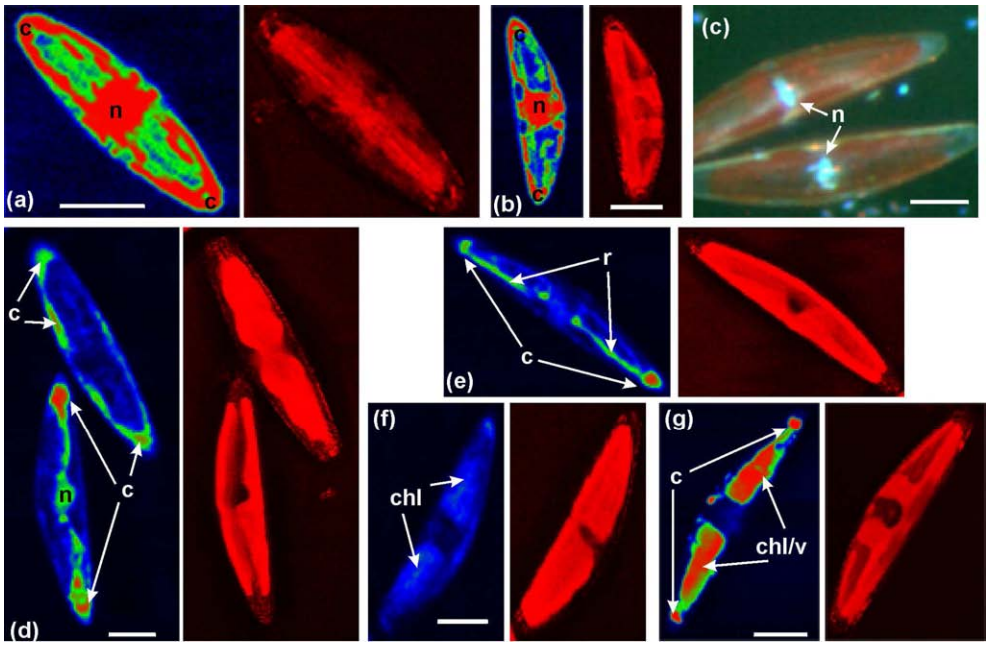

Figure 6-4 Localisation of nitric oxide production. Left image: False-colour (increase in fluorescence is shown from blue to red). Right: Chlorophyll autofluorescence. c = cytosol; n = nucleus; chl = chloroplast; v = vacuole. Bars = 10 µm. **a)** and **b)** Fluorescein diacetate was used to label the cytosol and revealed its presence at the ends, sides and middle of the cell. Two cells are shown, one in girdle view (a) and one in raphe view (b). **c)** The nucleus is labelled with DAPI (blue) and can be seen in the centre of the cell (red = chlorophyll autofluorescence). **d)**, **e)** and **f)** Cells loaded with DAF-FM most commonly showed labelling of the cytosol particularly around the raphe (d and e), with occasional labelling of the nucleus (d) and chloroplasts (f). **g)** Cells loaded with DAF-FM in high NO conditions due to incubation with the NO donor SNAP showed labelling of the chloroplasts and vacuoles as well as cytosol at the tips of the cells.

6.3.2.3 Comparison of nitric oxide production on glass and PDMSE

When overall NO production in cells settled on the two substrates for 2 h was compared, *Seminavis* showed significantly greater production of NO when settled on glass than on PDMSE (Table 6-1) with relative NO being 3-4.5-fold higher in cells settled on glass. Therefore the cells appear to be producing more NO when settled on a hydrophilic surface – a surface they show weaker attachment to – than when settled on a hydrophobic surface – a surface they show strong attachment to.

Table 6-1 Nitric oxide levels of *Seminavis* cells settled on glass and PDMSE. *Seminavis* cells settled on glass for 2 h had significantly higher levels of NO than those settled on PDMSE in all experiments. Relative NO values are minus control values of cells incubated in DMSO without DAF-FM.

		n	**Relative NO**	**% difference in relative NO**	***t***	***p***	**df**
1	**Glass**	69	13.83 +/- 1.27	294	9.03	<0.001	20
	PDMSE	59	3.51 +/- 0.45				
2	**Glass**	79	8.81 +/- 0.38	201	11.47	<0.001	20
	PDMSE	70	2.93 +/- 0.34				
3	**Glass**	90	11.97 +/- 0.83	353	11.33	<0.001	20
	PDMSE	77	2.64 +/- 0.29				

Using initial methods that involved some exposure to air, *Craspedostauros* showed variable NO production on glass and PDMSE. When the method involving no exposure to air was used there was no apparent NO production in *Craspedostauros*. When fluorescence values at 500-530 nm of control cells not incubated with DAF-FM were removed from cells incubated with DAF-FM, there was no net production of NO on either of the surfaces. It is thought that any DAF-FM fluorescence seen in previous experiments was due to stress from the cells passing though the air-water interface.

6.3.2.4 Nitric oxide production increases with increased settlement time

Seminavis cells showed increased NO production with increased settlement time on both glass and PDMSE (Figure 6-5). Nitric oxide production was significantly higher after 3 h settlement compared to after 1 h in all three experiments. Again, cells settled on glass showed higher NO production than cells settled on PDMSE. The rate of NO production over the time measured was similar between cells settled on glass and PDMSE (~60% increase) but it is likely that the dye may become saturated and/or compartmentalised after time and hence unable to respond to further increases in NO. Also it may be anticipated that it is during the first hour of settlement when cells are becoming accustomed to the surface that the biggest difference in production of NO is seen between the two surfaces.

6.3.2.5 Use of a nitric oxide donor

The NO donor S-nitroso-N-acetylpenicillamine (SNAP) was used to verify that DAF-FM was accurately reporting changes in NO in *Seminavis*. DAF-FM fluorescence was on average 3-fold higher in cells that were incubated with SNAP compared to control cells settled on glass (Table 6-2). The increase in DAF-FM fluorescence after the addition of NO indicates that DAF-FM is a reliable probe for NO detection in *Seminavis* cells.

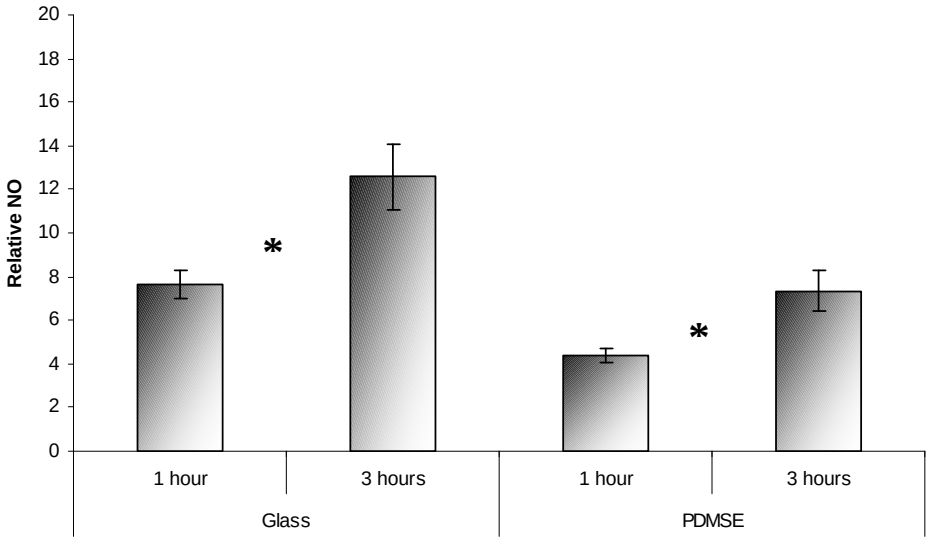

Figure 6-5 Effect of settlement time on the production of NO in *Seminavis* cells settled on glass and PDMSE. Cells settled on both glass and PDMSE for 3 h showed significantly higher production of NO than cells settled for 1 h. Nitric oxide production on glass was again higher than on PDMSE. Data shown is representative of three experiments. Approximately 50 cells were used for each time point. Error bars are +/- SE. * = significantly different to p <0.05.

Table 6-2 Nitric oxide levels of *Seminavis* cells incubated with the NO donor SNAP. *Seminavis* cells settled for 1 h had significantly higher levels of NO after incubation with 0.5 mM SNAP than cells incubated with an equivalent amount of DMSO (solute for SNAP) when settled on glass and PDMSE. Relative NO values are minus control values of cells incubated in DMSO without DAF-FM.

	Treatment	*n*	Relative NO	% difference in relative NO	*t*	*p*	df
1	SNAP Control	121 102	49.71 +/- 2.32 5.90 +/- 0.26	742.5	-33.25	<0.001	40
2	SNAP Control	54 59	35.84 +/- 2.50 12.34 +/- 0.73	190.4	-9.03	<0.001	16
3	SNAP Control	67 49	10.04 +/- 0.59 6.79 +/- 0.94	47.9	2.92	<0.001	20

6.3.2.6 Use of a nitric oxidase synthase inhibitor

To test whether the observed NO response involved NOS, cells were incubated with the NOS inhibitor NMMA whilst settled on glass. NMMA significantly reduced the production of NO (Table 6-3) by on average 30% implicating the possible involvement of NOS in NO generation in *Seminavis*. However, 70% of NO production was not inhibited in the presence of NMMA therefore there may be other pathways for NO production in *Seminavis*.

Table 6-3 Nitric oxide levels of *Seminavis* cells incubated with the NOS inhibitor NMMA. *Seminavis* cells settled for 1 h had significantly lower levels of NO after incubation with 0.5 mM NMMA than cells incubated with an equivalent amount of distilled water (solute for NMMA) when settled on glass. Relative NO values are minus control values of cells incubated in DMSO without DAF-FM.

	Treatment	*n*	Relative NO	% difference in relative NO	*t*	*P*	df
1	NMMA Control	68 72	18.17 +/- 1.25 26.07 +/- 2.07	-30.3	3.26	0.005	16
2	NMMA Control	79 113	23.43 +/- 3.16 31.77 +/- 2.41	-26.3	2.10	0.05	18
3	NMMA Control	65 95	23.00 +/- 1.86 34.59 +/- 2.00	-33.5	4.24	<0.001	18

6.3.3 Cells with higher nitric oxide levels show weaker adhesion

To assess whether artificially-enhanced levels of NO were associated with weaker adhesion, cells were pre-incubated with 0.5 mM SNAP in DMSO, or an equivalent amount of DMSO for the control treatment, settled on acid-washed glass for 2 h and then exposed to 2 Pa shear stress in the flow channel. Cells that had been pre-incubated with SNAP showed 24.9% higher percentage removal from glass than the control cells (Figure 6-6a). The increase in percentage removal was reproducible and highly significant ($p < 0.001$). Cells with higher intracellular NO production did not adhere as well as cells with lower NO; hence high NO levels are associated with reduced adhesion strength. The same trend was seen on PDMSE with cells showing

21.6% higher percentage removal in the presence of SNAP when subjected to a shear stress of ~21 Pa (Figure 6-6b). In the same experiment, cells settled on glass showed a very similar increase in percentage removal (20.4%) when exposed to SNAP (Figure 6-6b) hence increased NO causes the same effect in cells settled on glass as on PDMSE.

To eliminate the possibility that SNAP may have been affecting adhesion through indirect, non-specific effects on cell viability, the effect of SNAP on growth was examined. Cells were incubated with 0.5 mM SNAP, washed in fresh F2 and then growth rates were compared to control cells. Cells that had experienced high intracellular NO (3 times higher than normal) showed only a small, 6.4% increase in growth rate in the presence of SNAP over 48 h (control 0.469, SNAP 0.500 increase in cell number per day). Furthermore, assessments of cell viability using the mortal stain, revealed no difference in the percentage of dead cells on SNAP compared with control cells (SNAP 7.26 +/- 1.01% dead cells per 0.1 mm^2, control 7.91 +/- 2.07%). In addition, cells were still motile in the presence of SNAP.

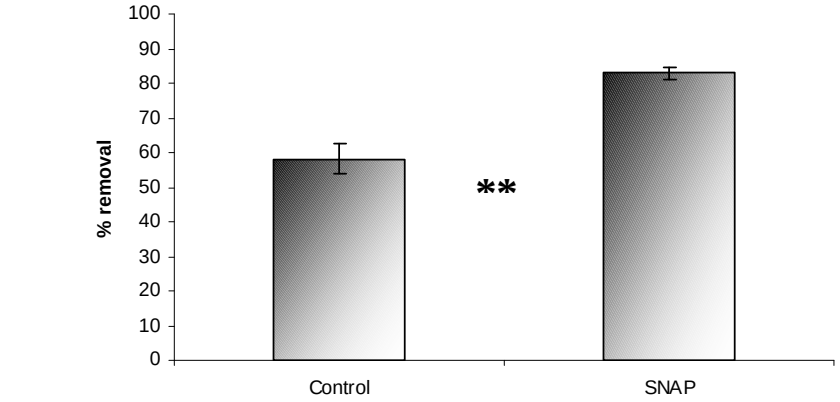

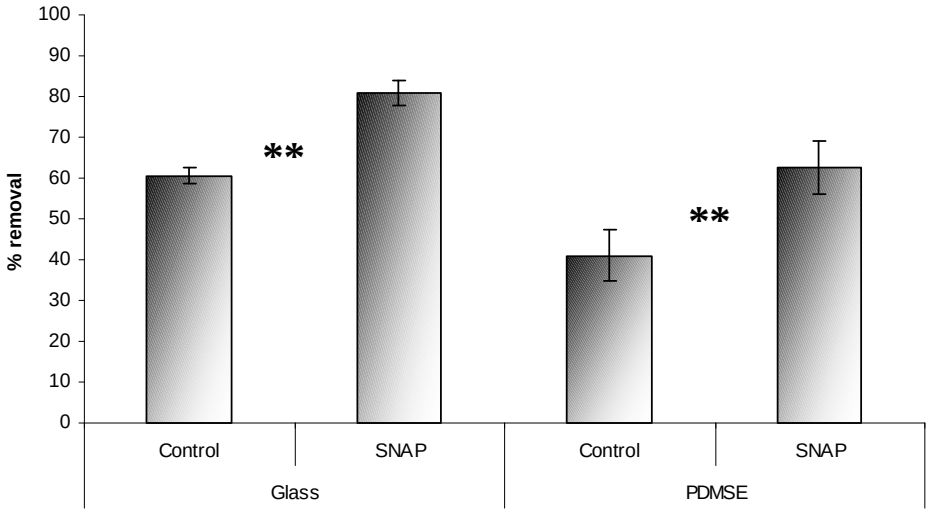

Figure 6-6 Addition of nitric oxide. a) Adhesion in the presence of high NO. Cells were incubated with SNAP or DMSO, settled for 2 h and then exposed to ~2 Pa in the flow channel. Cells incubated with SNAP (high NO) showed significantly higher percentage removal than control cells (data shown is representative of 5 experiments). **b)** Cells settled on PDMSE also showed significantly higher percentage removal when exposed to SNAP (data shown is representative of three experiments). Cells settled on glass were exposed to 2 Pa in the flow channel and cells settled on PDMSE were exposed to 21 Pa. Error bars are 95% confidence intervals from arcsine-transformed data. ** = significant difference to p <0.001.

6.3.4 Cells with lower nitric oxide show stronger adhesion

To assess the effect of lower NO production on adhesion, cells were incubated with 0.5 mM NMMA or an equivalent amount of distilled water, settled on acid-washed glass for 2 h and exposed to 2 Pa shear stress in the flow channel. Cells that had been incubated with NMMA showed significantly lower percentage removal (15%) than control cells (Figure 6-7). Cells with lower intracellular NO production therefore adhere more strongly. However, NMMA only reduced NO levels by 30% whereas SNAP increased NO levels by 300% which may explain the smaller difference seen in adhesion with the addition of NMMA compared to SNAP. Cells were still motile after the addition of NMMA and cell mortality assessed with Evans Blue was not significantly different to control cells (NMMA 3.02% +/- 0.85 dead cells per 0.1 mm^2, control 2.74% +/- 0.46). However the relative growth rate was significantly reduced by 27% over 72 h (two-way ANOVA, $F = 86.54$, $p < 0.001$) in cells that had been incubated previously with NMMA (but were washed after exposure) indicating that NO may be important for growth in *Seminavis*. The difference in growth rate was particularly apparent over the first 24 h with a 60.6% decrease in relative growth rate (control 0.66, NMMA 0.26 increase in cell number per day).

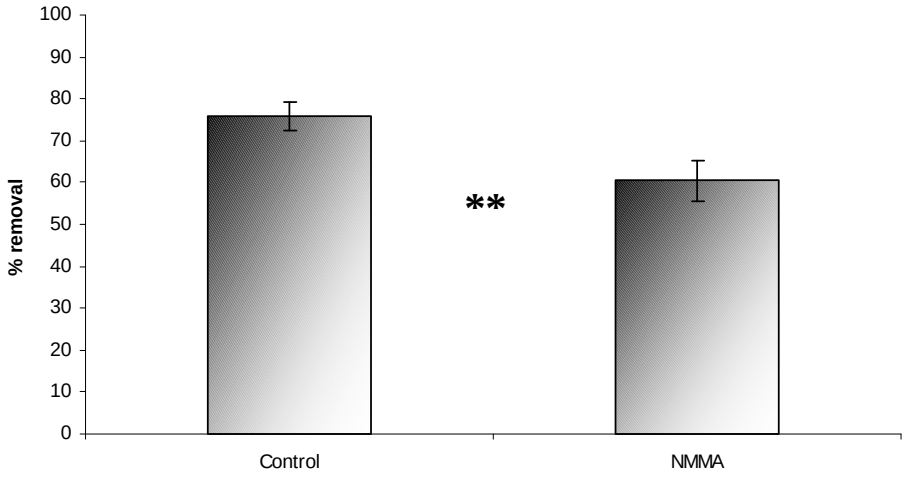

Figure 6-7 Addition of a nitric oxidase synthase inhibitor. Cells were incubated with NMMA or distilled water, settled for 2 h on glass and then exposed to ~2 Pa in the flow channel. Cells incubated with NMMA (lower NO) showed significantly lower percentage removal than control cells (data shown is representative of two experiments). Error bars are 95% confidence intervals from arcsine-transformed data. ** = significant difference to p <0.001.

6.4 Discussion

Adhesion of *Seminavis* was stronger on the hydrophobic PDMSE surface than to glass which agrees with observations made on other raphid diatoms (Holland *et al.*, 2004). *Seminavis* showed a similar strength of attachment to *Navicula perminuta* (Holland *et al.*, 2004) in that only a small percentage of cells were removed from PDMSE at wall shear stresses up to 53 Pa (the highest pressure in the flow channel). Adhesion of *Seminavis* was stronger than either *Craspedostauros australis* or *Amphora coffeaeformis* which required 17 and 24 Pa respectively for 50% removal from PDMSE (Holland *et al.*, 2004). Therefore *Seminavis* can be described as a strongly adhering diatom that is difficult to remove from hydrophobic surfaces whereas *Craspedostauros* can be described as a weakly adhering diatom.

The cytosol was the most common area for NO production in *Seminavis* in response to surfaces. Production of NO was also seen in the chloroplast and nucleus. However there may be differential accumulation of the dye in cellular compartments and this cannot be ruled out when using a single-wavelength dye (Foissner *et al.*, 2000). These results are consistent with results reported by Foissner *et al*. (2000) and Huang *et al*. (2002) who found NO production and/or accumulation particularly in the cytosol, chloroplast and along the plasma membrane when stimulating cell death in epidermal tobacco cells with the fungal elicitor cryptogein. Gould *et al.* (2003) also discovered NO production in the cytosol and chloroplast in tobacco leaf cells in response to stress. The diatom *P. tricornutum* showed NO production/accumulation closely associated with the nucleus (Vardi *et al.*, 2006). It is therefore likely that the cytosol and chloroplasts are acting as a source of NO in plant cells with possible additional production in diatoms associated with the nucleus. Nitric oxide synthases have been

reported in the cytosol (Ribeiro Jr. *et al.*, 1999) and chloroplasts of plant cells (Barroso *et al.*, 1999).

Nitric oxide production was predominantly seen in the cytosol adjacent to the raphe. The raphe is where EPS is secreted from (Hoagland *et al.*, 1993) and hence is the site of adhesion and motility processes in raphid diatoms such as *Seminavis*. It is therefore possible that NO production is concentrated in the area where it can affect adhesion/motility.

Seminavis showed greater production of NO on a hydrophilic surface that it weakly attaches to than on a hydrophobic surface that it strongly adheres to. Hence the cell appears to be producing NO in response to the adhesive properties of the surface it is adhered to. The possibility that DAF-FM is absorbed by the silicone surface PDMSE so that less is available for uptake into the cell can be dismissed as NO production occurred at a similar rate in cells settled on glass and PDMSE when measured over 3 h.

In *Craspedostauros* there was no detectable NO production in response to hydrophilic vs. hydrophobic surfaces. This difference, compared to the strong differential response shown for *Seminavis*, could be related to that fact that *Craspedostauros* shows weak adhesion to both of the substrates tested (Holland et al. 2004). If *Craspedostauros* is only weakly attached in the first place then it may be less able to sense differences in the surface compared to *Seminavis*. Therefore the difference shown by the two species in NO production in response to the substratum may be due to their differing strengths of attachment.

Results have shown that care must be taken when using hydrophobic surfaces as taking the cells through the air-water interface causes stress to diatoms. The high hydrophobicity of PDMSE means that when the surface is removed from seawater the water very quickly runs off and can leave cells exposed to air. Being exposed to air for just 30 s caused death in over 50% of *Craspedostauros* cells. In diatoms cell dehydration causes a decrease in ATP which in turn inhibits photosynthesis. Iron may accumulate which can then catalyse a stress response through the Fenton reaction (Rijstenbil, 2003). Under natural conditions the diatoms would be part of a biofilm in which the exopolymers (EPS) produced for movement and adhesion prevent desiccation by keeping a hydrated layer around the diatoms (Bhosle *et al.*, 1996). In the experiment cells were only settled for 1 h so there would not have been time for mucilage to accumulate.

Nitric oxide can act as a messenger or can itself be a regulator of physiological processes (Delledonne, 2005). Downstream events of NO production in mammals are mediated by the stimulation of soluble guanylate cyclase and subsequent production of cyclic GMP (cGMP) (Bicker, 2005). In animals, NO is a regulator of motility of cells (Bicker, 2005) and it is proposed that the regulation of cell motility by NO/cGMP signalling has been conserved through evolution predating diversification in plants and animals (Bicker, 2005). It is therefore possible that NO signalling could control motility in diatoms and by reducing adhesion to the surface, NO could allow *Seminavis* to move off a surface more easily and find a more suitable microhabitat. It would be interesting to determine if motility was increased by the addition of the NO donor SNAP but assays for motility are difficult to quantify as movement in diatoms can vary significantly from day to day (Poulsen *et al.*, 1999).

In *Seminavis*, increased levels of NO induced by the use of an exogenous NO donor caused a significant reduction in cell adhesion to both glass and PDMSE. Nitric oxide acts as a regulator of cell adhesion in animals (eg. Lefer & Lefer (1996)) causing inhibition of adhesion in platelets and other cell types such as neutrophils (Loscalzo & Welch, 1995). Our findings suggest that in *Seminavis*, NO may also cause inhibition of adhesion either through blocking the secretion of adhesive making the cell more likely to detach and move off the surface, or alternatively NO could cause the production of a less sticky adhesive or prevent cross-linking of the polymer (Wigglesworth-Cooksey & Cooksey, 1992) leading to an adhesive that is more conducive to movement. It has already been shown that diatoms can modify the production of EPS in relation to environmental changes indicating a high degree of genetic control (Abdullahi *et al.*, 2006); hence it is possible that *Seminavis* can modify the production of EPS in response to the substratum. On a surface that the cell sticks well to such as PDMSE, there is no signal to produce NO so the cell remains adhered to the surface. For a summary of the proposed mechanism of action of NO on hydrophilic and hydrophobic surfaces see Figure 6-8.

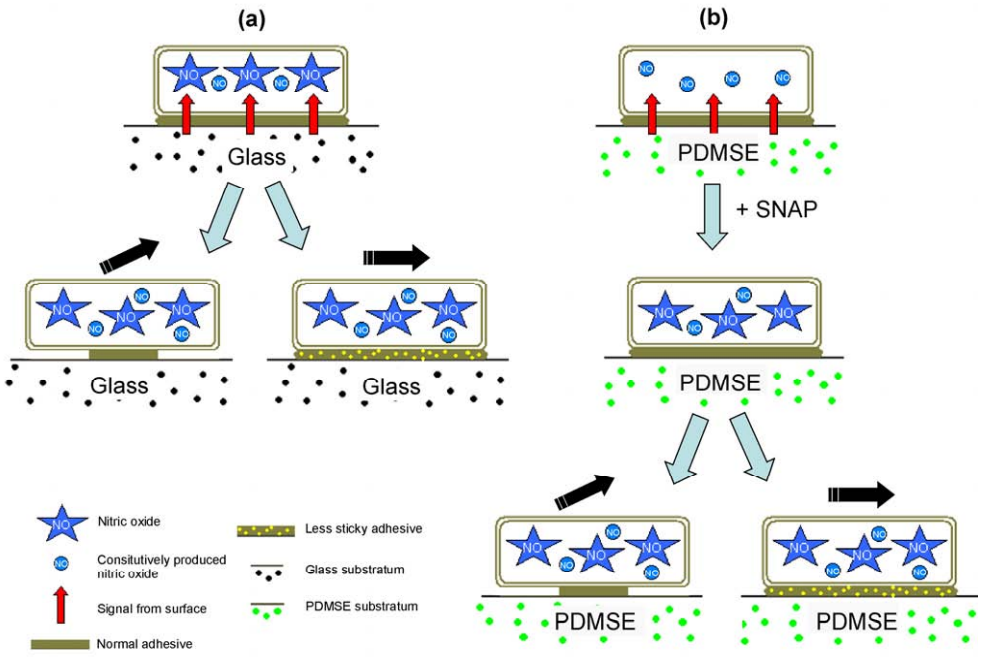

Figure 6-8 Summary of the possible action mechanisms of nitric oxide in relation to surfaces in *Seminavis*. a) *Seminavis* detects the adhesiveness of a surface through an unknown signal. A signal from a surface that the cell does not adhere to strongly causes the production of NO in the cell. Nitric oxide then either blocks the secretion of adhesive making the cell more likely to detach and move off the surface and/or NO causes the production of a less sticky adhesive which is more conducive to movement resulting in reduced attachment strength. **b)** When *Seminavis* is adhered to a surface that it sticks well to such as PDMSE the signal from the surface does not cause the production of NO. There is however some constitutively produced NO in the cell that is necessary for growth. Nitric oxide is not elevated so the cell does not move off the surface. When NO is added to the cell through the addition of the NO donor SNAP, NO levels in the cell are increased causing reduced adhesion through the same pathways given in a).

Levels of NO that are 3-fold those under normal conditions do not appear to be toxic to cells or inhibit growth. In fact when production of NO was inhibited by the NOS inhibitor NMMA, growth was inhibited implying that NO may play a protective role in *Seminavis*. Inhibition of growth by addition of NOS inhibitors was also seen in sea urchin embryos (Semenova & Ozernyuk, 2004) and in Antarctic *Chlorella* and *Chlamydomonas* (Estevez & Puntarulo, 2005). Nitric oxide is known to be a stress-coping factor aiding survival (Beligni & Lamattina, 2001). In the chlorophyte algae *Scenedesmus* addition of NO via a NO donor was found to ameliorate the damage caused by reactive oxygen species produced in stress responses (Mallick *et al.*, 2002).

The NOS inhibitor NMMA significantly reduced the production of NO implicating the possible involvement of NOS in NO generation in *Seminavis* as Vardi *et al.* (2006) also found in the diatom *P. tricornutum*. When NO production was reduced through incubation with NMMA, adhesion to glass was stronger enforcing the idea that NO is important in adhesion. However only 30% of the NO production was stopped by inhibiting NOS indicating that non-enzymatic production of NO may also be important or that the inhibitor used was not totally effective. Production of NO from nitrite is common in algal cultures grown with nitrate (Mallick *et al.*, 2000) and the culture media used in this experiment (F2) contained ~0.1 mM nitrate. Nitrite can either be reduced non-enzymatically under acidic conditions in compartments or nitrate reductase can catalyse the reduction of nitrite over a wide pH range (Beligni & Lamattina, 2001). It has been found that NOS inhibitors including NMMA, although inhibiting enzymatic production of NO through NOS, can encourage non-enzymatic production of NO possibly due to the release of nitrite from the inhibitor (Moroz *et al.*, 1998). Hence the application of NMMA can lead to a lower decrease than expected in NO production (Moroz *et al.*, 1998). Therefore the NO production not

prevented by NMMA may be due to non-enzymatic production of NO that either occurred naturally in the cell or as a result of the addition of the NOS inhibitor. In addition, the two plant NOS genes that have been identified are structurally different to mammalian NOS (del Río *et al.*, 2004) hence NMMA designed as an inhibitor of mammalian NOS may not be as effective on plant NOS.

6.5 Conclusions

Seminavis cells produce NO in relation to surfaces. The intracellular NO levels created by addition of an NO donor do not result in cell death, prevent motility or growth and hence may instead be a signalling mechanism for detecting surfaces. Increased intracellular NO levels reduced attachment strength. This may be of benefit to a diatom in that if it produces NO in response to a surface that it does not stick to well (such as a hydrophilic surface) this could signal the cell to detach from the surface and move off to a surface to which it can stick better (a hydrophobic surface).

7: GENERAL DISCUSSION

7.1 Aims and objectives

The aim of the research presented in this thesis was to investigate the cell biology behind the settlement and adhesion processes of biofouling algae in order to understand the various membrane and other signalling events that are involved in the adhesive systems. This was carried out using zoospores of the macroalga *Ulva* during the spring and summer months, and microalgal, raphid diatoms during the autumn and winter.

In the life cycle of *Ulva*, zoospores are produced in order to disperse and colonise new surfaces. Therefore it is the settlement and establishment of this stage of the life cycle that is most important to understand so that cells can be prevented from settling on man-made submerged structures. Previous studies on *Ulva* zoospores have revealed that mass exocytosis of the adhesive occurs at settlement (Callow *et al.*, 1997; Stanley *et al.*, 1999). It was therefore of interest to investigate the cellular events surrounding settlement in order to determine what triggers the mass secretion of adhesive. It was hypothesized that during settlement of *Ulva* zoospores, plasma membrane recycling would be required in order to balance the exocytosis of vesicles that occurs during adhesive secretion.

Calcium is a major regulator of exocytosis in the plant cell (Battey & Blackbourn, 1993) and an increase in $[Ca^{2+}]_{cyt}$ has been shown to regulate exocytosis in the algae *Fucus serratus* (Roberts *et al.*, 1994) and *Phaeocystis globosa* (Chin *et al.*, 2004). It was therefore hypothesized that an increase in $[Ca^{2+}]_{cyt}$ triggers exocytosis of the adhesive from *Ulva* zoospores.

In addition to the glycoprotein adhesive released at settlement, there is also thought to be release of products that cure the adhesive through cross-linking (Evans & Christie, 1970; Stanley *et al.*, 1999; Humphrey *et al.*, 2005). It was hypothesized that there is vesicular secretion of products after settlement that cross-link the zoospore adhesive and that these products may be redox-active.

Diatoms have been shown to possess sensing mechanisms to allow them to perceive changes in the environment such as turbulence, osmotic stress and dissolved oxygen levels (Falciatore *et al.*, 2000). Therefore, it was hypothesized that detection of an unfavourable surface i.e. one that they do not stick well to, could trigger a stress response. Nitric oxide has been shown to be involved in stress responses in algae (Vardi *et al.*, 2006) hence the hypothesis was that diatoms produce NO upon detection of an unfavourable surface.

In order to address these hypotheses, the following experimental objectives were set:

1. To investigate membrane dynamics during the settlement process.
2. To evaluate AM ester and dextran Ca^{2+} indicators for use with *Ulva* zoospores.
3. To determine whether changes in cytosolic calcium are involved in zoospore settlement and adhesion.
4. To investigate whether oxidisable products are released to cure the adhesive and if so, over what timescale after settlement.
5. To determine if there is any difference in NO production by diatoms showing differential adhesion to surfaces of different wettability.

6. To determine if manipulating the levels of NO through the use of inhibitors and promoters of NO production affects adhesion properties.

7.2 Technical achievements of the research

7.2.1 Confocal imaging

One of the most important method developments presented in this thesis was the evolution of techniques for capturing images of motile cells on the CLSM. The CLSM forms an image from individual scan lines which limits the speed of imaging (see Chapter 2) and therefore to measure changes in fluorescence over time, cells need to remain in one place. Initial techniques encouraged spore settlement in one particular location. Although this was adequate for cells loaded with AM-esters or the styryl dye FM 1-43, for cells that had been shot with pellets of dye, the proportion of cells settling was reduced (personal observation). In these cases it was necessary to induce settlement through the addition of low-melting point agarose.

The development of protocols for immobilizing cells, to a large extent solved the problems of imaging motile cells. However, an additional difficulty was created by the change in shape of the spore as it settled (from pear-shaped to spherical), which can result in a change in fluorescence signal. Ratio imaging whereby both a Ca^{2+}-dependent fluorescence signal and a Ca^{2+}-independent fluorescence signal are obtained was therefore used to minimise any Ca^{2+}-independent changes in dye fluorescence.

7.2.2 Calcium indicator loading

Evaluation of AM-ester and dextran Ca^{2+} indicators showed conclusively that the use of dextran-conjugated indicators was essential with such a motile and morphologically dynamic organism as the *Ulva* zoospore. Initially it was hoped that AM-ester dyes would be suitable as there were no convenient methods available for loading dextran-conjugated indicators. However, when loaded into cells as AM esters, the dyes were sequestered into subcellular compartments leaving insufficient dye in the cytosol and resulting in significant contamination of the fluorescence signal from compartmentalised dye. Biolistic bombardment allowed routine delivery of multiple dextran-conjugated indicators into a motile cell, allowing ratio imaging to minimize potential artifacts arising from changes in cell shape and movement. The biolistic procedure is quick and simple resulting in ~10% of cells being loaded with the dye as opposed to microinjection of dextran dyes which would be impossible on a mass scale in such a small and motile organism.

Oregon Green BAPTA-1 dextran showed a 5-fold greater response in apparent cytosolic Ca^{2+} levels to Ca^{2+} ionophores than the AM-ester Oregon Green BAPTA-5N indicating that the AM-ester dye was sequestered into compartments in the cell and that dextran dyes provide a significantly more accurate measurement of $[Ca^{2+}]_{cyt}$. Cells of the dinoflagellate *Crypthecodinum cohnii* loaded with the AM-ester Calcium Orange (Lam *et al.*, 2005) showed a similar increase in Ca^{2+} dye fluorescence in response to Ca^{2+}-ionophores to that seen in *Ulva* using the AM-ester Oregon Green BAPTA-5N, suggesting that significant dye compartmentalisation was occurring.

7.2.3 Amperometric measurements

Using the amperometric technique it was possible to detect individual secretory redox-active events from mechano-stimulated settled spores. The secretory events detected in *Ulva* spores are one of the first demonstrations of algal or plant single secretory events. Individual exocytotic events have also been recorded in protoplasts from coleoptiles of *Zea mays* using cell attached capacitance measurements (Thiel *et al.*, 1998) although measurements have not yet been made with intact cells like the *Ulva* spore and protoplast preparation procedures may result in loss of receptors and components of signalling pathways (Thiel & Battey, 1998).

7.2.4 Measuring stress responses in diatoms

Production of NO in diatoms was measured in individual cells using the fluorescent dye DAF-FM diacetate. This probe had previously been used in the diatom *Phaeodactylum tricornutum* (Vardi *et al.*, 2006) and has been shown to be specific to NO (Balcerczyk *et al.*, 2005) and to not react with reactive oxygen species (ROS) (Foissner *et al.*, 2000). Trials were conducted with the ROS probe 2',7'-dichlorodihydrofluorescein diacetate (H_2DCFDA) but the cells did not appear to load with the probe as when adding H_2O_2 to the solution there was no increase in fluorescence.

Initial experiments with diatoms and DAF-FM were hampered by the sensitivity of diatoms to exposure to air when settled on hydrophobic surfaces on slides. Removing slides through the air-water interface caused water to rapidly withdraw across the surface, which caused large elevations in [NO] within the cells and cell death. Imaging experiments were therefore designed to prevent any exposure to air by using

a water-immersion objective and washing slides *in situ* by replacing old solutions with new. However such modifications were not possible when using the flow channel and the fact that nearly 100% cell death can occur after only 1 min exposure to air has implications for method development when testing hydrophobic surfaces in the future.

When NO production was measured in diatoms previously, quantification of DAF-FM fluorescence was made using a Fluorescence Microplate Reader or flow cytometer (Vardi *et al.*, 2006). Therefore only production of NO by the whole population was measured, not in individual cells. It was not possible to measure NO production by the whole population for this study as a Fluorescence Microplate Reader and flow cytometer require cells that are in suspension. Therefore it would not be possible to measure NO production in cells attached to surfaces. Use of the CLSM allowed measurement of NO in individual cells attached to surfaces. However, because of the high variability involved in such a method, it was necessary to find a raphid diatom with a sufficiently large expanse of cytosol. Initial trials were conducted with *Navicula perminuta* (length 5 µm), however the small size of the cell and the large proportion of the cell taken up by the chloroplast meant that the DAF-FM signal from the cytosol was too small. *Seminavis* is significantly larger (length 30-50 µm) and the cytosol is easily visible at the tips of the cell hence DAF-FM fluorescence can be more accurately recorded.

7.3 Novel outcomes of the research

7.3.1 Membrane dynamics during settlement of Ulva *zoospores*

Mass membrane recycling occurs rapidly at settlement

The fluorescent styryl dye FM 1-43 was used to assess membrane dynamics in the *Ulva* zoospore at settlement. Intracellular FM 1-43 labelling indicated that internalisation of the plasma membrane occurred both in swimming and settled spores but mass endocytosis only occurred in spores undergoing settlement. The *Ulva* zoospore system was found to be highly dynamic at settlement with rapid membrane recycling occurring to balance the mass exocytosis of adhesive. This appears to be one of the most dynamic membrane recycling processes observed to date in a plant or algal cell and it is likely that the rapid internalisation in *Ulva* zoospores is closely associated with the rapid secretory characteristics of this cell during settlement. The only other published example of plasma membrane recycling at a similar speed in an alga is in *Fucus serratus* embryos where hypoosmotic treatment resulted in rapid internalization of FM 1-43 within 20 s of the shock (Battey *et al.*, 1999).

Plasma membrane is recycled to an endosomal-like compartment

The retrieved membrane is targeted to an endosomal-like compartment that had not previously been shown in published electron micrographs (Evans & Christie, 1970). The existence of endosomes in plants has been shown (Meckel *et al.*, 2004), however their presence in algae had previously not been documented. Endosomes are formed as a result of receptor-mediated endocytosis involving coated pits and vesicles. Clathrin forms the protein coat in coated pits and vesicles (Battey *et al.*, 1999) hence further support for the existence of targeted membrane retrieval is provided by

molecular data indicating the presence of clathrin vesicle coat proteins in sporulating *Ulva* tissue (Stanley *et al.*, 2005).

Settlement marker

The plasma membrane recycling that occurs after zoospore settlement to an endosomal-like compartment in a FM 1-43 labelled cell results in a spot of intracellular FM 1-43. This can be used as a visual marker for settlement of individual cells on a surface and indicates that the cell has extruded its adhesive.

7.3.2 Calcium dynamics during settlement

Elevations in cytosolic calcium accompany settlement

Initial investigations with AM-ester Ca^{2+}-indicators suggested that there were elevations of $[Ca^{2+}]_{cyt}$ during settlement. Use of dextran-conjugated Ca^{2+}-indicators confirmed that there were both transient and prolonged elevations of $[Ca^{2+}]_{cyt}$ at settlement. The elevations were concomitant with loss of the flagella sheaths and the cell rounding up which both occur as the cell secretes adhesive. Calcium-regulated secretion has been shown in other algae such as *Fucus* (Roberts *et al.*, 1994) and *Phaeocystis* (Chin *et al.*, 2004). It is therefore proposed that a major role of elevated $[Ca^{2+}]_{cyt}$ during *Ulva* zoospore settlement is in the regulation of exocytosis of the adhesive vesicles.

Localised elevations in cytosolic calcium may be associated with loss of the flagella sheaths at settlement

The localised elevations in $[Ca^{2+}]_{cyt}$ which occurred near the base of the flagella during settlement may be associated with loss of the flagella sheaths. In motile

Chlamydomonas cells, deflagellation is associated with a localised elevation in $[Ca^{2+}]_{cyt}$ at the base of the flagella (Quarmby, 1996; Bothwell *et al.*, 2006). Although deflagellation in *Chlamydomonas* is different in that the whole flagella are excised, it is possible that loss of the flagella sheaths in *Ulva* is also a Ca^{2+}-dependent process.

Calcium channel inhibitors reduce settlement

The reduction in settlement of *Ulva* zoospores in the presence of the Ca^{2+}-channel inhibitors verapamil and Gd^{3+} at concentrations that did not reduce swimming speed indicates that an influx of extracellular Ca^{2+} is required for settlement and that a rise in $[Ca^{2+}]_{cyt}$ is required to allow settlement to proceed. Verapamil and Gd^{3+} have been used to show the Ca^{2+}-dependence of chemotaxis (Ermilova *et al.*, 1998) and deflagellation (Quarmby, 1996) respectively in *Chlamydomonas*.

7.3.3 Redox related processes during settlement

There is a population of vesicles containing redox-active molecules in* Ulva *zoospores

The question of post-settlement secretion of redox-active substrates that aid curing of the adhesive was explored using amperometry. This provided further evidence for exocytosis in *Ulva* spores but release of redox-active substances was only detected after mechano-stimulation of settled spores or in the bulk medium of settling populations of cells. Release of oxidisable products from *Fucus* eggs occurred spontaneously (Taylor, A.R. in prep.). It is thought that spontaneous release of redox-active substrates may not have been detected from individual cells undergoing settlement due to contamination of the CFME active surface with spore adhesive

resulting in reduced sensitivity. When a settled cell is prodded the CFME tip may be wiped clean allowing closer access to the plasma membrane.

The mechano-stimulated secretory characteristics of* Ulva *are very similar to bovine chromaffin cells

When bovine chromaffin cells were mechanically stimulated by non-destructive but forceful contact, secretory events had a similar duration (25 cf 26 ms half-width) and charge (amount of molecules released per event) (Wightman *et al.*, 1991; Moser *et al.*, 1995) to those detected from *Ulva* spores. *Fucus* eggs spontaneously secrete oxidisable products with a slower half-width (3x slower) and larger charge (4x) than *Ulva* (Taylor, A.R. in prep.). The secretory characteristics of *Ulva* therefore seem more similar to those of animal cells than of the brown alga *Fucus*, which probably reflects the similarity in size of the intracellular secretory vesicles in these smaller cells.

A fusion pore may be involved in exocytosis in* Ulva *spores

The high temporal resolution that the amperometric technique allows has provided information on the kinetics of vesicle release in *Ulva* spores. The foot signal sometimes seen preceding the main peak of current may represent leakage of molecules out of a narrow 'fusion pore' before full fusion of the vesicle with the plasma membrane (Chow *et al.*, 1992; Monck & Fernandez, 1992). The low frequency of foot events compared to chromaffin (Zhou *et al.*, 1996) and *Fucus* cells (Taylor, A.R. in prep.) may signify that the kinetics of fusion pores in the release of the redox-active substance in *Ulva* spores differ from other cells in that they dilate at a

greater rate so that there is little leakage of vesicle contents before full fusion with the plasma membrane.

7.3.4 Substrate-related signalling in diatoms

Seminavis *cells produce nitric oxide in relation to surfaces*

Experiments with the diatom *Seminavis robusta* revealed substantial basal NO production in relation to the substratum. Nitric oxide production increased with settlement time and was 4-fold greater on a surface to which the cells adhered weakly than on a surface to which they attached more strongly. *Craspedostauros australis* did not show any significant NO production on surfaces, possibly due to its comparatively weak attachment to all surfaces (Holland *et al.*, 2004). Nitric oxide production has also been recorded in the diatom *P. tricornutum* (Vardi *et al.*, 2006) but not in response to surfaces.

Increased intracellular nitric oxide levels in* Seminavis *causes reduced attachment strength

By increasing NO production 3-fold through the addition of the NO donor SNAP, adhesion strength was reduced by 25%. By decreasing NO production by only 30% using the NOS inhibitor NMMA, adhesion strength was increased by 15%. Hence NO appears to reduce adhesion strength in *Seminavis*. It is proposed that NO has a signalling role in *Seminavis* so that a cell produces NO in response to a surface that it does not adhere well to (such as a hydrophilic surface), which could then signal the cell to detach from the surface and move away to a surface where it can attach more strongly (a hydrophobic surface). Nitric oxide has been shown to be a regulator of

adhesion in animals causing inhibition of adhesion in platelets and other cell types such as neutrophils (Loscalzo & Welch, 1995).

Five of the six initial objectives have therefore been achieved by the work undertaken in this thesis (see Section 7.1). Objective number four ('to investigate whether oxidisable products are released to cure the adhesive and if so over what timescale after settlement') could not be completed, as it was not possible to clearly link the secretion of oxidisable products with settlement. Moreover, the work accomplished has raised many further questions that hopefully will be considered by future researchers in this field.

7.4 Potential areas for future work

To elucidate the structure of the endosomal compartment, transmission electron microscopy (TEM) can be used to view the spore ultrastructure (Evans & Christie, 1970). Both swimming and settled spores could be sectioned for use in the TEM and images compared to look for the presence of a large (~1 µm in diameter), membranous compartment in the anterior of the cell.

To investigate single secretory events at settlement, a Total Internal Reflection Fluorescence (TIRF) system (see Chapter 1, section 1.4.2) of sufficient resolution may be used. Exocytosis could be viewed by loading with the Ca^{2+} indicator Calcium Orange-AM that is shown in Chapter 4 (section 4.3.1) to accumulate in the adhesive vesicles. Exocytosis of single vesicles loaded with the Calcium Orange 'cargo' could then be viewed at the immediate plasma membrane before, during and after fusion and release of the fluorescent cargo (Zenisek *et al.*, 2002). Using this technique,

fusion characteristics of the vesicles and the location of their release from the plasma membrane could be investigated.

The secretory process in *Ulva* zoospores has been found to be highly dynamic with evidence of targeted membrane retrieval. In order to investigate the secretory process in more depth, various molecular studies could be undertaken to answer the question – ***what are the components of the zoospore secretory pathway?*** Molecular studies of sporulating tissue of *Ulva linza* have already revealed expressed sequence tags (ESTs) for a clathrin vesicle coat protein and a putative membrane transporter protein (Stanley *et al.*, 2005). Further elucidation of ESTs from sporulating tissue could be undertaken to investigate the presence of the docking proteins SNAREs which are responsible for the correct targeting and fusion of secretory vesicles and have been discovered in *Arabidopsis* (Surpin & Raikhel, 2004) and RabGTPases which are endomembrane-compartment-specific small GTP binding proteins that are involved in the docking and fusion of vesicles (Vernoud *et al.*, 2003).

If the study organism were *Arabidopsis* then there would be multiple options for interfering with functionality to determine if SNAREs are involved in secretion e.g. to create knockout mutants. In *Ulva* zoospores however the options are limited. It is possible that RNA interference (RNAi) technology could be used where synthetic double-stranded RNA (dsRNA) introduced into cells can suppress specific genes of interest. Biolistic delivery of dsRNA has been performed in plants (Klahre *et al.*, 2002) where the gold particles instead of being coated with dye (Chapter 4) are coated with DNA or RNA (Watson *et al.*, 2005). It may then be possible to shoot dsRNA specific for the SNARE genes for *Arabidopsis* into *Ulva* zoospores and then test for functionality.

If it is possible to isolate and purify the endosomal compartment from settled spores then proteomics could be used to identify what proteins are present in the compartment and could therefore be involved in membrane trafficking. This type of study has been undertaken with vacuoles in *Arabidopsis*. SNARE proteins were found to be present in the vacuole which is a major part of the membrane recycling pathway in *Arabidopsis* (Carter *et al.*, 2004).

Which processes are Ca^{2+} dependent? The discovery of elevated $[Ca^{2+}]_{cyt}$ at settlement merits further investigation: this should focus on the detailed characteristics of the $[Ca^{2+}]_{cyt}$ signals which may underlie the three processes occurring at settlement, namely secretion, loss of flagella sheaths and cell shape changes. To distinguish between the various processes taking place at settlement, a higher temporal resolution is required. With the CLSM used for this project, the maximum imaging speed was 1 image per 100 ms, the actual speed used for Ca^{2+} imaging was 1 image per 667 ms since at higher imaging speeds resolution deteriorated. There is a trade-off between spatial and temporal resolution with confocal imaging. The desired spatial resolution may be unobtainable at the desired temporal resolution. This is because as the acquisition rate increases, the spatial resolution decreases as fewer lines are scanned to make up the same sized image. The size of the region scanned can be reduced in size to a 'slot' or spot which increases the scanning speed allowing imaging at a temporal rate of 5 ms or less without the loss of spatial resolution (Hernández-Cruz *et al.*, 1990). Using a CLSM that has a maximum scan speed of 0.5 ms per line, a 50 x 50 pixel box which should have sufficient resolution for a single cell will take approximately 25 ms to scan.

Techniques have been developed to achieve fast Ca^{2+} imaging (faster than video-rate) using epi-fluorescent microscopes. Both high spatial and temporal resolution of Ca^{2+}-indicator fluorescence signals has been achieved using epi-fluorescent illumination from a xenon excitation source by measuring fluorescence using a fast CCD camera (Canepari & Mammano, 1999). Imaging at full frame resolution (128 x 128 pixels) was possible with a minimal 2.5 ms inter-frame interval. The temporal resolution was only limited by the kinetic properties of the fluorescent indicator used (Canepari & Mammano, 1999).

What concentrations of $[Ca^{2+}]_{cyt}$ are reached during the settlement response? Accurate quantification of $[Ca^{2+}]_{cyt}$ reached during the settlement response was not possible using Oregon Green BAPTA-1-dextran due to the dye becoming saturated to the same degree as that achieved when Ca^{2+}-ionophore was added. Therefore to achieve exact measurements of $[Ca^{2+}]_{cyt}$ lower affinity Ca^{2+} indicators should be tested that can cope with higher Ca^{2+} concentrations.

What is the source of the Ca^{2+} required for settlement? Calcium channel inhibitor experiments suggest that extracellular Ca^{2+} is required for settlement, but internal release of Ca^{2+} from stores such as the ER and vacuole may also be important and may be induced by Ca^{2+} influx through the plasma membrane (Sanders *et al.*, 1999). Internal release of Ca^{2+} can be tested through the use of inhibitors such as the aminosteroid U73122 which blocks phospholipase C-mediated intracellular Ca^{2+} release (Lee & Shen, 1998) and has been used in *Fucus* to block release of Ca^{2+} from intracellular stores (Coelho *et al.*, 2002).

Do Ca^{2+} channels mediate elevations in $[Ca^{2+}]_{cyt}$ at settlement and are they clustered at the anterior of the cell where the adhesive vesicles are released? To investigate

calcium channels in the plasma membrane patch clamping could be used. Patch clamping is a powerful technique which is used to study the function and regulation of ion channels in the plasma membrane including ion channel gating kinetics. For example, the technique can be used to determine how frequently a channel opens and closes and from this the duration it stays open for (Taylor & Brownlee, 1992). Patch clamp studies have shown that specific Ca^{2+} channels exist in plant cells (Trewavas & Knight, 1994) and could be used to provide an insight into the presence of Ca^{2+} channels in *Ulva* spores, in particular their location in the plasma membrane. Studies with amperometry provided evidence for the presence of mechanosensitive channels in the plasma membrane. If these channels are present they could provide a mechanism for the initiation of settlement. For example, when a zoospore detects a surface that is favourable for settlement it begins to spin, sensing the surface with its apical papilla. Favourable signals from the surface may induce settlement which could be mediated by the opening of mechanosensitive Ca^{2+} channels allowing Ca^{2+} to flood into the cell resulting in an elevation in $[Ca^{2+}]_{cyt}$, in turn triggering the release of the adhesive vesicles. The presence of mechanosensitive channels could be further investigated using patch clamping.

Preliminary attempts to use patch clamping on zoospores met with limited success due to the motility of the cells and the flexibility of the plasma membrane which prevented a good electrical seal forming between the cell membrane and glass micropipette (see Appendix III). If a gigaseal could be achieved with whole-cell patch clamping then capacitance changes could be measured at settlement. The capacitance of the plasma membrane is linearly proportional to its surface area (Thiel & Battey, 1998), and hence an increase in capacitance indicates an increase in plasma

membrane surface area that can only be brought about by exocytosis. The kinetics of exocytosis and endocytosis can be elucidated using capacitance measurements.

Further studies to link settlement with Ca^{2+}-regulated secretion could include dual imaging experiments using FM 1-43 as a settlement marker and Oregon Green BAPTA-1 dextran however there may be some overlap of the two dye emissions as FM 1-43 has a broad emission spectra peaking at 600 nm when bound to phospholipid bilayer membranes (Haughland, 2002). FM 1-43 could also be used as a settlement marker in conjunction with patch clamping so that the exact point of secretion and mass membrane recycling could be tied in with electrophysiological measurements. In addition, caged Ca^{2+} reagents such as Ca^{2+}-nitrophenyl-EGTA (Ca^{2+}-NP-EGTA) which deliver Ca^{2+} upon photolysis could be used to transiently elevate $[Ca^{2+}]_{cyt}$ to see if this triggers cells to secrete their adhesive and hence settle. In mouse pancreatic ß-cells both exocytosis and endocytosis were triggered by photorelease of Ca^{2+} from Ca^{2+}-NP-EGTA (Eliasson *et al.*, 1996).

In order to link settlement with the release of the redox-active substrate detected using micro-amperometry, the question remains – ***what is the product that is being secreted in response to mechano-stimulation?*** The question could be tackled using fast cyclic voltammetry, which provides information regarding the chemical species being studied. The technique involves the application of a periodic voltage pattern to the electrode in the absence and presence of the reactant. The background trace obtained without the reactant present is then subtracted from subsequent traces, to reveal the current resulting from the reduction and oxidation of the reactant. Characteristic voltammograms are obtained for specific compounds due to their redox potentials and rates of electron transfer (Chow & von Rüden, 1995). If the chemical constituents of

the vesicles could be elucidated it would allow comparison with compounds that are involved in cross-linking of the cell wall. If a compound has not been studied before it may not be possible to determine whether the signature belongs to it or not, but it may be possible to distinguish whether the product released on cell rupture is the same product released during vesicular release.

One of the biggest questions raised by the work on NO production in diatoms is – ***does NO production affect motility in* Seminavis*?*** Through this study it has been found that elevated levels of NO reduce adhesion and that cells produce more NO on a surface to which they adhere to weakly. Nitric oxide production on an unfavourable surface could therefore provide a signal for *Seminavis* to move away from a surface (even detach) and find a more suitable microhabitat. The question could easily be answered if there was a marked difference between the motility of control cells and cells incubated with the NO donor SNAP, but due to the inherent variability in motility seen in diatoms (Poulsen *et al.*, 1999) it is likely to be a lengthy study.

Experiments have recently been conducted using NOS-overexpressing transformants of *P. tricornutum* that show elevated NO production. Adhesion assays have shown a 2-fold reduction in adhesion of the transformants compared to adhesion of the wild-type (Thompson *et al.* in prep). These experiments corroborate the idea that NO reduces adhesion in diatoms.

Is there secretion of different adhesives when settled on hydrophilic and hydrophobic surfaces? Adhesive production could be tested on the two surfaces – glass and PDMSE – to see whether the surfaces cause the cells to produce different adhesive polymers. Characterisation of polysaccharides in the adhesive could be achieved by growing cells on glass and PDMSE, followed by harvesting of the cells

and fractional carbohydrate analysis of the polymeric substances extracted using various extraction procedures as has been performed for the pennate diatom *Pinnularia viridis* (Chiovitti *et al.*, 2003). An alternative molecular method could involve growth of the cells on glass and PDMSE, followed by harvesting and screening the mRNA for adhesion-related genes to determine if different genes are active in cells grown on the two surfaces.

Is the generation of NO in* Seminavis *caused by an elevation in $[Ca^{2+}]_{cyt}$***?*** In *P. tricornutum* $[Ca^{2+}]_{cyt}$ transients lead to the production of NO via a calcium-dependent NOS (Vardi *et al.*, 2006). Calcium was measured using t ransgenic lines of *P. tricornutum* expressing the aequorin gene. Transgenic approaches are not possible with *Seminavis* hence to see if there is a Ca^{2+} flux, a dextran Ca^{2+}-indicator could be loaded into the cell using the biolistic technique together with a dextran version of DAF-FM. To achieve separation of dye emissions, the Ca^{2+} indicator would be required to emit above 530 nm. Suitable Ca^{2+}-indicators include X-rhod-1, which emits at 600 nm and Rhod-2, which emits at 580 nm.

Understanding the cell biology of fouling algae will aid developments in antifouling coatings. Nitric oxide-releasing surfaces have already been produced and tested for use in humans to reduce thrombosis following procedures such as balloon angioplasty by the addition of NO donors to hydrogels (Bohl & West, 2000). If an NO donor could be tethered to antifouling coatings applied to ships then diatom removal from the submerged surface should be increased, as diatom attachment strength would be reduced. Whether NO could reduce settlement and/or attachment strength of other fouling organisms such as *Ulva* zoospores and barnacle cypris larvae is of interest

because antifouling surfaces that are effective against multiple target organisms are highly sought after.

References

ABDULLAHI, A. S., UNDERWOOD, G. J. C., GRETZ, M. R. (2006). Extracellular matrix assembly in diatoms (Bacillariophyceae). V. Environmental effects on polysaccharide synthesis in the model diatom, *Phaeodactylum tricornutum*. *J. Phycol.* **42**: 363-378.

ALLEN, A. E., VARDI, A., BOWLER, C. (2006). An ecological and evolutionary context for integrated nitrogen metabolism and related signaling pathways in marine diatoms. *Curr. Opin. Plant Biol.* **9**: 264-273.

ALZIEU, C. L., SANJUAN, J., DELTREIL, J. P., BOREL, M. (1986). Tin contamination in Arcachon Bay: effects on oyster shell anomalies. *Mar. Pollut. Bull.* **17**(11): 494-498.

ANDERSON, L. L. (2006). Discovery of the 'porosome'; the universal secretory machinery in cells. *J. Cell. Mol. Med.* **10**(1): 126-131.

ARMBRUST, E. V., BERGES, J. A., BOWLER, C., GREEN, B. R., MARTINEZ, D., PUTNAM, N. H., ZHOU, S. G., ALLEN, A. E., APT, K. E., BECHNER, M., BRZEZINSKI, M. A., CHAAL, B. K., CHIOVITTI, A., DAVIS, A. K., DEMAREST, M. S., DETTER, J. C., GLAVINA, T., GOODSTEIN, D., HADI, M. Z., HELLSTEN, U., HILDEBRAND, M., JENKINS, B. D., JURKA, J., KAPITONOV, V. V., KROGER, N., LAU, W. W. Y., LANE, T. W., LARIMER, F. W., LIPPMEIER, J. C., LUCAS, S., MEDINA, M., MONTSANT, A., OBORNIK, M., PARKER, M. S., PALENIK, B., PAZOUR, G. J., RICHARDSON, P. M., RYNEARSON, T. A., SAITO, M. A., SCHWARTZ, D. C., THAMATRAKOLN, K., VALENTIN, K., VARDI, A., WILKERSON, F. P., ROKHSAR, D. S. (2004). The genome of the diatom Thalassiosira pseudonana: Ecology, evolution, and metabolism. *Science* **306**(5693): 79-86.

ATKINSON, H. A., DANIELS, A., READ, N. D. (2002). Live-cell imaging of endocytosis during conidial germination in the rice blast fungus, *Magnaporthe grisea*. *Fungal Genet. Biol.* **37**: 233-244.

BALCERCZYK, A., SOSZYNSKI, M., BARTOSZ, G. (2005). On the specificity of 4-amino-5-methylamino-2',7'-difluorofluorescein as a probe for nitric oxide. *Free Radic. Biol. Med.* **39**: 327-335.

BARCLAY, J. W., MORGAN, A., BURGOYNE, R. D. (2005). Calcium-dependent regulation of exocytosis. *Cell Calcium* **38**: 343-353.

BARROSO, J. B., CORPAS, F. J., CARRERAS, A., SANDALIO, L. M., VALDERRAMA, R., PALMA, J. M., LUPIÁÑEZ, J. A., DEL RÍO, L. A. (1999). Localization of nitric-oxide synthase in plant peroxisomes. *J. Biol. Chem.* **274**(51): 36729-36733.

BATTEY, N. H., BLACKBOURN, H. D. (1993). The control of exocytosis in plant-cells. *New Phytol.* **125**(2): 307-338.

BATTEY, N. H., JAMES, N. C., GREENLAND, A. J., BROWNLEE, C. (1999). Exocytosis and endocytosis. *The Plant Cell* **11**: 643-659.

BELANGER, K. D., QUATRANO, R. S. (2000). Membrane recycling occurs during asymmetric tip growth and cell plate formation in *Fucus distichus* zygotes. *Protoplasma* **212**: 24-37.

BELIGNI, M. V., LAMATTINA, L. (2001). Nitric oxide in plants: the history is just beginning. *Plant, Cell Environ.* **24**: 267-278.

BETZ, W. J., BEWICK, G. S. (1992). Optical analysis of synaptic vesicle recycling at the frog neuromuscular junction. *Science* **255**(5041): 200-203.

BETZ, W. J., MAO, F., BEWICK, G. S. (1992). Activity-dependent fluorescent staining and destaining of living vertebrate motor nerve terminals. *J. Neurosci.* **12**(2): 363-375.

BHOSLE, N. B., SAWANT, S. S., GARG, A., WAGH, A. B., EVANS, L. V. (1996). Chemical characterization of exopolysaccharides from the marine fouling diatom *Amphora coffeaeformis*. *Biofouling* **10**(4): 301-307.

BICKER, G. (2005). STOP and GO with NO: nitric oxide as a regulator of cell motility in simple brains. *BioEssays* **27**: 495-505.

BOHL, K. S., WEST, J. L. (2000). Nitric oxide-generating polymers reduce platelet adhesion and smooth muscle cell proliferation. *Biomaterials* **21**: 2273-2278.

BOTHWELL, J. H. F., BROWNLEE, C., HETHERINGTON, A. M., NG, C. K.-Y., WHEELER, G. L., MCAINSH, M. R. (2006). Biolistic delivery of Ca2+ dyes into plant and algal cells. *The Plant Journal* **46**: 327-335.

BRAUN, F. J., HEGEMANN, P. (1999). Direct measurement of cytosolic calcium and pH in living *Chlamydomonas reinhardtii* cells. *Eur. J. Cell Biol.* **78**(3): 199-208.

BROWNLEE, C., PULSFORD, A. L. (1988). Visualization of the cytoplasmic free Ca2+ gradient in growing rhizoid cells of *Fucus serratus*. *J. Cell Sci.* **91**: 249-256.

BUCHANAN, B. B., GRUISSEM, W., JONES, R. L. (eds.) (2000). *Biochemistry and molecular biology of plants* First edition. American Society of Plant Physiologists, Rockville, USA.

BUSH, D. S., JONES, R. L. (1987). Measurement of cytoplasmic calcium in aleurone protoplasts using indo-1 and fura-2. *Cell Calcium* **8**: 455-472.

CALENBERG, M., BROHSONN, U., ZEDLACHER, M., KREIMER, G. (1998). Light- and Ca2+-modulated heterotrimeric GTPases in the eyespot apparatus of a flagellate green alga. *The Plant Cell* **10**: 91-103.

CALLOW, J. A., CALLOW, M. E. (2006). The *Ulva* Spore Adhesive System. In *Biological Adhesives* (A. M. SMITH, J. A. CALLOW editors), pp. 63-78. Springer-Verlag, Berlin, Heidelberg.

CALLOW, J. A., CALLOW, M. E., ISTA, L. K., LOPEZ, G. P., CHAUDHURY, M. K. (2005). The influence of surface energy on the wetting behaviour of the spore adhesive of the marine alga *Ulva linza* (synonym *Enteromorpha linza*). *Journal of the Royal Society Interface* **2**(4): 319-325.

CALLOW, J. A., CRAWFORD, S. A., HIGGINS, M. J., MULVANEY, P., WETHERBEE, R. (2000a). The application of atomic force microscopy to topographical studies and force measurements on the secreted adhesive of the green alga *Enteromorpha*. *Planta* **211**(5): 641-647.

CALLOW, J. A., OSBORNE, M. P., CALLOW, M. E., BAKER, F., DONALD, A. M. (2003). Use of Environmental Scanning Electron Microscopy to image the spore adhesive of the marine alga *Enteromorpha* in its natural hydrated state. *Colloids and Surfaces B: Biointerfaces* **27**: 315-321.

CALLOW, M. E., CALLOW, J. A. (2000). Substratum location and zoospore behaviour in the fouling alga *Enteromorpha*. *Biofouling* **15**(1-3): 49-56.

CALLOW, M. E., CALLOW, J. A. (2002). Marine biofouling: a sticky problem. *Biologist* **49**(1): 10-14.

CALLOW, M. E., CALLOW, J. A., ISTA, L. K., COLEMAN, S. E., NOLASCO, A. C., LOPEZ, G. P. (2000b). The use of self-assembled monolayers of different

wettabilities to study surface selection and primary adhesion processes of green algal (*Enteromorpha*) zoospores. *Appl. Environ. Microbiol.* **66**(8): 3249-3254.

CALLOW, M. E., CALLOW, J. A., PICKETT-HEAPS, J. D., WETHERBEE, R. (1997). Primary adhesion of *Enteromorpha* (Chlorophyta, Ulvales) propagules: quantitative settlement studies and video microscopy. *J. Phycol.* **33**: 938-947.

CALLOW, M. E., CRAWFORD, S., WETHERBEE, R., TAYLOR, K., FINLAY, J. A., CALLOW, J. A. (2001). Brefeldin A affects adhesion of zoospores of the green alga *Enteromorpha*. *J. Exp. Bot.* **52**(360): 1409-1415.

CALLOW, M. E., EVANS, L. V. (1974). Studies on the ship-fouling alga *Enteromorpha* III. Cytochemistry and autoradiography of adhesive production. *Protoplasma* **80**: 15-27.

CALLOW, M. E., EVANS, L. V. (1977). Studies on the ship-fouling alga *Enteromorpha* (Chlorophyceae, Ulvales) IV. Polysaccharide and nucleoside diphosphatase localization. *Phycologia* **16**(3): 313-320.

CALLOW, M. E., JENNINGS, A. R., BRENNAN, A. B., SEEGERT, C. E., GIBSON, A., WILSON, L., FEINBERG, A., BANEY, R., CALLOW, J. A. (2002). Microtopographic cues for settlement of zoospores of the green fouling alga *Enteromorpha*. *Biofouling* **18**(3): 237-245.

CANEPARI, M., MAMMANO, F. (1999). Imaging neuronal calcium fluorescence at high spatio-temporal resolution. *J. Neurosci. Methods* **87**: 1-11.

CARROLL, A. D., MOYEN, C., KESTEREN, P. V., TOOKE, F., BATTEY, N. H., BROWNLEE, C. (1998). Ca^{2+}, annexins, and GTP modulate exocytosis from maize root cap protoplasts. *The Plant Cell* **10**: 1267-1276.

CARTER, C., PAN, S., ZOUHAR, J., AVILA, E. L., GIRKE, T., RAIKHEL, N. V. (2004). The vegetative vacuole proteome of *Arabidopsis thaliana* reveals predicted and unexpected proteins. *The Plant Cell* **16**: 3285-3303.

CASSÉ, F., STAFSLIEN, S. J., BAHR, J. A., DANIELS, J., FINLAY, J. A., CALLOW, J. A., CALLOW, M. E. (2007). Combinatorial materials research applied to the development of new surface coatings V. Application of a spinning water-jet for the semi-high throughput assessment of the attachment strength of marine fouling algae. *Biofouling* **23** (2): 121-130.

CHAMP, M. C. (2000). A review of organotin regulatory strategies, pending actions, related costs and benefits. *Sci. Total Environ.* **258**: 21-71.

CHEPURNOV, V. A., MANN, D. G., VYVERMAN, W., SABBE, K., DANIELIDIS, D. B. (2002). Sexual reproduction, mating system, and protoplast dynamics of *Seminavis* (Bacillariophyceae). *J. Phycol.* **38**: 1004-1019.

CHIN, W.-C., ORELLANA, M. V., QUESADA, I., VERDUGO, P. (2004). Secretion in unicellular marine phytoplankton: demonstration of regulated exocytosis in *Phaeocystis globosa*. *Plant Cell Physiol.* **45**(5): 535-542.

CHIOVITTI, A., HIGGINS, M. J., HARPER, R. E., WETHERBEE, R., BACIC, A. (2003). The complex polysaccharides of the raphid diatom *Pinnularia viridis* (Bacillariophyceae). *J. Phycol.* **39**: 543-554.

CHO, M.-S., QUINN, A. S., STROMER, M. H., DASH, S., CHO, J., TAATJES, D. J., JENA, B. P. (2002). Structure and dynamics of the fusion pore in live cells. *Cell Biol. Int.* **26**(1): 35-42.

CHOW, R. H., VON RÜDEN, L. (1995). Electrochemical detection of secretion from single cells. In *Single-channel recording* (B. SAKMANN, E. NEHER editors), Plenum Press, New York.

CHOW, R. H., VON RÜDEN, L., NEHER, E. (1992). Delay in vesicle fusion revealed by electrochemical monitoring of single secretory events in adrenal chromaffin cells. *Nature* **356**: 60-63.

CLAISSE, D., ALZIEU, C. L. (1993). Copper contamination as a result of antifouling paint regulations? *Mar. Pollut. Bull.* **26**(7): 395-397.

CLAYTON, M. N., ASHBURNER, C. M. (1994). Secretion of phenolic bodies following fertilisation in *Durvillaea potatorum* (Durvillaeales, Phaeophyta). *E. J. Phycol.* **29**: 1-9.

COELHO, S. M., TAYLOR, A. R., RYAN, K. P., SOUSA-PINTO, I., M.T., B., BROWNLEE, C. (2002). Spatiotemporal patterning of reactive oxygen production and Ca^{2+} wave propagation in fucus rhizoid cells. *The Plant Cell* **14**: 2369-2381.

COOKSEY, K. E., COOKSEY, B. (1986). Adhesion of fouling diatoms to surfaces: some biochemistry. In *Algal biofouling* (L. V. EVANS, K. D. HOAGLAND editors), pp. 41-53. Elsevier, Amsterdam.

COSGROVE, D. J., HEDRICH, R. (1991). Stretch-activated chloride, potassium and calcium channels coexisting in plasma membranes of guard cells of *Vicia faba* L. *Planta* **186**: 143-153.

COUPLAND, R. E. (1968). Determining sizes and distribution of sizes of spherical bodies such as chromaffin granules in tissue sections. *Nature* **217**: 384-388.

COUSIN, M. A., ROBINSON, P. J. (1999). Mechanisms of synaptic vesicle recycling illuminated by fluorescent dyes. *J. Neurochem.* **73**: 2227-2239.

CRAWFORD, N. M., GALLI, M., TISCHNER, R., HEIMER, Y. M., OKAMOTO, M., MACK, A. (2006). Response to Zemojtel *et al*: Plant nitric oxide synthase: back to square one. *Trends Plant Sci.* **11**(11): **526-527**.

DAVIES, I. M., HARDING, M. J. C., BAILEY, S. K., SHANKS, A. M., LÄNGE, R. (1997). Sublethal effects of tributyltin oxide on the dogwhelk *Nucella lapillus*. *Mar. Ecol. Prog. Ser.* **158**: 191-204.

DEL RÍO, L. A., CORPAS, F. J., BARROSO, J. B. (2004). Nitric oxide and nitric oxide synthase activity in plants. *Phytochemistry* **65**: 783-792.

DELLEDONNE, M. (2005). NO news is good news for plants. *Curr. Opin. Plant Biol.* **8**: 390-396.

DUNINA-BARKOVSKAYA, A. Y., LEVINA, N. N., LEW, R. R., HEATH, L. B. (2004). Gadolinium effects on gigaseal formation and the adhesive properties of a fungal amoeboid cell, the slime mutant of *Neurospora crassa*. *J. Membr. Biol.* **198**: 77-87.

ELIASSON, L., PROKS, P., ÄMMÄLÄ, C., ASHCROFT, F. M., BOKVIST, K., RENSTRÖM, E., RORSMAN, P., SMITH, P. A. (1996). Endocytosis of secretory granules in mouse pancreatic ß-cells evoked by transient elevation of cytosolic calcium. *J. Physiol. (Lond).* **493**: 755-767.

EMANS, N., ZIMMERMANN, S., FISCHER, R. (2002). Uptake of a fluorescent marker in plant cells is sensitive to Brefaldin A and Wortmannin. *The Plant Cell* **14**: 71-86.

ERMILOVA, E., ZALUTSKAYA, Z., MUNNIK, T., VAN DER ENDE, H., GROMOV, B. (1998). Calcium in the control of chemotaxis in *Chlamydomonas*. *Biologia (Bratisl).* **53**(4): 577-581.

ESPINOSA, M., NOÉ, G., TRONSCOSO, C., HO, S. B., VILLALÓN, M. (2002). Acidic pH and increasing [Ca^{2+}] reduce the swelling of mucins in primary cultures of human cervical cells. *Hum. Reprod.* **17**(8): 1964-1972.

ESTEVEZ, M. S., PUNTARULO, S. (2005). Nitric oxide generation upon growth of Antarctic Chlorella sp cells. *Physiol. Plant.* **125**(2): 192-201.

EVANS, L. V., CHRISTIE, A. O. (1970). Studies on the ship-fouling alga *Enteromorpha*. I. Aspects of the fine structure and biochemistry of swimming and newly settled zoospores. *Ann. Bot.* **34**: 451-456.

EVANS, S. M. (1999). Tributytin pollution: the catastrophe that never happened. *Mar. Pollut. Bull.* **38**(8): 629-636.

EVANS, S. M., BIRCHENOUGH, A. C., BRANCATO, M. S. (2000). The TBT ban: out of the frying pan into the fire? *Mar. Pollut. Bull.* **40**(3): 204-211.

FALCIATORE, A., CASOTTI, R., LEBLANC, C., ABRESCIA, C., BOWLER, C. (1999). Transformation of nonselectable reporter genes in marine diatoms. *Mar. Biotechnol.* **1**: 239-251.

FALCIATORE, A., D'ALCALÁ, M. R., CROOT, P., BOWLER, C. (2000). Perception of environmental signals by a marine diatom. *Science* **288**: 2363-2366.

FALKOWSKI, P. G., BARBER, R. T., SMETACEK, V. (1998). Biogeochemical controls and feedbacks on ocean primary production. *Science* **281**: 200-206.

FINLAY, J. A., CALLOW, M. E., ISTA, L. K., LOPEZ, G. P., CALLOW, J. A. (2002a). The influence of surface wettability on the adhesion strength of settled spores of the green alga *Enteromorpha* and the diatom *Amphora*. *Integrative and Comparative Biology* **42**: 1116-1122.

FINLAY, J. A., CALLOW, M. E., SCHULTZ, M. P., SWAIN, G. W., CALLOW, J. A. (2002b). Adhesion strength of settled spores of the green alga *Enteromorpha*. *Biofouling* **18**(4): 251-256.

FOISSNER, I., WENDEHENNE, D., LANGEBARTELS, C., DURNER, J. (2000). *In vivo* imaging of an elicitor-induced nitric oxide burst in tobacco. *The Plant Journal* **23**(6): 817-824.

GEESEY, G. G., WIGGLESWORTH-COOKSEY, B., COOKSEY, K. E. (2000). Influence of calcium and other cations on surface adhesion of bacteria and diatoms: a review. *Biofouling* **15**(1-3): 195-205.

GELDNER, N. (2004). The plant endosomal system - its structure and role in signal transduction and plant development. *Planta* **219**: 547-560.

GHAZI, A., BERRIER, C., AJOUZ, B., BESNARD, M. (1998). Mechanosensitive ion channels and their mode of activation. *Biochimie* **80**: 357-362.

GILROY, S., BETHKE, P. C., JONES, R. L. (1993). Calcium homeostasis in plants. *J. Cell Sci.* **106**: 453-462.

GLOSSMANN, H., STRIESSNIG, J. (1988). Calcium channels. *Vitamins and Hormones - Advances in Research and Applications* **44**: 155-328.

GONZÁLEZ-GAITÁN, M. (2003). Endocytic trafficking during *Drosophila* development. *Mech. Dev.* **120**: 1265-1282.

GOULD, K. S., LAMOTTE, O., KLINGUER, A., PUGIN, A., WENDEHENNE, D. (2003). Nitric oxide production in tobacco leaf cells: a generalised stress response? *Plant, Cell Environ.* **26**: 1851-1862.

GUILLARD, R. R. L., RYTHER, J. H. (1962). Studies of marine planktonic diatoms: I. *Cyclotella nana* Hustedt and *Detonula confervacea* Cleve. *Can. J. Microbiol.* **8**: 229-239.

HARZ, H., HEGEMANN, P. (1991). Rhodopsin-regulated calcium currents in Chlamydomonas. *Nature* **351**(6326): 489-491.

HARZ, H., NONNENGÄSSER, C., HEGEMANN, P. (1992). The photoreceptor current of the green alga *Chlamydomonas*. *Phil. Trans. R. Soc. London, Ser. B* **338**: 39-52.

HAUGHLAND, R. P. (2002). *Molecular Probes. Handbook of fluorescent probes and research chemicals*, Ninth edition edition. Molecular Probes, Inc., Eugene, USA.

HERNÁNDEZ-CRUZ, A., SALA, F., ADAMS, P. R. (1990). Subcellular calcium transients visualized by confocal microscopy in a voltage-clamped vertebrate neuron. *Science* **247**: 858-862.

HETHERINGTON, A. M., BROWNLEE, C. (2004). The generation of Ca2+ signals in plants. *Annu. Rev. Plant Biol.* **55**: 410-427.

HIGGINS, M. J., MOLINO, P., MULVANEY, P., WETHERBEE, R. (2003). The structure and nanomechanical properties of the adhesive mucilage that mediates diatom-substratum adhesion and motility. *J. Phycol.* **39**: 1181-1193.

HOAGLAND, K. D., ROSOWSKI, J. R., GRETZ, M. R., ROEMER, S. C. (1993). Diatom extracellular polymeric substances: Function, fine structure, chemistry, and physiology. *J. Phycol.* **29**(5): 537-566.

HOFFMAN, L. R. (1967). Observations on the fine structure of *Oedogonium*. III. Microtubular elements in the chloroplasts of *Oe. Cardiacum*. *J. Phycol.* **3**: 212-221.

HOLLAND, E.-M., BRAUN, F. J., NONNENGÄSSER, C., HARZ, H., HEGEMANN, P. (1996). The nature of rhodopsin-triggered photocurrents in *Chlamydomonas*. I. Kinetics and influence of divalent ions. *Biophys. J.* **70**: 924-931.

HOLLAND, R., DUGDALE, T. M., WETHERBEE, R., BRENNAN, A. B., FINLAY, J. A., CALLOW, J. A., CALLOW, M. E. (2004). Adhesion and motility of fouling diatoms on a silicone elastomer. *Biofouling* **20**(6): 323-329.

HOMANN, U., TESTER, M. (1997). Ca^{2+}-independent and Ca^{2+}/GTP-binding protein-controlled exocytosis in a plant cell. *Proc. Natl. Acad. Sci. U. S. A.* **94**: 6565-6570.

HUANG, X., KIEFER, E., VON RAD, U., ERNST, D., FOISSNER, I., DURNER, J. (2002). Nitric oxide burst and nitric oxide-dependent gene induction in plants. *Plant Physiol. Biochem.* **40**: 625-631.

HUMPHREY, A. J., FINLAY, J. A., PETTITT, M. E., STANLEY, M. S., CALLOW, J. A. (2005). Effect of Ellman's reagent and dithiothreitol on the curing of the spore adhesive glycoprotein of the green alga *Ulva*. *J. Adhes.* **81**: 791-803.

HWANG, I., SHEEN, J. (2001). Two-component circuitry in *Arabidopsis* cytokinin signal transduction. *Nature* **413**: 383-389.

JEFFREY, S. W., HUMPHREY, G. F. (1975). New spectrophotometric equations for determining chlorophylls a, b, c1 and c2 in higher plants, algae and natural phytoplankton. *Biochem. Physiol. Pflanzen (BPP)* **167**: 191-194.

JENA, B. P., CHO, S. J., JEREMIC, A., STROMER, M. H., ABU-HAMDAH, R. (2003). Structure and composition of the fusion pore. *Biophys. J.* **84**: 1337-1343.

JOINT, I., CALLOW, M. E., CALLOW, J. A., CLARKE, K. R. (2000). The attachment of *Enteromorpha* zoospores to a bacterial biofilm assemblage. *Biofouling* **16**(2-4): 151-158.

JOINT, I., TAIT, K., CALLOW, M. E., CALLOW, J. A., MILTON, D., WILLIAMS, P., CÁMARA, M. (2002). Cell-to-cell communication across the prokaryote-eukaryote boundary. *Science* **298**(5596): 1207.

KIEBER, J. J. (1997). The ethylene signal transduction pathway in *Arabidopsis*. *J. Exp. Bot.* **48**(307): 211-218.

KIM, K.-T., KOH, D.-S., HILLE, B. (2000). Loading of oxidizable transmitters into secretory vesicles permits carbon-fiber amperometry. *J. Neurosci.* **20**: RC101 (101-105).

KIRKMAN-BROWN, J. C., BRAY, C., STEWART, P. M., BARRATT, C. L. R., PUBLICOVER, S. J. (2000). Biphasic elevation of $[Ca^{2+}]_i$ in individual human spermatozoa exposed to progesterone. *Dev. Biol.* **222**: 326-335.

KLAHRE, U., CRÉTÉ, P., LEUENBERGER, S. A., IGLESIAS, V. A., MEINS, F. (2002). High molecular weight RNAs and small interfering RNAs induce systemic posttranscriptional gene silencing in plants. *Proc. Natl. Acad. Sci. U. S. A.* **99**(18): 11981-11986.

KNIGHT, M. R., CAMPBELL, A. K., SMITH, S. M., TREWAVAS, A. J. (1991). Transgenic plant aequorin reports the effects of touch and cold-shock and elicitors on cytoplasmic calcium. *Nature* **352**: 524-526.

KOHN, R. (1975). Ion binding on polyuronates - alginate and pectin. *Pure Appl. Chem.* **42**: 371-397.

KOJIMA, H., URANO, Y., KIKUCHI, K., HIGUCHI, T., HIRATA, Y., NAGANO, T. (1999). Fluorescent indicators for imaging nitric oxide production. *Angew. Chem. Int. Ed.* **38**(21): 3209-3212.

KREIMER, G., WITMAN, G. B. (1994). Novel touch-induced, Ca^{2+}-dependent phobic response in a flagellate green alga. *Cell Motil. Cytoskeleton* **29**: 97-109.

KRISHNAN, S., WANG, N., OBER, C. K., FINLAY, J. A., CALLOW, M. E., CALLOW, J. A., HEXEMER, A., SOHN, K. E., KRAMER, E. J., FISCHER, D. A. (2006). Comparison of the Fouling Release Properties of Hydrophobic Fluorinated and Hydrophilic PEGylated Block Copolymer Surfaces: Attachment Strength of the Diatom *Navicula* and the Green Alga *Ulva*. *Biomacromolecules* **7**: 1449-1462.

KUBITSCHECK, U., HOMANN, U., THIEL, G. (2000). Osmotically evoked shrinking of guard-cell protoplasts causes vesicular retrieval of plasma membrane into the cytoplasm. *Planta* **210**: 423-431.

KÜHN, S. F., BROWNLEE, C. (2005). Membrane organisation and dynamics in the marine diatom *Coscinodiscus wailesii* (Bacillariophyceae). *Bot. Mar.* **48**(4): 297-305.

LAM, C. M. C., YEUNG, P. K. K., WONG, J. T. Y. (2005). Monitoring cytosolic calcium in the dinoflagellate *Crypthecodinium cohnii* with Calcium Orange-AM. *Plant Cell Physiol.* **46**(6): 1021-1027.

LAW, R. J., BLAKE, S. J., JONES, B. R., ROGAN, E. (1998). Organotin compounds in liver tissue of harbour porpoises (*Phocoena phocoena*) and grey seals (*Halichoerus grypus*) from the coastal waters of England and Wales. *Mar. Pollut. Bull.* **36**(3): 241-247.

LEE, S.-J., SHEN, S. S. (1998). The calcium transient in sea urchin eggs during fertilization requires the production of Inositol 1,4,5-Trisphosphate. *Dev. Biol.* **193**: 195-208.

LEFER, A. M., LEFER, D. J. (1996). The role of nitric oxide and cell adhesion molecules on the microcirculation in ischaemia-reperfusion. *Cardiovasc. Res.* **32**: 743-751.

LODISH, H., BERK, A., MATSUDAIRA, P., KAISER, C. A., KREIGER, M., SCOTT, M. P., ZIPURSKY, S. L., DARNELL, J. (2004). *Molecular Cell Biology*. Fifth edition. W.H. Freeman and Company, New York, USA. 973 pp.

LOPEZ, P. J., DESCLÉS, J., ALLEN, A. E., BOWLER, C. (2005). Prospects in diatom research. *Curr. Opin. Biotechnol.* **16**: 180-186.

LOSCALZO, J., WELCH, G. (1995). Nitric oxide and its role in the cardiovascular system. *Prog. Cardiovasc. Dis.* **38**(2): 87-104.

MAGGS, C. A., CALLOW, M. E. (2003). Algal spores, version 1.0. In *Encyclopedia of Life Sciences*, Nature Publishing Group, London.

MALLICK, N., MOHN, F. H., RAI, L., SOEDER, C. J. (2000). Impact of physiological stresses on nitric oxide formation by green alga, Scenedesmus obliquus. *J. Microbiol. Biotechnol.* **10**(3): 300-306.

MALLICK, N., MOHN, F. H., SOEDER, C. J., GROBBELAAR, J. U. (2002). Ameliorative role of nitric oxide on H2O2 toxicity to a chlorophycean alga *Scenedesmus obliquus*. *J. Gen. Appl. Microbiol.* **48**: 1-7.

MARCOTE, M. J., GU, F., GRUENBERG, J., ANIENTO, F. (2000). Membrane transport in the endocytic pathway: animal versus plant cells. *Protoplasma* **210**: 123-132.

MCAINSH, M. R., HETHERINGTON, A. M. (1998). Encoding specificity in Ca2+ signalling systems. *Trends Plant Sci.* **3**(1): 32-36.

MECKEL, T., HURST, A. C., THIEL, G., HOMANN, U. (2004). Endocytosis against high turgor: intact guard cells of *Vicia faba* constitutively endocytose fluorescently labelled plasma membrane and GFP-tagged K+-channel KAT1. *The Plant Journal* **39**: 182-193.

MIRALTO, A., BARONE, G., ROMANO, G., POULET, S. A., IANORA, A., RUSSO, G. L., BUTTINO, I., MAZZARELLA, G., LAABIR, M., CABRINI, M., GIACOBBE, M. G. (1999). The insidious effect of diatoms on copepod reproduction. *Nature* **402**: 173-176.

MONCK, J. R., FERNANDEZ, J. M. (1992). The exocytotic fusion pore. *J. Cell Biol.* **119**: 1395-1404.

MOROZ, L. L., NORBY, S. W., CRUZ, L., SWEEDLER, J. V., GILLETTE, R., CLARKSON, R. B. (1998). Non-enzymatic production of nitric oxide (NO) from NO synthase inhibitors. *Biochem. Biophys. Res. Commun.* **253**: 571-576.

MOSER, T., CHOW, R. H., NEHER, E. (1995). Swelling-induced catecholamine secretion recorded from single chromaffin cells. *Pflugers Archiv* **431**: 196-203.

NAKANO, I., KOBAYASHI, T., YOSHIMURA, M., SHINGYOJI, C. (2003). Central-pair-linked regulation of microtubule sliding by calcium in flagellar axonemes. *J. Cell Sci.* **116**: 1627-1636.

NONNENGÄSSER, C., HOLLAND, E.-M., HARZ, H., HEGEMANN, P. (1996). The nature of rhodopsin-triggered photocurrents in *Chlamydomonas*. II. Influence of monovalent ions. *Biophys. J.* **70**: 932-938.

OHATA, H., TANAKA, K., MAEYAMA, N., YAMAMOTO, M., MOMOSE, K. (2001). Visualization of elementary mechanosensitive Ca^{2+}-influx events, Ca^{2+} spots, in bovine lens epithelial cells. *J. Physiol. (Lond).* **532**(1): 31-42.

PARTON, R. M., FISCHER-PARTON, S., WATAHIKI, M. H., TREWAVAS, A. J. (2001). Dynamics of the apical vesicle accumulation and the rate of growth are related in individual pollen tubes. *J. Cell Sci.* **114**(14): 2685-2695.

PATEL, P., CALLOW, M. E., JOINT, I., CALLOW, J. A. (2003). Specificity in the settlement - modifying response of bacterial biofilms towards zoospores of the marine alga *Enteromorpha*. *Environ. Microbiol.* **5**(5): 338-349.

PAWLEY, J. B. (ed.) (1995). *Handbook of biological confocal microscopy* 2nd edition. Springer, New York.

PINONTOAN, R., YUASA, T., ANDERCA, M. I., MATSUOKA, T., UOZUMI, N., MORI, H., MUTO, S. (2000). Cloning of a cDNA encoding a 66-kDa Ca2+-dependent protein kinase (CDPK) from *Dunaliella tertiolecta* (Chlorophyta). *J. Phycol.* **36**(3): 545-552.

POULSEN, N. C., SPECTOR, I., SPURCK, T. P., SCHULTZ, T. F., WETHERBEE, R. (1999). Diatom gliding is the result of an actin-myosin motility system. *Cell Motil. Cytoskeleton* **44**: 23-33.

QUARMBY, L. M. (1996). Ca2+ influx activated by low pH in *Chlamydomonas*. *J. Gen. Physiol.* **108**: 351-361.

QUESADA, I., CHIN, W.-C., VERDUGO, P. (2006). Mechanisms of signal transduction in photo-stimulated secretion in *Phaeocystis globosa*. *FEBS Lett.* **580**: 2201-2206.

READ, N. D., SHACKLOCK, P. S., KNIGHT, M. R., TREWAVAS, A. J. (1993). Imaging calcium dynamics in living plant cells and tissues. *Cell Biol. Int.* **17**(2): 111-125.

REIZE, I. B., MELKONIAN, M. (1989). A new way to investigate living flagellated/ciliated cells in the light microscope: immobilization of cells in agarose. *Bot. Acta* **102**: 145-151.

RIBEIRO JR., E. A., CUNHA, F. Q., TAMASHIRO, W. M. S. C., MARTINS, I. S. (1999). Growth phase-dependent subcellular localization of nitric oxide synthase in maize cells. *FEBS Lett.* **445**: 283-286.

RIJSTENBIL, J. W. (2003). Effects of UVB radiation and salt stress on growth, pigments and antioxidative defence of the marine diatom *Cylindrotheca closterium*. *Mar. Ecol. Prog. Ser.* **254**: 37-48.

ROBERTS, S. K., GILLOT, I., BROWNLEE, C. (1994). Cytoplasmic calcium and *Fucus* egg activation. *Development* **120**: 155-163.

ROUND, F. E., CRAWFORD, R. M., MANN, D. G. (1990). *The Diatoms: Biology and Morphology of the Genera*. Cambridge University Press, Cambridge.

RUSS, J. C. (1990). *Computer-assisted microscopy. The measurement and analysis of images*. Plenum Press, New York.

RYAN, T. A., SMITH, S. J., REUTER, H. (1996). The timing of synaptic vesicle endocytosis. *Proc. Natl. Acad. Sci. U. S. A.* **93**: 5567-5571.

SAKIHAMA, Y., NAKAMURA, S., YAMASAKI, H. (2002). Nitric oxide production mediated by nitrate reductase in the green alga *Chlamydomonas reinhardtii*: an alternative NO production pathway in photosynthetic organisms. *Plant Cell Physiol.* **43**(3): 290-297.

SAMUELS, A. L., BISALPUTRA, T. (1990). Endocytosis in elongating root cells of *Lobelia erinus*. *J. Cell Sci.* **97**: 157-165.

SANDERS, D., BROWNLEE, C., HARPER, J. F. (1999). Communicating with calcium. *The Plant Cell* **11**: 691-706.

SCALA, S., BOWLER, C. (2001). Molecular insights into the novel aspects of diatom biology. *Cell. Mol. Life Sci.* **58**: 1666-1673.

SCHOENWAELDER, M. E. A., CLAYTON, M. N. (1998). Secretion of phenolic substances into the zygote wall and cell plate in embryos of *Hormosira* and *Acrocarpia* (Fucales, Phaeophyceae). *J. Phycol.* **34**: 969-980.

SCHOENWAELDER, M. E. A., CLAYTON, M. N. (1999). The role of the cytoskeleton in brown algal physode movement. *Eur. J. Phycol* **34**: 223-229.

SCHULTE, A., CHOW, R. H. (1996). A simple method for insulating carbon-fiber microelectrodes using anodic electrophoretic deposition of paint. *Anal. Chem.* **68**: 3054-3058.

SCHULTE, A., CHOW, R. H. (1998). Cylindrically etched carbon-fiber microelectrodes for low-noise amperometric recording of cellular secretion. *Anal. Chem.* **70**: 985-990.

SCHULTZ, M. P., FINLAY, J. A., CALLOW, M. E., CALLOW, J. A. (2000). A turbulent channel flow apparatus for the determination of the adhesion strength of microfouling organisms. *Biofouling* **15**: 243-251.

SCHULTZ, M. P., SWAIN, G. W. (2000). The influence of biofilms on skin friction drag. *Biofouling* **15**(1-3): 129-139.

SEMENOVA, M. N., OZERNYUK, N. D. (2004). Effects of NO-synthase inhibitors on development of sea urchin embryos. *J. Evol. Biochem. Physiol.* **40**: 282-288.

SHEPHERD, V. A., BEILBY, M. J., BISSON, M. A. (2004). When is a cell not a cell? A theory relating coenocytic stucture to the unusual electrophysiology of *Ventricaria ventricosa* (*Valonia ventricosa*). *Protoplasma* **223**: 79-91.

SHOAF, T. W., LIUM, B. S. (1976). Improved extraction of chlorophyll a and b from algae using dimethyl sulfoxide. *Limn. Ocean.* **21**: 926-928.

SIDERIUS, M., HENSKENS, H., PORTOLEBLANCHE, A., VANHIMBERGEN, J., MUSGRAVE, A., HARING, M. (1997). Characterisation and cloning of a calmodulin-like domain protein kinase from *Chlamydomonas moewusii* (Gerloff). *Planta* **202**(1): 76-84.

STANLEY, M. S., CALLOW, M. E., CALLOW, J. A. (1999). Monoclonal antibodies to adhesive cell coat glycoproteins secreted by zoospores of the green alga *Enteromorpha*. *Planta* **210**: 61-71.

STANLEY, M. S., PERRY, R. M., CALLOW, J. A. (2005). Analysis of Expressed Sequence Tags (ESTs) from the green alga Ulva linza (Chlorophyta). *J. Phycol.* **41**(6): 1219-1226.

STATZ, A., FINLAY, J., DALSIN, J., CALLOW, M., CALLOW, J. A., MESSERSMITH, P. B. (2006). Algal antifouling and fouling-release properties of metal surfaces coated with a polymer inspired by marine mussels. *Biofouling* **22**: 391-399.

STEER, M. W. (1988). The role of calcium in exocytosis and endocytosis in plant cells. *Physiol. Plant.* **72**: 213-220.

STEWART, R. J., WEAVER, J. C., MORSE, D. E., WAITE, J. H. (2004). The tube cement of *Phragmatopoma californica*: a solid foam. *J. Exp. Biol.* **207**: 4727-4734.

STRICKER, S. A., CENTONZE, V. E., PADDOCK, S. W., SCHATTEN, G. (1992). Confocal microscopy of fertilization-induced calcium dynamics in sea urchin eggs. *Dev. Biol.* **149**: 370-380.

SURPIN, M., RAIKHEL, N. (2004). Traffic jams affect plant development and signal transduction. *Nat. Rev. Mol. Cell Biol.* **5**: 100-109.

SUTTER, J.-U., HOMANN, U., THIEL, G. (2000). Ca^{2+}-stimulated exocytosis in maize coleoptile cells. *The Plant Cell* **12**: 1127-1136.

TAYLOR, A. R., BROWNLEE, C. (1992). Localized patch clamping of plasma membrane of a polarised plant cell. *Plant Physiol.* **99**(4): 1686-1688.

TAYLOR, A. R., CHOW, R. H. (2001). A microelectrochemical technique to measure trans-plasma membrane electron transport in plant tissue and cells *in vivo*. *Plant, Cell Environ.* **24**: 749-754.

TAYLOR, A. R., MANISON, N. F. H., FERNANDEZ, C., WOOD, J., BROWNLEE, C. (1996). Spatial organization of calcium signalling involved in cell volume control in the Fucus rhizoid. *The Plant Cell* **8**: 2015-2031.

THIEL, G., BATTEY, N. (1998). Exocytosis in plants. *Plant Mol. Biol.* **38**: 111-125.

THIEL, G., KREFT, M., ZOREC, R. (1998). Unitary exocytotic and endocytotic events in *Zea mays* L. coleoptile protoplasts. *The Plant Journal* **13**(1): 117-120.

THIEL, G., SUTTER, J.-U., HOMANN, U. (2000). Ca2+-sensitive and Ca2+-insensitive exocytosis in maize coleoptile protoplasts. *Pflügers Archiv* **439**: R152-R153.

TRAVIS, E. R., WIGHTMAN, R. M. (1998). Spatio-temporal resolution of exocytosis from individual cells. *Annu. Rev. Biophys. Biomol. Struct.* **27**: 77-103.

TREWAVAS, A., KNIGHT, M. (1994). Mechanical signalling, calcium and plant form. *Plant Mol. Biol.* **26**: 1329-1341.

UEDA, T., YAMAGUCHI, M., UCHIMIYA, H., NAKANO, A. (2001). Ara6, a plant-unique novel type Rab GTPase, functions in the endocytic pathway of *Arabidopsis thaliana*. *EMBO J.* **20**(17): 4730-4741.

VAN BREUSEGEM, F., VRANOVÁ, E., DAT, J. F., INZÉ, D. (2001). The role of active oxygen species in plant signal transduction. *Plant Science* **161**: 405-414.

VARDI, A., FORMIGGINI, F., CASOTTI, R., DE MARTINO, A., RIBALET, F., MIRALTO, A., BOWLER, C. (2006). A stress surveillance system based on calcium and nitric oxide in marine diatoms. *PLoS Biol.* **4**(3): e60.

VERDUGO, P., ALLDREDGE, A. L., AZAM, F., KIRCHMAN, D. L., PASSOW, U., SANTSCHI, P. H. (2004). The oceanic gel phase: a bridge in the DOM-POM continuum. *Mar. Chem.* **92**: 67-85.

VERNOUD, V., HORTON, A. C., YANG, Z., NIELSEN, E. (2003). Analysis of the small GTPase gene superfamily of Arabidopsis. *Plant Physiol.* **131**: 1191-1208.

VREELAND, V., WAITE, J. H., EPSTEIN, L. (1998). Polyphenols and oxidases in substratum adhesion by marine algae and mussels. *J. Phycol.* **34**: 1-8.

WATSON, J. M., FUSARO, A. F., WANG, M., WATERHOUSE, P. M. (2005). RNA silencing platforms in plants. *FEBS Lett.* **579**: 5982-5987.

WETHERBEE, R., LIND, J. L., BURKE, J. (1998). The first kiss: establishment and control of initial adhesion by raphid diatoms. *J. Phycol.* **34**: 9-15.

WHEELER, G. L., TAIT, K., TAYLOR, A., BROWNLEE, C., JOINT, I. (2005). Acyl-homoserine lactones modulate the settlement rate of zoospores of the marine alga *Ulva intestinalis* via a novel chemokinetic mechanism. *Plant, Cell Environ.*

WHITE, P. J. (2000). Calcium channels in higher plants. *Biochim. Biophys. Acta* **1465**: 171-189.

WIGGLESWORTH-COOKSEY, B., COOKSEY, K. E. (1992). Can diatoms sense surfaces?: State of our knowledge. *Biofouling* **5**: 227-238.

WIGHTMAN, R. M., JANKOWSKI, J. A., KENNEDY, R. T., KAWAGOE, K. T., SCHROEDER, T. J., LESZCZYSZYN, D. J., NEAR, J. A., DILIBERTO JR., E. J., VIVEROS, O. H. (1991). Temporally resolved catecholamine spikes correspond to single release from individual chromaffin cells. *Proc. Natl. Acad. Sci. U. S. A.* **88**: 10754-10758.

WILSON, S. M., PICKETT-HEAPS, J. D., WEST, J. A. (2006). Vesicle transport and the cytoskeleton in the unicellular alga *Glaucosphaera vacuolata*. *Phycol. Res.* **54**: 15-20.

WOOD, A. M., EVERROAD, R. C., WINGARD, L. M. (2005). Measuring growth in microalgal cultures. In *Algal Culturing Techniques* (R. A. ANDERSEN editor), p. 596. Elsevier Academic Press, London.

YEBRA, D. M., KIIL, S., DAM-JOHANSEN, K. (2004). Antifouling technology - past, present and future steps towards efficient and environmentally friendly antifouling coatings. *Prog. Org. Coat.* **50**: 75-104.

YOSHIMURA, K. (1996). A novel type of mechanoreception by the flagella of *Chlamydomonas*. *J. Exp. Biol.* **199**(2): 295-302.

YOSHIMURA, K. (1998). Mechanosensitive channels in the cell body of *Chlamydomonas*. *J. Membr. Biol.* **166**(2): 149-155.

YOUNGBLOOD, J. P., ANDRUZZI, L., OBER, C. K., HEXEMER, A., KRAMER, E. J., CALLOW, J. A., FINLAY, J. A., CALLOW, M. E. (2003). Coatings based on side-chain ether-linked poly(ethylene glycol) and fluorocarbon polymers for the control of marine biofouling. *Biofouling* **19 (supplement)**: 91-98.

YUASA, T., HASHIMOTO, H. (2006). A calcium-dependent protein kinase (CDPK) in the unicellular green alga *Closterium ehrenbergii*. *Microbes Environ.* **21**(4): 278-283.

ZEMOJTEL, T., FRÖHLICH, A., PALMIERI, M. C., KOLANCZYK, M., MIKULA, I., WYRWICZ, L. S., WANKER, E. E., MUNDLOS, S., VINGRON, M., MARTASEK, P., DURNER, J. (2006). Plant nitric oxide synthase: a never-ending story? *Trends Plant Sci.* **11**: 524-525.

ZENISEK, D., STEYER, J. A., ALMERS, W. (2000). Transport, capture and exocytosis of single synaptic vesicles at active zones. *Nature* **406**: 849-854.

ZENISEK, D., STEYER, J. A., FELDMAN, M. E., ALMERS, W. (2002). A membrane marker leaves synaptic vesicles in milliseconds after exocytosis in retinal bipolar cells. *Neuron* **35**: 1085-1097.

ZHANG, Z.-B., LUI, C.-Y., WU, Z.-Z., XING, L., LI, P.-F. (2006). Detection of nitric oxide in culture media and studies on nitric oxide formation by marine microalgae. *Med. Sci. Monit.* **12**(2): BR75-85.

ZHOU, Z., MISLER, S., CHOW, R. H. (1996). Rapid fluctuations in transmitter release from single vesicles in bovine adrenal chromaffin cells. *Biophys. J.* **70**: 1543-1552.

ZOREC, R., TESTER, M. (1992). Cytoplasmic calcium stimulates exocytosis in a plant secretory cell. *Biophys. J.* **63**(3): 864-867.

APPENDIX I

STACKS MACROS FOR RATIO IMAGES IN SCION IMAGE

- For Pic files – first open in Thumbsplus and split into bmps
- Open bmps in Scion Image
- Windows to Stack
- Save as a tif file
- Load Macros
- Open Oregon Green stack first
- To Texas Red stack apply macro ‘Divide 250/255 and add 5’
- Apply macro ‘Ratio two stacks’
- Apply macro ‘Smooth’ to ratioed stack

```
macro 'divide 250/255 and add 5';
var
  i:integer;
begin
  CheckForStack;
  for i:= 1 to nSlices do begin
    SelectSlice(i);
    MultiplyByConstant(0.98);
AddConstant(5)
  end;
end;
```

```
macro 'ratio two stacks';
{Creates ratio image.}
```

```
var
  i,w1,w2,w3,h1,h2,h3,d1,d2,d3,rat:integer;
begin
  RequiresVersion(1.53);
  SaveState;
  if nPics<>2 then begin
    PutMessage('This macro operates on exactly two stacks.');
    exit;
  end;
  SelectPic(1);
  KillRoi;
  GetPicSize(w1,h1);
  d1:=nSlices;
  SelectPic(2);
  KillRoi;
  GetPicSize(w2,h2);
  d2:=nSlices;
  if d1>=d2
    then d3:=d1
    else d3:=d2;
  if (w1<>w2) or (h1<>h2) or (d1<>d2) or (d1=0)  then begin
    PutMessage('This macro requires two stacks that are the same size.');
    exit;
  end;
  SetNewSize(w1,h1);
  MakeNewStack('ratio');
  rat:=PicNumber;
```

```
  for i:=1 to d1 do begin
    SelectPic(1);
    SelectSlice(i);
    SelectPic(2);
    SelectSlice(i);
   ImageMath('div', 1, 2, 60, 1, 'Temp');
    SelectAll;
    Copy;
    dispose;
    SelectPic(rat);
    if i<>1 then AddSlice;
    paste;
   end;
  RestoreState;
end;



macro 'Smooth';
var
  i:integer;
begin
  CheckForStack;
  for i:= 1 to nSlices do begin
    SelectSlice(i);
    SetOption; Smooth;
  end;
end;
```

APPENDIX II

GUILLARDS F/2 MEDIUM FOR DIATOMS

1) Steam 1L of natural seawater for 4h and then allow to cool.
2) Make up 0.1 M $Na_2SiO_3.5H_2O$ stock
    a. Add 12.5 g $Na_2SiO_3.5H_2O$ to 400 ml distilled water.
    b. pH to pH 2.0 using HCl.
    c. Make up to 500 ml with distilled water.
3) Make up 0.9 M $NaNO_3$ stock
    a. Add 7.4 g of $NaNO_3$ to 100 ml distilled water
4) Make up 36 mM $NaH_2PO_42H_2O$ stock
    a. Add 0.566g of $NaH_2PO_42H_2O$ to 100 ml distilled water
5) Make up Trace Mineral stock
    a. Add the following to 500 ml distilled water
        i. 11.5 mg $ZnSO_4.7H_2O$ (80 µM)
        ii. 89 mg $MnCl_2.4H_2O$ (900 mM)
        iii. 18.5 mg $(NH_4)_6.Mo_7O_{24}$ (30 µM)
        iv. 7 mg of $CoSO_4.7H_2O$ (50 µM)
        v. 5 mg of $CuSO_4.5H_2O$ (40 µM)
6) Make up Fe/EDTA stock
    a. Add 0.392 g of ferric citrate (16 mM) and 0.393 g of EDTA (10 mM) and add to 100 ml distilled water.
7) Make up 1 M Tris stock
    a. Add 12.4 g of Tris to 100 ml distilled water
8) Make up B_{12}/Biotin stick
    a. Add 1 mg of biotin (41 µM) and 1 mg of vitamin B_{12} (7 µM) to 100 ml of water

9) Make up 0.3 mM Thiamine stock

    a. Add 10 mg of thiamine to 100 ml distilled water and pH to pH4 using HCl

10) Add to seawater the following:

    a. 8.0 ml/L of $Na_2SiO_3.5H_2O$
    b. 1.0 ml/L of $NaNO_3$
    c. 1.0 ml/L of $NaH_2PO_42H_2O$
    d. 1.0 ml/L of Trace Mineral
    e. 1.0 ml/L Fe/EDTA
    f. 1.0 ml/L Tris
    g. 50 µl/L of B_{12}/biotin
    h. 1.0 ml/L of Thiamine

11) Filter through 0.22 µm pore-size bottle-top filter (Nalgene, New York, US) into sterile schott bottle.

APPENDIX III

PATCH CLAMPING

Introduction

Patch clamping is a powerful technique used to study the function and regulation of ion channels in the plasma membrane and ion channel gating kinetics such as how often a channel opens and closes and how long it stays open for (Taylor & Brownlee, 1992). Patch clamp studies have shown the existence of specific calcium channels in plant cells (Trewavas & Knight, 1994).

The technique involves a filled glass micropipette being brought into contact with the cell membrane of interest which is bathed in a defined solution. If conditions permit, an electrical seal will form between the micropipette and membrane, isolating electrical currents from ion channels that are present only in the patch of membrane. Patch clamping is technically demanding as a good electrical seal (referred to as a giga-seal as it has a resistance of $10^9 – 10^{11}$ Ω) is required between the cell membrane and micropipette. Suction is often required to create a giga-seal (Hamill *et al.*, 1981). A patch clamp amplifier is used to control voltage flow through the membrane and record currents passing through the ion channels as they open (Garrill, 2000).

There are four main recording configurations in patch clamping and the methods used to achieve them are illustrated in Figure 9. Cell-free membrane patches are possible without a loss in seal resistance by slowly withdrawing the micropipette from the membrane. A tight vesicle sealing off the pipette tip is formed allowing effects of ion concentration changes on single channel currents to be studied (Hamill *et al.*, 1981). Whole-cell patch clamping is achieved by breaking the membrane patch separating the pipette from the cell interior by applying suction (Figure 9). The seal is not damaged in the process and recordings can then be made from the whole cell. Whole-

cell recording allows control of the cytosolic composition and the measurement of electrical parameters from the whole cell and is best used when the likelihood of finding an active channel in a patch is low (Homann & Tester, 1998). It is possible that any calcium channels present in the *Ulva* zoospore plasma membrane will be fairly clustered at the anterior plasma membrane to allow a localised influx of calcium ions and a polarised release of the adhesive vesicles.

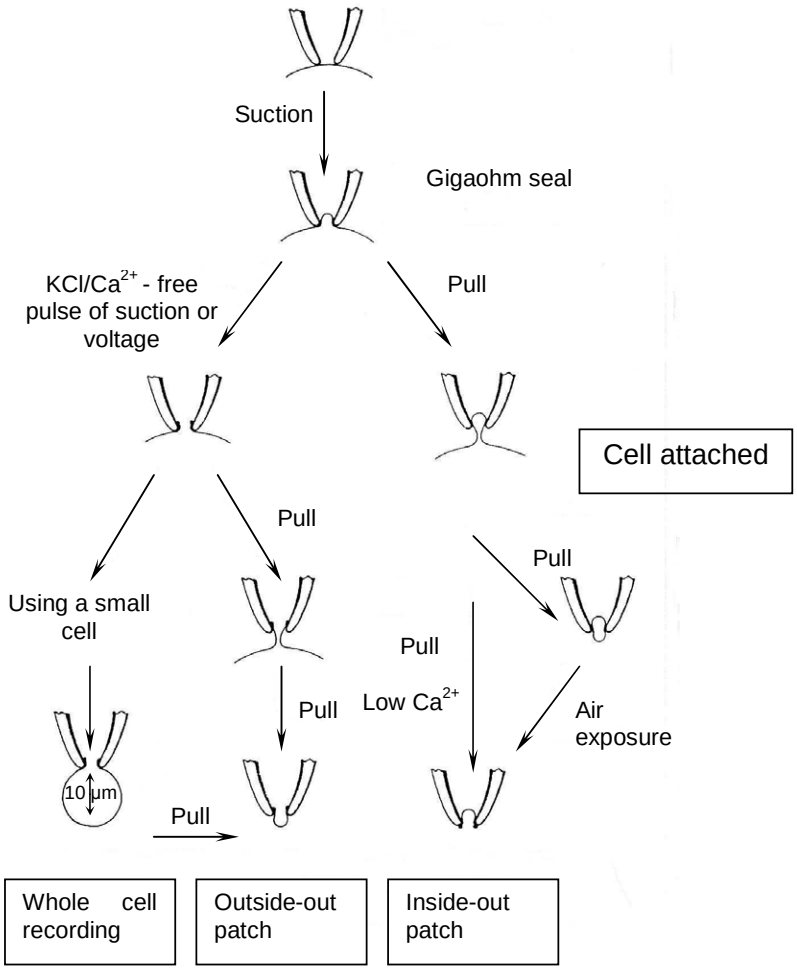

Figure 9 Illustrating the four recording configurations possible with patch clamping – cell-attached, whole-cell, outside-out and inside out patches (taken from Hamill *et al*. (1981)). Applying slight suction to a cell forms a cell-attached patch. Manipulations can then be made to a cell-attached patch to achieve the three other recording configurations.

Methods

Four different solutions were tried for patch clamping experiments (see Table 4). Zoospores swam noticeably slower in the solutions with sorbitol presumably due to an increase in viscosity.

Table 4 Solutions used for patch clamping. Solutions 3 and 4 are the same as 1 and 2 minus sorbitol. pH was adjusted using CaOH.

Chemical	**1**	**2**	**3**	**4**
$CaCl_2$	20 mM	20 mM	20 mM	20 mM
HEPES	5 mM	5 mM	5 mM	5 mM
Sorbitol	1 M	700 mM	/	/
NaCl	/	100 mM	/	100 mM
$MgCl_2$	/	15 mM	/	15 mM
pH	8.2	8.2	8.2	8.2

Zoospores were released from adult thalli in solution 4 (Table 4) as the composition is close to that of seawater but the exact ions present and their concentration are known. Conventional patch clamp techniques (Hamill *et al.*, 1981) were used to attempt to form seals in a cell-attached configuration. The reference electrode consisted of an Ag/AgCl pellet connected to the bath via a bridge containing solution 1. Patch pipettes were fabricated from borosilicate glass (GC150F-10; Harvard, Edenbridge, UK) with a Narashige pipette puller (P-833; Narishige, Tokyo, Japan). Pipettes were coated with beeswax to reduce capacitance. Electrodes were back filled with ultra-filtered (0.22 µm; Millipore, Watford, UK) pipette solution no. 1. Patch pipettes were connected via a pipette holder to the head stage of a patch clamp amplifier (Axopatch 200A; Axon Instruments, Union City, USA). Slight positive pressure was applied

until the pipette was in view after which suction was applied to attract a swimming zoospore. After contact with a zoospore gentle suction was applied to promote seal formation. Electrodes with a resistance of 15-25 MΩ were used (~1 µm diameter), as the tips of lower resistance electrodes were too large resulting in zoospores being sucked up the tip.

Results and Discussion

Zoospores behaved normally when they were in the NaCl solution without sorbitol (#4) and zoospores could be released from the parent material when rehydrated in this solution. Active zoospores were not released when hydrated in the $CaCl_2$ solutions (1 & 3). Zoospores moved very slowly and normal settlement rates were only seen to occur when the bath solution was diluted 50:50 with seawater. However better seals were formed in the $CaCl_2$ solutions hence most experiments used these as bath solutions. Cells formed better seals when they were freshly added to the bath solution.

In the $CaCl_2$ solution without sorbitol (#3), cells stopped moving and appeared to swell up. The cells were very delicate to excess suction in this state. When cells moved slowly it was easier to form a seal as when they moved at their natural speed it was very difficult to keep them on the end of the electrode without the cell entering the electrode. Although the cells are not physiologically healthy in the $CaCl_2$ solutions once the appropriate conditions are found for seal formation the health of the cells can hopefully be improved through modifications in the bath composition.

Figure 10 shows a seal being formed between the micropipette and cell. A seal only tended to form when a large proportion of the cell membrane was drawn up the

pipette (Figure 10). However when the cell was in this state it was unstable and the whole cell was likely to enter the electrode, as the zoospore membrane is very flexible. The instability of the membrane is illustrated by the internalisation of FM 1-43 in Figure 10 indicating that the membrane had been disrupted allowing dye to enter the cytosol. Narrow high resistance pipette tips were needed (~1 µm) as if the tip was any larger the whole cell entered the electrode when applying negative pressure. However the tip had to be sufficiently large to allow enough suction to attract and hold zoospores on the end.

Seals of 250 MΩ were commonly achieved but the seal then stopped forming and despite applying negative and positive voltage as well as negative pressure further improvement in the seal did not occur. With a seal of 250 MΩ there was too much noise to distinguish single channel responses.

It appears that zoospores will settle on a micropipette as long as they are still free to move such as when the end of the pipette is blocked so a seal is not formed. Hence it is unlikely that a cell will undergo settlement voluntarily whilst being patch clamped, as a seal with the membrane is required and movement of the cell is prevented when the cell is held tightly. Therefore stimulation of settlement will be needed. Addition of low melting point agarose could be used to initiate settlement of a cell on the end of an electrode.

References

GARRILL, A. (2000). Studying ion channels in undergraduate laboratories. *Biochem. Mol. Biol. Educ.* **28**: 318-321.

HAMILL, O. P., MARTY, A., NEHER, E., SAKMANN, B., SIGWORTH, F. J. (1981). Improved patch-clamp techniques for high-resolution current recording from cells and cell-free membrane patches. *Pflügers Archiv* **391**: 85-100.

HOMANN, U., TESTER, M. (1998). Patch-clamp measurements of capacitance to study exocytosis and endocytosis. *Trends Plant Sci.* **3**(3): 110-114.

TAYLOR, A. R., BROWNLEE, C. (1992). Localized patch clamping of plasma membrane of a polarised plant cell. *Plant Physiol.* **99**(4): 1686-1688.

TREWAVAS, A., KNIGHT, M. (1994). Mechanical signalling, calcium and plant form. *Plant Mol. Biol.* **26**: 1329-1341.

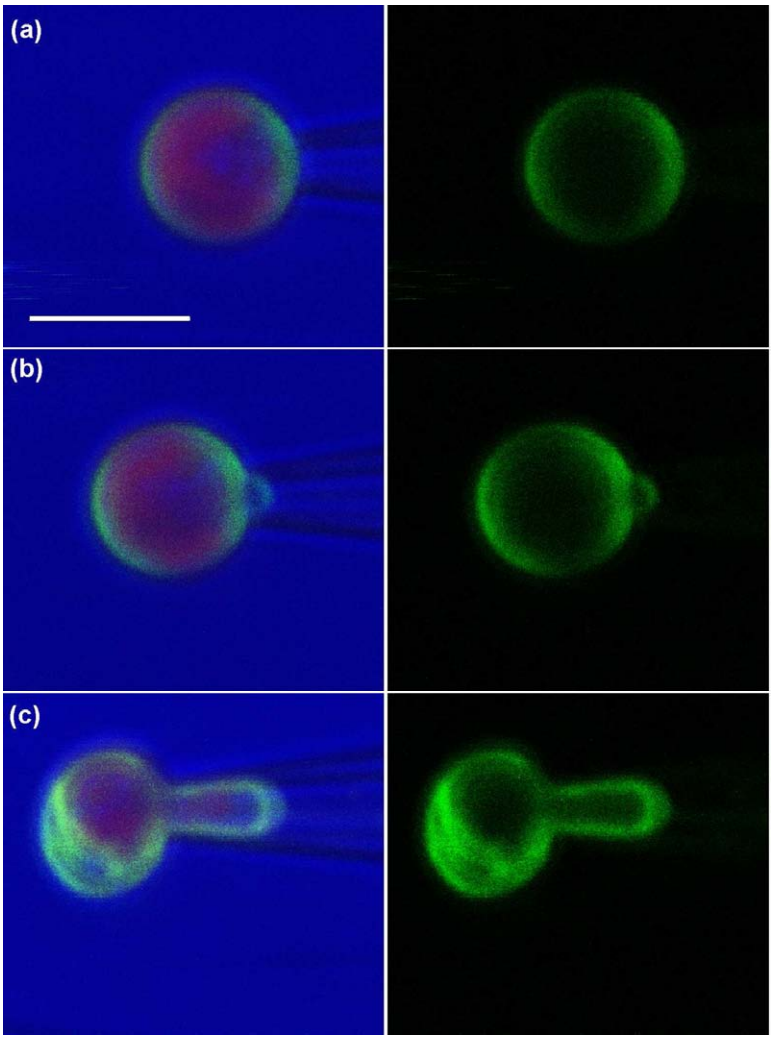

Figure 10 Left: Autofluorescence (red) and FM 1-43 fluorescence (green) of a tethered zoospore **Right:** FM 1-43 fluorescence only a) 8 minutes b) 10 minutes and c) 14 minutes after addition of FM 1-43. Bar = 5 µm.